

In presenting the dissertation as a partial fulfillment of the requirements for an advanced degree from the Georgia Institute of Technology, I agree that the Library of the Institute shall make it available for inspection and circulation in accordance with its regulations governing materials of this type. I agree that permission to copy from, or to publish from, this dissertation may be granted by the professor under whose direction it was written, or, in his absence, by the Dean of the Graduate Division when such copying or publication is solely for scholarly purposes and does not involve potential financial gain. It is understood that any copying from, or publication of, this dissertation which involves potential financial gain will not be allowed without written permission.

D.
REMOVED FROM FILE

7/25/68

SENSITIVITY ANALYSIS OF THE
SYSTEM RESPONSE FUNCTIONS OF LINEAR HYDROLOGIC MODELS

A THESIS

Presented to

The Faculty of the Division of Graduate
Studies and Research

by

Richard Hamilton McCuen

In Partial Fulfillment
of the Requirements for the Degree
Doctor of Philosophy
in the School of Civil Engineering

Georgia Institute of Technology

March, 1971

SENSITIVITY ANALYSIS OF THE
SYSTEM RESPONSE FUNCTIONS OF LINEAR HYDROLOGIC MODELS

Approved:

Chairman

Date approved by Chairman:

March 1, 1971

ACKNOWLEDGMENTS

My sincerest appreciation goes to Dr. James R. Wallace, my thesis advisor, without whose encouragement, enthusiasm, generous contribution of time, and competent advice this thesis would not have been possible. Thanks are also due to the other members of my reading committee, Mr. Willard M. Snyder and Dr. Alan M. Lumb, who also gave unselfishly of their time and effort to this endeavor.

The author also wishes to thank Dr. L. Douglas James and Dr. George M. Slaughter for their helpful comments in preparation of the final manuscript.

This thesis is dedicated to the author's wife, Amelia, for typing each draft of my thesis and especially for her encouragement and patience during this endeavor.

TABLE OF CONTENTS

ACKNOWLEDGMENTS	Page ii
LIST OF TABLES	v
LIST OF ILLUSTRATIONS	vii
SUMMARY	ix
 Chapter	
I. INTRODUCTION	1
II. LITERATURE REVIEW	5
Representation of the Watershed as a System	
Conceptual Models	
Sensitivity Analysis	
Critique and Motivation	
III. PREPARATION OF DATA	18
Hydrologic Data	
Determination of Precipitation Excess	
Physiographic Data	
Use of Data	
IV. ANALYSIS OF DATA FOR THE SELECTED CONCEPTUAL MODELS . .	22
Measurement of Model Regeneration Capability	
The Single Linear Reservoir Model	
Single Linear Reservoir with Feedback Model	
The Nash Model	
Double Routing Model	
Double Routing with Feedback Model	
Linear Channel-Linear Reservoir Model	
Comparative Evaluation of Conceptual Models	
Unique Parameter Values for a Watershed	
Analysis of Results	

Chapter	Page
V. FACTORS AFFECTING THE DERIVATION OF THE SYSTEM RESPONSE FUNCTION OF SELECTED CONCEPTUAL MODELS	61
The Watershed and Conceptual Model Response Functions	
The Distribution of Precipitation Excess	
Types and Magnitude of Data Error	
Experimental Design	
Experimental Procedure	
Results	
Summary of Results	
The Importance of Considering the Shape Characteristics of Conceptual Model Response Functions	
VI. PREDICTION OF CONCEPTUAL MODEL RESPONSE FUNCTIONS . . .	94
Factor Analysis of Topographic Characteristics and Model Parameters	
Conceptual Model Parameter Prediction Equations	
Parameter Prediction for Ungaged Watersheds	
Analysis of Prediction Equations	
VII. SENSITIVITY ANALYSIS	111
The Sensitivity Function	
The Sensitivity Equation	
Sources of Parametric Error	
The Sensitivity Functions of the Conceptual Models	
The Sensitivity-Regeneration Capability Trade-Off	
Comparison of Conceptual Model Sensitivity	
Inverse Sensitivity Analysis	
VIII. DISCUSSION AND CONCLUSIONS	147
Adequacy of Linear Conceptual Models	
Prediction of Model Parameter Values	
Sensitivity Analysis	
Conclusions	
IX. RECOMMENDATIONS	155
Optimum Sensitivity	
Parameter Sensitivity and Parameter Importance	
Comparison of Model Sensitivity	
Structural Analysis of Multi-parameter Models Using Parametric Sensitivity	
Summary	
REFERENCES	159
APPENDICES	163

LIST OF TABLES

Table	Page
4-1. Regeneration for SLR Model	29
4-2. Regeneration for SLRWF Model	33
4-3. Regeneration for Nash Model	38
4-4. Regeneration for Double Routing Model	40
4-5. Regeneration for DRWF Model	44
4-6. System Response Functions of the LCLR Models	47
4-7. Regeneration for LCLR Models	50
4-8. Summary of Correlation Coefficients for Six Models . . .	51
4-9. Comparison of Regeneration by Rank	51
4-10. Correlation Coefficients Resulting from Joint Parameter Regeneration	55
4-11. Standard Error Values Resulting from Joint Parameter Regeneration	56
5-1. Watershed Response Function Parameters	66
5-2. Total Error Distribution	78
5-3. Averaged Effects : Models Versus Watershed Response Function	83
5-4. Averaged Effects : Models Versus Data Error	85
5-5. Averaged Effects : Models Versus PE Distribution	85
5-6. Model Regeneration Capability	93
6-1. Correlation Coefficients for Prediction Equations . . .	98
6-2. Model Parameter Prediction Equations	100

Table	Page
6-3. Watershed and Storm Characteristic Values	100
6-4. Model Parameter Prediction Equations	103
6-5. Prediction Equation Regeneration Comparison	105
6-6. Regeneration for Ungaged Watersheds	109
7-1. Regeneration Capability Measured by Correlation Coefficient	133
7-2. Regeneration Capability Measured by Standard Error . . .	133
7-3. Rank of Sensitivity Estimates	133
7-4. Comparison of Two-Parameter Model Sensitivity for Storm Event 18	138

LIST OF FIGURES

Figure	Page
2-1. Linear Channel Action	8
4-1. Block Diagram of Single Linear Reservoir Model	25
4-2. Regeneration of Storm Event 2 Using SLR Models	30
4-3. Regeneration of Storm Event 14 Using SLR Models	30
4-4. Block Diagram of SLRWF Model	31
4-5. Nash Model Regeneration of Storm Event 8	35
4-6. Block Diagram Representation of Double Routing Model	36
4-7. Double Routing Model Regeneration of Storm Event 8	41
4-8. Block Diagram Representation of the DRWF Model	42
4-9. Regeneration Using Averaged Parameter Values	59
5-1. Watershed Response Functions	66
5-2. True Precipitation Excess Distributions	67
5-3. Introduction of a Uniform Loss Function Data Error	68
5-4. Experimental Procedure	74
5-5. Comparison of Model Response Functions and Watershed Response Function I_1	81
5-6. Comparison of Watershed Response Functions	91
6-1. Regeneration Using Predicted Parameter Value	106
7-1. Sensitivity Functions : SLR Model	119
7-2. Sensitivity Functions : SLRWF Model	119
7-3. Sensitivity Functions : DR Model	121

Figure	Page
7-4. Sensitivity Functions : DRWF Model	121
7-5. Sensitivity Functions : Nash Model	123
7-6. Sensitivity Functions : LCLR-R Model	125
7-7. Sensitivity Functions : LCLR-LT Model	126
7-8. Sensitivity Functions : LCLR-RT Model	127
7-9. Comparison of Sensitivity Functions	131
7-10. Regeneration of Storm Event 2	136
7-11. Example : Inverse Sensitivity Analysis	144
7-12. Sensitivity Function for Inverse Sensitivity Example . .	145
7-13. Adjusted Storm Runoff for Inverse Sensitivity Example .	145

SUMMARY

The purpose of a model is prediction. Such predictions are potentially limited in two ways. First, the mathematical structure of a model can effectively limit the flexibility of the model. Once the mathematical form of the model has been selected, parameters of the model must be evaluated. There are a number of factors which influence the process of parameter evaluation. These factors represent a limitation in the utilization of the associated model. This research was focused on the development and use of techniques for model structure analysis and the identification of factors which influence the computed value of model parameters.

The data used for the study were obtained from twenty small agricultural watersheds located in various parts of the continental United States. The area of the watersheds ranged from one-quarter of an acre to 2000 acres with fourteen of the twenty watersheds having an area less than 15 acres.

The following conceptual models were used in the analysis of the data: the single linear reservoir model, the single linear reservoir with feedback model, the double routing model, the double routing with feedback model, the Nash model, and the linear channel-linear reservoir model (LCLR). Each of these models can be classified as a linear, time invariant, storage model. One parameter value for both of the two-parameter models (the Nash and LCLR models) was set equal to the differ-

ence between the first moments of the observed runoff and the precipitation excess. The second parameter value for these two models and the parameter value for each of the four one-parameter models was determined by minimizing the sum of the squares of the differences between the observed and computed storm hydrographs. The optimized parameter values were used to regenerate the storm hydrographs and a correlation coefficient was used to measure the level of output reproduction. The poor regeneration obtained using the optimized parameter values indicated that the storage models were not capable of consistently providing a high level of output reproduction.

An analysis of artificial data indicated that the poor regeneration obtained from the analysis of hydrological data was due primarily to the limited flexibility of the storage models. The effect of error introduced into the data through the collection or processing of data was minor compared with the constraining shape of the storage model response functions.

Multivariate statistical techniques were used to identify and quantify the relationship between the optimized model parameter values and topographic characteristics. Factor analysis indicated that the basin area was the only significant topographic characteristic. Principal components regression provided prediction equations which could be used to predict model parameter values from the basin area and two storm characteristics.

Model parameter sensitivity was defined mathematically and the mathematical definition was used to derive functional relationships

(sensitivity functions) for the sensitivity of the storage model parameters. The sensitivity functions allow the dynamic and parametric natures of sensitivity to be examined. Correspondence between model parameter sensitivity and the potential regeneration of a model is revealed. The sensitivity equation which relates the parameter sensitivity and the change in a parameter value to the resulting change in output is discussed.

CHAPTER I

INTRODUCTION

Hydrologic data, including precipitation and stream flow measurements, are important in the design of hydraulic structures and in the planning and management of water resource systems. Existing data is usually quite limited and hydrologists have proposed techniques to analyze the data for the purpose of predicting storm runoff for watershed conditions not included in the available data for ungaged watersheds. Prediction of the hydrologic behavior of a watershed for a variety of conditions can be made using a mathematical model of the watershed. Models range in complexity from single parameter models used to predict peak discharges or individual storm hydrographs to more complex models involving subsystem representation of the various parts of the hydrologic cycle which simulate the continuous behavior of the watershed. Some (1) believe that only hydrologic models having a sound hydrologic basis should be used in hydrologic and hydraulic design. Additionally, the model structure should be of sufficient complexity to provide the desired level of accuracy but limited in structural complexity to the level which is necessary to achieve such accuracy.

Important advancements in hydrologic model analysis would be the development of techniques through which the structure of a model can be analyzed. For example, techniques which determine the relative importance of the individual subsystems of a model could be used to determine

whether or not a particular subsystem is a necessary part of the model. To this date, research into the analysis of model structure has been largely qualitative. Qualitative analysis, as contrasted with quantitative analysis, has consisted of the examination of the rationality of optimized model parameters. Having optimized a set of model parameters using a set of hydrologic data, the parameter values, and the computed output, are examined for correspondence to expectations. Thus, the qualitative analysis of the model structure, which is a necessary test of the concept, is subjective and "a posteriori."

A quantitative and more objective means of analyzing the structure of a model is needed. Such a technique would be more valuable if it could be performed prior to the optimization of the model parameters. Such a need was the motivation behind this study. The investigation into the problem was conducted with the following specific objectives:

1. To investigate the potential adequacy of the simple linear system representation of the rainfall-runoff process of individual storm events on small watersheds;
2. To investigate the possibility of determining model parameter values which are unique for any given watershed;
3. To identify factors which influence the computed value of the parameters of linear rainfall-runoff conceptual models;
4. Using empirically derived prediction equations, to investigate the possibility of adequately predicting model parameter values for ungaged watersheds;

5. To use the analytical definition of sensitivity to compute the sensitivity of model parameters;
6. To investigate the relationship between the sensitivity of model parameters and the ability of a model response function to represent the hydrologic response of a watershed.

The structure of a model determines the ability of the model to represent the rainfall-runoff process. Since the sensitivity of the model parameters depend on the structure of the model, the sensitivity can be used as a quantitative indicator of the model structure and as an indication of the ability of the model to represent the hydrologic response of a watershed. In Chapter VII the correspondence between model parameter sensitivity and regeneration capability will be detailed. Since the sensitivity of a model parameter depends on the values of the model parameters it would be helpful to examine the influence of various factors on the computed values of the model parameters. Chapter V is devoted to an investigation (using artificially generated data) of the influence of error present in the data on the computed model parameter values and of the need to consider the type of data to be analyzed when selecting a specific model structure for data analysis. One indication of the quality of a model is the ability of the model to represent the rainfall-runoff process. The analysis of hydrologic data in Chapter IV is an attempt to determine if the model structure is flexible enough to adequately reproduce observed hydrologic data. A more crucial test of a model is the ability of the model to predict storm runoff on ungaged

watersheds. The empirically derived prediction equations developed in Chapter VI are then an additional test of the flexibility of the model structure.

CHAPTER II

LITERATURE REVIEW

The transformation of precipitation to streamflow is a part of the hydrologic cycle which is of concern to many hydrologists. To date the level of knowledge concerning the various flow regimes and the relationship between each is not sufficient to provide a full quantitative description of the natural hydrologic system (2). This has led to the development and use of a multitude of models of varying complexity to represent the rainfall-runoff process. In order to simplify the transformation of precipitation to streamflow, the precipitation excess, the observed precipitation distribution minus the time distribution of losses, is often used as the input to the model representation of the watershed instead of the precipitation. Similarly, direct runoff, which is that portion of the total streamflow resulting from surface runoff and subsurface flow that flows rapidly into the stream channel network, is often separated from the total streamflow and used as the system output. Thus, "direct runoff" is the data used for evaluating model parameter values.

Representation of the Watershed as a System

Using precipitation excess data as input, the watershed is often represented by a "black box" system, a system for which the system response function is derived from measurements of system input and output without any assumptions about the internal form of the system. The output from the system representation of the watershed is the direct runoff. For a

system representation of the watershed (see Appendix B) the components and the relationships between components are usually represented by equations derived from empirical studies of the watershed processes. For example, the loss function has been represented by

$$L(t) = f_1 + (f_2 - f_1) e^{-Kt} \quad (2-1)$$

Precipitation and runoff are distributed both in time and space. Similarly, the watershed is spatially distributed and could be represented as such (3). The complexity of such spatially distributed and time-varying systems can be reduced by using single-valued, or lumped-sum, parameters to represent the distributed characteristics.

A watershed system can be classified by its properties (see Appendix C). The system representation can be classified as linear or nonlinear, static or dynamic, time-varying or time-invariant, lumped or distributed, deterministic or stochastic, etc. Models of relatively simple form are often linear, lumped and deterministic. Many models classified as linear, lumped, dynamic, and deterministic have been proposed and used to represent the transformation of rainfall to runoff. Such models, which are used exclusively in this study, were selected for study to avoid the problems which would arise in the examination of more complex models.

Conceptual Models

All models must maintain a balance between input, output and storage. That is, the law of conservation of mass must be obeyed. This law can be represented by the continuity equation

$$I - Q = dS / dt \quad (2-2)$$

where I, Q and S are the input, output and storage, respectively. The conceptual models used in this study obey the law of conservation of mass.

Conceptual models transform rainfall excess to direct runoff using elements which represent pure storage and translation. The conceptual models discussed herein consist of linear elements which serve to store and translate in time the distribution of excess rainfall. The linear elements used in the conceptual models are the linear channel, which serves to translate in time a given input function, and the linear reservoir, which serves to change the time distribution of an input function. The structure of a conceptual model is supposedly based on knowledge of the processes which transform rainfall to runoff. The linear elements are combined and described by a set of equations, and the parameters of the model are adjusted such that the model output is similar, as measured by a specified objective function, to the observed distribution of direct runoff.

Using a linear channel, each ordinate of the inflow hydrograph is delayed by the time of translation. The time delay does not change the time distribution of the inflow hydrograph $I(t)$ (see Fig. 2-1). Thus,

the output from a linear channel due to input $I(t)$ is $I(t - T)$, where T is the time of translation through the channel.

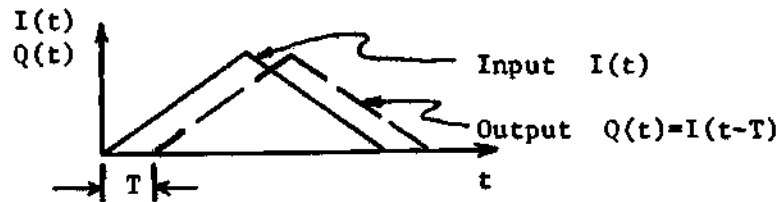


Figure 2-1. Linear Channel Action

While a linear channel involves the pure translation of inflow, the linear reservoir shows the effect of pure storage action. The pure storage action is represented by the equation

$$S = KQ \quad (2-3)$$

where S , Q and K are the storage, outflow and storage coefficient, respectively.

A single linear reservoir (SLR) model, which consists of a single linear storage element, was introduced by Zoch (4). The response of the SLR model to a constant input of finite duration T is given by

$$q_t = \begin{cases} 1 - e^{-t/K} & 0 \leq t \leq T \\ q_0 e^{-(t-T)/K} & T \leq t \leq \infty \end{cases} \quad (2-4)$$

where q_0 is the discharge at $t = T$ and K is the storage coefficient. For a unit impulse input function (see Appendix D) the SLR model response function is

$$q_t = (e^{-t/K}) / K \quad 0 \leq t \leq \infty \quad (2-5)$$

The outflow for any input function $I(t)$ can be determined using the convolution integral (see Appendix F)

$$Q(t) = \int_0^t I(\tau) U(t - \tau) d\tau \quad (2-6)$$

where $U(t)$ is the system response function and τ is a variable of integration.

The response function of a linear channel-linear reservoir (LCLR) model can be determined by using a time-area-concentration curve as the input to a single linear reservoir model. A time-area-concentration diagram can be derived (5) by dividing the watershed into subareas of equal travel time (the derivation of the time-area-concentration diagram will be discussed in more detail in Chapter IV). O'Kelly (6) represented the time-area-concentration diagram by a smooth geometric shape having a time base equal to the time of concentration, which was defined as the time of travel for a particle of water from the most remote part of the basin to the gaging station.

Using n linear reservoirs connected in series, each reservoir having the same storage coefficient K , Nash (7) derived the following system response function

$$h(t) = t^{n-1} e^{-t/K} / K^n \Gamma(n) \quad (2-7)$$

where n is the number of reservoirs, K is the value of the common storage coefficient and $\Gamma(n)$ is the gamma function. Nash (7,8) showed that the first moment about the origin of the response function equaled nK while the second moment about the center of area equaled nK^2 .

Holtan and Overton (9) and Overton (10) proposed using the Nash model, equation 2-7, with $n = 2$ as a model. The resulting response function

$$h(t) = te^{-t/K} / K^2 \quad (2-8)$$

can be determined by routing a unit impulse function through two linear reservoirs in series, each with an identical storage coefficient. The response function, equation 2-8, is called the double routing (DR) model.

Sensitivity Analysis

Parametric sensitivity is the effect on the output of a model caused by variation in the parameters of the model. According to Dawdy (11), "A valid field of research which is to date almost untouched is the methodology of developing and using sensitivity analysis for comparing different models . . ." The need for a sensitivity analysis of an optimum

solution has been expressed by others (12, 13, 14, 15).

One of the earliest and most complete investigations of the sensitivity of dynamic systems was reported by Tomovic (16). Tomovic was concerned with the stability of electronic systems, but introduced and applied the theoretical foundation of the dynamic and parametric nature of sensitivity. Specifically, Tomovic discussed how sensitivity coefficients, which were defined as the change in the solution of a differential equation for a change in the value of a coefficient of the differential equation, can be determined. Also, an equation, called the sensitivity equation, which relates the change in the system output to changes in the system parameters, was introduced and applied to electrical systems. Tomovic recognized that the sensitivity equation was inadequate in the design of dynamic systems and, thus, introduced the notion of inverse sensitivity analysis so that the tolerable level of parametric variation could be determined for a given model and a specified change in system performance. Tomovic applied the theoretical framework of sensitivity analysis to electronic systems.

The theoretical work of Tomovic (16) was restated and its application to the design of hydraulic systems was presented by Vemuri, et al. (15). The authors briefly discussed the computation of sensitivity coefficients for the following nonlinear ordinary differential equation

$$\frac{d^2x}{d\theta^2} + \psi \frac{dx}{d\theta} \left| \frac{dx}{d\theta} \right| + w^2x = f(\theta) \quad (2-9)$$

where θ , ψ and w are the dimensionless time, damping parameter and a constant, respectively, which occurs in the design of hydraulic systems. A solution to the problem for systems stimulated by random inputs was also briefly discussed.

Recognizing the variation of the interactions between the parameters of the Stanford Watershed Model, Crawford and Linsley (17) discussed the variation of parameters for different watershed conditions and input data. Analyses of the sensitivity of certain model parameters to variation in the input data and various watershed conditions resulted in recommendations for the estimation of initial values of these parameters. Specifically, a plot presented by the authors of discharge versus time for different levels of the parameter CC, a model parameter which governs the proportion of interflow, might enable a user of the model to make a more accurate initial estimate of the parameter value than would normally be made in the absence of such a plot. Such plots would also enable users to better estimate the magnitude of any necessary changes in numerical estimates of the parameters.

Recognizing the need for automatic parameter adjustment, Dawdy and O'Donnell (13) developed a simulation model, less complex than the Stanford Model, to test the feasibility of model parameter optimization. Using artificial data the authors investigated the sensitivity of the nine model parameters. The parameters were optimized using the Rosenbrock technique (18) and the objective function

$$U = \min \sum_{i=1}^n [Q_c(i) - Q_o(i)]^2 \quad (2-10)$$

where $Q_c(i)$ and $Q_o(i)$ are the i^{th} computed and observed storm hydrograph ordinates, respectively, and n is the number of ordinates. The model was also discussed by O'Donnell (19).

Lichty, et al. (14) proposed a model for simulating the surface-runoff component of a storm hydrograph. The model, which consisted of eight parameters, was optimized using the Rosenbrock technique (18) and the objective function U_3

$$U_3 = U_1 + 0.5 U_2 \quad (2-11)$$

where

$$U_1 = \min \sum [\log_e (\text{simulated peak}) - \log_e (\text{observed peak})]^2 \quad (2-12)$$

and

$$U_2 = \min \sum [\log_e (\text{simulated volume}) - \log_e (\text{estimated volume})]^2 \quad (2-13)$$

The sensitivity of the objective function to changes in the model parameters was used to evaluate the significance of the optimum solution and illustrate the interaction between individual parameters and groups of parameters. Sensitivity plots, objective function value versus the percent deviation of the parameter value from the optimum value, were used to show the sensitivity of the individual parameters.

Dawdy and O'Donnell (13) concluded that "any further development of automatic parameter optimization techniques must use some criterion of response sensitivity in selecting what can be considered adequately optimized parameters." DeCoursey and Snyder (20) recently used a technique involving parametric sensitivity for optimizing four hydrologic models. The technique partitions the total error, defined as the total difference between the individual observed and computed observations, by using estimates of parametric sensitivity as weighting functions. Principal components regression (see Appendix I) was used to partition the total error since the "independent variables" are usually not uncorrelated.

Critique and Motivation

It is apparent from the preceding review of the literature that several important factors concerning model sensitivity have not been considered. The most serious problem is the gap that exists between the theoretical developments of parametric sensitivity analysis and the use of such theory for the analysis of hydrologic models. The theoretical developments of Tomovic (16) provide a means of analyzing the sensitivity of a dynamic system representation of a watershed. Application of such theoretical developments is a first step towards understanding the potential usefulness of sensitivity analysis.

By nature sensitivity is both dynamic (see Appendix C) and parametric. In a hydrological context the dynamic nature of model parameter sensitivity has not been considered even though it has important hydrological implications. For example, if a model which can be used to

predict a storm hydrograph must be selected from several possible models the following sensitivity considerations are important. First, if the estimation of the peak discharge is of primary importance, and the rising and recession limbs of secondary importance, a model which is highly sensitive to parameter variation at the peak of the storm hydrograph might be preferred. Second, if each ordinate of the storm hydrograph is of equal importance then a model with uniformly distributed sensitivity might be preferable. Reasons for preferring high or low sensitivity will be discussed in detail as part of this study.

The parametric nature of sensitivity is also of importance. For multiparameter models the sensitivity of each parameter will usually depend on the numerical values of the other model parameters. Therefore, making general statements about the importance of any specific model parameter from the analysis of one set, or a few sets, of data can be misleading. Only by analyzing the entire parametric nature of sensitivity can general statements about parameter importance be made prior to using a model.

To date sensitivity analysis has been used primarily for identifying the model parameters which have the greatest influence on the output. Parameter sensitivity can also be used to compare the potential regeneration capability of different models, to determine which of several objective functions is the best estimator of the level of regeneration, and to indicate the effect on the output of various factors, such as data error (error introduced into the data during the collection or processing of the data) or the distribution of the input function.

Dawdy and O'Donnell (13) observed that the more sensitive model parameters approached the true parameter value (which were known to the authors since artificial data was used) after fewer rounds of optimization than did the less sensitive parameters. Although sensitivity can be defined as the change in output for a specified change in a parameter value there is an important implication of parametric sensitivity that accounts for the observations of Dawdy and O'Donnell (13). High sensitivity of the parameters of a response function implies better adjustment capability in the form of the response function. The concept of response function adjustment capability is important and shall be considered in more detail.

Parameter sensitivity, and thus the adjustment capability of the response function of a model, is related to the capability of a model to reproduce observed storm events and also to the effect of parametric error. To a certain point, increasing the sensitivity of a model will increase the likelihood of good reproduction of the observed output. But error contained in the data, error involved in the estimation of the model parameters and nonlinearity of the true hydrologic response of a watershed will induce larger error in the output of the more sensitive models. Thus, it is important to consider the "trade-off" that exists between increasing model sensitivity for the purpose of better output reproduction and the necessity to decrease the sensitivity in order to reduce the influence of the above mentioned sources of error. Identification of the exact nature of this "trade-off" might lead to an objective means of comparing models and to defining an optimum level of sensitivity.

The preceding paragraphs have briefly described the many facets of parametric sensitivity which will be developed and discussed in much greater depth as part of this study.

CHAPTER III

PREPARATION OF DATA

The purpose of this chapter is to detail the preparation of the hydrologic and physiographic data used in this study. Hydrologic and physiographic data were obtained from twenty watersheds and experimental plots. The area of the basins ranged in size from 0.243 acres to 2000 acres with fourteen of the twenty basins having areas less than fifteen acres. The basins are located in different parts of the continental United States, and thus, were subject to different meteorological conditions.

Hydrologic Data

Precipitation and runoff data were obtained from United States Department of Agricultural Reports (21, 22, 23). Hydrologic data were acquired only for storm events with hydrographs characterized by a single peak and well defined rising and recession limbs. The data as listed in the USDA Reports were reported at unequal time intervals. Using the assumption that the precipitation intensity remained constant over each recorded time interval, the recorded precipitation hyetograph was converted to an equal time interval hyetograph. The recorded storm hydrograph was converted to an equal time interval storm hydrograph by visually fitting a curve to the observed points on a mass curve and estimating the hydrograph ordinates at equal intervals of time. The time

interval selected depended on the storm length. All hydrographs analyzed contained at least five time intervals between the beginning of runoff and the hydrograph peak, and had a time base of at least twenty time intervals.

Determination of Precipitation Excess

Only that part of the precipitation which emerges as direct runoff was used in the derivation of model parameters. The remainder of the precipitation, which includes infiltration, evaporation, interception and temporary surface storage, is considered as losses. Since the volume of precipitation excess must equal the volume of direct runoff, it is necessary to compute the volume and estimate the time distribution of losses. Before estimating the loss function an initial abstraction of all precipitation occurring prior to the start of runoff was eliminated. The volume of losses was set equal to the difference in the volume of precipitation, after the elimination of the initial abstraction, and the volume of direct runoff. For this study the observed storm hydrograph was considered to be the distribution of direct runoff; that is, the distribution of base flow was considered negligible.

Infiltration is often the main source of loss. Studies (24) have indicated that the infiltration rate is a maximum at the start of precipitation and progressively decreases to a constant rate. But since it is difficult to estimate the infiltration rate at any time, the loss function is often taken to be constant. The phi-index method (25), or uniform loss function method, was used herein to estimate the true loss function.

Determination of the precipitation excess distribution was performed on a B5500 digital computer. Prior to computer computations the rainfall and runoff data were determined for equal intervals of time. The input to the computer program consisted of the equal time interval distributions of precipitation and direct runoff. The program eliminated the initial abstraction, i.e., all rainfall prior to the start of direct runoff, and determined the distribution of precipitation excess using the phi-index method. The distributions of precipitation excess and direct runoff were then available for analysis.

Physiographic Data

Hydrologic data were assembled only for basins for which adequate topographic maps were available. All the topographic maps showed the boundary and contour lines of the basin. The values of twenty-six topographic characteristics were determined for sixteen watersheds. The topographic characteristics measured (see Appendix J) included the watershed area, three hypsometric curve parameters, eleven slope parameters, and eleven parameters representing basin shape. The topographic parameters selected for use were used because land use and land condition data were not available and are usually not available. The method of computing each parameter is also given in Appendix J.

Use of Data

A total of twenty-six storm events from twenty watersheds were used in this study. Twenty-two of the storm events, storm events 1 through 22, were used in the development of prediction equations. The

remaining four storm events, E1, E2, E3 and E4, were used for storm hydrograph synthesis. That is, the storm characteristics of the four storm events were not used in the determination of prediction equation parameters. The names of the watersheds and the numbers of the storm events associated with the individual watersheds are given in Appendix K.

CHAPTER IV

ANALYSIS OF DATA FOR THE SELECTED CONCEPTUAL MODELS

Linear conceptual models have, in many instances, been used for hydrologic analysis and synthesis because the ease in computation is accompanied by an acceptable level of storm hydrograph regeneration. Because of their adjustment capability more complex simulation models may provide better prediction estimates. But simulation models, when compared with closed-form models, require more detailed computational algorithms and usually more input data which sometimes is not available. Since many conceptual models have been proposed, it is desirable to analyze and compare the ability of conceptual models to regenerate observed storm hydrographs.

Six conceptual models were analyzed for this study. The following models were selected for study: [1] the single linear reservoir model (SLR), [2] the single linear reservoir with feedback model (SLRWF), [3] the double routing model (DR), [4] the double routing with feedback model (DRWF), [5] the Nash model, and [6] the linear channel-linear reservoir model (LCLR). Two models, the Nash and LCLR models, are a function of two model parameters while the remaining four models depend only on the value of the storage coefficient K . The Nash model depends on a storage coefficient K and the number of storage elements n . The LCLR model is defined using parameters representing the basin time of concentration and the storage coefficient.

Two models containing feedback (see Appendix G) were developed for this study. Prior to this study the SLRWF and DRWF models have not been used for the prediction of storm runoff. They were developed to study the effect of feedback on model regeneration capability and model sensitivity. Although non-unity feedback could have been used for the models investigated herein only negative unity feedback was used.

The model parameters for each of the six conceptual models were estimated using the twenty-two storm events from sixteen basins. The model response function defined by such parameters were convolved with the observed precipitation excess. The regenerated storm output was then compared with the observed storm hydrograph to estimate the model regeneration capability.

Past investigators (26, 27, 28, 29) have indicated that the storm-to-storm variation is quite significant. Thus, for five basins included in this study each having two storm events analyzed, an average model parameter was computed for each of the five watersheds and the model regeneration capability measured.

Measurement of Model Regeneration Capability

Output regeneration is the process of convolving the distribution of precipitation excess and the computed model response function. The criterion function selected for measuring the regeneration capability of a model can be completely subjective, such as visual inspection, or somewhat more objective, such as a correlation coefficient or the error sum of squares. Naturally, the criterion function selected for such measurement will affect the results.

For this study, the correlation coefficient, defined as

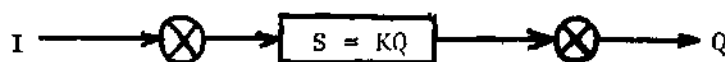
$$R = \frac{\sum_{i=1}^N Q_o(i) Q_c(i) - \left[\sum_{i=1}^N Q_o(i) \right] \left[\sum_{i=1}^N Q_c(i) \right]}{\left\{ \left[N \sum_{i=1}^N (Q_o(i))^2 - \left(\sum_{i=1}^N Q_o(i) \right)^2 \right] \left[N \sum_{i=1}^N (Q_c(i))^2 - \left(\sum_{i=1}^N Q_c(i) \right)^2 \right] \right\}^{1/2}} \quad (4-1)$$

was selected as the method of comparing the observed storm hydrograph, $Q_o(i)$, and the computed storm hydrograph, $Q_c(i)$. The special correlation coefficient and the integral square error have also been used (29) for this purpose. The sum of the squares of the differences between the computed and observed storm hydrographs could have also been used, and in some instances in this study, the error sum of squares values will be reported. Unfortunately, the "sum of squares" criterion is not invariant to changes in scale and thus, the magnitude of the criterion function does not reflect the regeneration capability when comparing storm hydrographs of different magnitudes. The correlation coefficient is commonly used to express the degree of association between samples of two variables which for this study are represented by two storm hydrographs. The ordinates of a storm hydrograph are serially correlated. Thus, the value of the correlation coefficient when comparing storm hydrographs will be comparatively higher. Since the correlation coefficient defined by equation 4-1 was not developed for comparison of serially correlated variables it would be best to consider the value of R only as a correlation index. Recognizing the limitation imposed by data which is serially

correlated, the correlation coefficient will be used as an index of the association between storm hydrographs. The value of the correlation coefficient varies from -1 to $+1$. A value near $+1$ indicates that the computed hydrograph closely approximates the observed storm hydrograph. A value of R near zero indicates that a relatively poor association between the hydrographs exists. The correlation coefficient is not a valid means of comparing storm hydrographs which differ in the volume of total runoff.

The Single Linear Reservoir Model

The single linear reservoir model is shown in block diagram (see Appendix B) form in Figure 4-1. For this model, and all other models



I = Input
 Q = Output
 K = Storage Coefficient
 S = Storage

Figure 4-1. Block Diagram of Single Linear Reservoir Model

investigated in this study, the storage in the channel system is represented by a hypothetical reservoir in which the storage in the reservoir is assumed to be linearly related to the outflow

$$S = KQ \quad (4-2)$$

where S is the storage, K is a storage coefficient, and Q is the outflow. Differentiating equation 4-2 and substituting the result into the hydrologic continuity equation

$$I - Q = dS / dt \quad (4-3)$$

where I is the input function, results in the differential equation

$$dQ / dt + KQ = KI \quad (4-4)$$

A solution to the differential equation can be determined using the Laplace Transform (see Appendix A for a discussion of the Laplace Transform). The Laplace Transform of equation 4-4 is

$$sQ(s) + KQ(s) = (s + K)Q(s) = KI(s) \quad (4-5)$$

where s is the complex variable ($s = j\omega$). Manipulation of equation 4-5 provides the transfer function, the ratio of the output $Y(s)$ to the input $X(s)$, of the single linear reservoir model

$$H(s) = Q(s) / I(s) = K / (s + K) \quad (4-6)$$

The inverse Laplace transform (also discussed in Appendix A) of the transfer function is the system response function. Thus,

$$L^{-1}[H(s)] = h(t) = (e^{-t/K}) / K \quad (4-7)$$

Since the model is linear, the output for any input function can be determined using the convolution integral (see Appendix F).

$$Q(t) = \int_0^t I(\tau)h(t - \tau)d\tau \quad (4-8a)$$

or

$$Q(t) = \sum_{\tau=0}^t I(\tau)h(t - \tau) \quad (4-8b)$$

Determination of Model Parameter

The response function of the single linear reservoir model is a function of the storage coefficient K and time t . Nash (7, 31) demonstrated that the storage coefficient, which has the units of time, is equal to the time interval T_L between the centers of mass of precipitation excess and direct runoff. Unfortunately, the rainfall-runoff process is not linear. The non-linearity of the watershed and variations in storm characteristics cause computed values of the time lag T_L to vary from storm to storm. This variation of the storage coefficient has been observed by others (32, 33). When the storage coefficient for the SLR model is estimated by the time lag the response function will be represented by SLR_1 .

Storage coefficient values can also be computed using the objective function

$$\min \sum_{i=1}^n [Q_o(i) - Q_c(i)]^2 \quad (4-9)$$

This objective function, which minimizes the sum of the squares of the deviations between the observed storm hydrograph $Q_o(i)$ and computed storm hydrograph $Q_c(i)$, is widely used (34) as a measure of the "best fit." SLR_2 will be used to represent the model where the storage coefficient has been determined using equation 4-9.

Results

Storage coefficient values for the twenty-two storm events were computed using the objective function of equation 4-9 and the time lag T_L computed from data. The computed values are given in Table 4-1. The computed parameter values were used to regenerate storm hydrographs and correlation coefficients were computed. The correlation values are also listed in Table 4-1. For fourteen of the twenty-two storm events the objective function of equation 4-9 provided higher correlation than the model with the storage coefficient set equal to the time lag T_L . When K was set equal to the time lag T_L only seven of the twenty-two storm events resulted in correlation above 0.90. Using equation 4-9 to determine K resulted in correlation coefficients exceeding 0.90 for eight storm events. Figures 4-2 and 4-3 show the storm hydrographs, computed and observed, for storm events 2 and 14, respectively. The graphs of the computed and observed storm hydrographs indicate that even a correlation coefficient 0.98 does not necessarily represent good regeneration. With a correlation coefficient of 0.969, the computed storm hydrograph for storm event 2, using the time lag value for the storage coefficient, has a peak discharge at least forty percent greater than the peak of the observed storm discharge. Lower correlation coefficients, as for example

Table 4-1. Regeneration for SLR Model

Storm Event	Storage Coefficient		Correlation Coefficient	
	$K=T_L$	K (Eq 4-9)	R (T_L)	R (Eq 4-9)
1	8.617	12.437	0.643	0.738
2	2.864	5.254	0.969	0.985
3	11.474	16.205	0.856	0.921
4	15.646	22.918	0.425	0.553
5	4.372	8.569	0.601	0.728
6	46.042	27.226	0.877	0.753
7	14.994	11.847	0.749	0.674
8	10.844	15.935	0.925	0.972
9	27.469	22.716	0.713	0.653
10	14.168	1.911	0.956	0.717
11	4.633	6.642	0.951	0.979
12	5.187	7.599	0.758	0.817
13	10.156	8.666	0.549	0.499
14	9.686	14.365	0.761	0.834
15	64.637	10.403	0.829	0.757
16	28.176	2.671	0.901	0.555
17	4.640	6.612	0.944	0.972
18	10.299	13.527	0.893	0.925
19	6.626	8.928	0.984	0.995
20	13.271	18.354	0.794	0.844
21	11.566	15.949	0.889	0.933
22	11.651	7.120	0.859	0.750

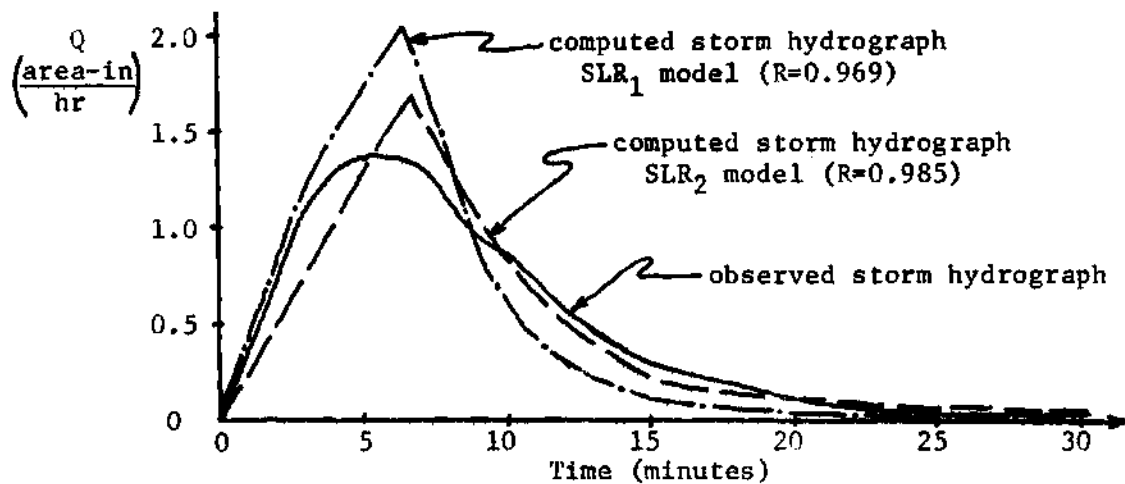


Figure 4-2. Regeneration of Storm Event 2 Using SLR Models

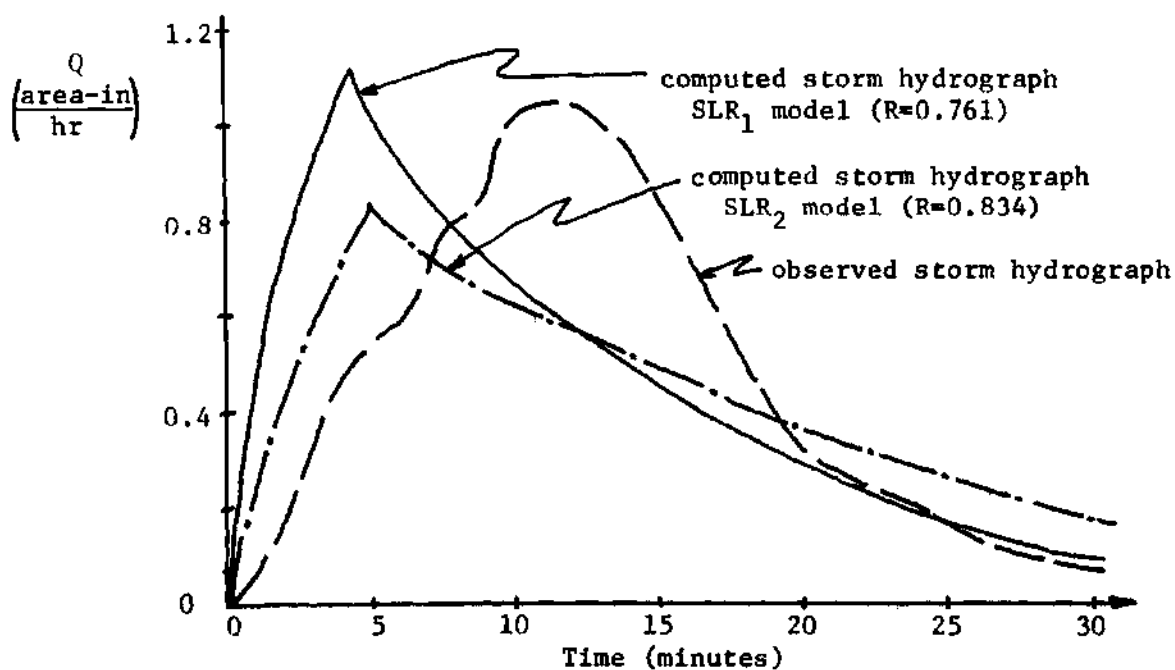


Figure 4-3. Regeneration of Storm Event 14 Using SLR Models

The inverse Laplace transform of the transfer function yields the model response function

$$h(t) = (e^{-t/2K}) / K \quad (4-12)$$

Determination of Model Parameter

The storage coefficient for the SLRWF model was determined using the objective function given by equation 4-9. The resulting parameter values are given in Table 4-2.

Results

Using the computed model parameters the storm hydrographs were regenerated. The resulting correlation coefficients are given in Table 4-2. The correlation coefficients indicate that the SLRWF model is not capable of providing a good representation of the watershed response. Only two storm events were regenerated with correlation greater than 0.94, and the correlation coefficient was less than 0.50 for four of the twenty-two storm events.

The Nash Model

The conceptual model proposed by Nash (7) consists of n linear reservoirs each having a storage coefficient K . The response function of the Nash Model is given by

$$h(t) = t^{n-1} e^{-t/K} / K^n \Gamma(n) \quad (4-13)$$

Table 4-2. Regeneration for SLRWF Model

Storm Event	Storage Coefficient	Correlation Coefficient
1	16.192	0.622
2	4.790	0.953
3	20.632	0.830
4	30.710	0.418
5	10.899	0.655
6	45.470	0.693
7	18.810	0.589
8	18.520	0.893
9	39.534	0.604
10	1.625	0.960
11	5.821	0.879
12	9.460	0.737
13	16.745	0.487
14	19.182	0.759
15	5.749	0.740
16	2.638	0.553
17	7.681	0.915
18	17.695	0.864
19	9.678	0.948
20	24.013	0.771
21	20.248	0.860
22	1.403	0.705

where $\Gamma(n)$ is the gamma function with argument n . The response function is a function of the two model parameters, K and n , and time t .

Determination of Model Parameters

Nash (31) proposed equating the model parameters, K and n , to the first and second moments of the precipitation excess and direct runoff distributions. Specifically, Nash derived the equations

$$nK = M_{10} - M_{1I} \quad (4-14)$$

$$n(n+1)K^2 = M_{20} - M_{2I} - 2nKM_{1I} \quad (4-15)$$

where M_{10} is the first moment of the direct runoff hydrograph, M_{1I} is the first moment of the precipitation excess hyetograph, M_{20} is the second moment of the direct runoff hydrograph, and M_{2I} is the second moment of the precipitation excess hyetograph. Parameter values computed from equations 4-14 and 4-15 have resulted in good ("good" being defined as correlation coefficients greater than 0.90) storm hydrograph regeneration on watersheds larger than five square miles (29). A preliminary investigation using equations 4-17 and 4-18 of five storm events resulted in small negative values for the model parameters. Negative values of the storage coefficients, which caused negative values of n , occur because the center of mass of direct runoff occurs before the center of mass of precipitation excess. To provide consistency in model parameter derivation, the objective function of equation 14-9 was used to compute the model parameters instead of equations 4-14 and 4-15. Since there is no

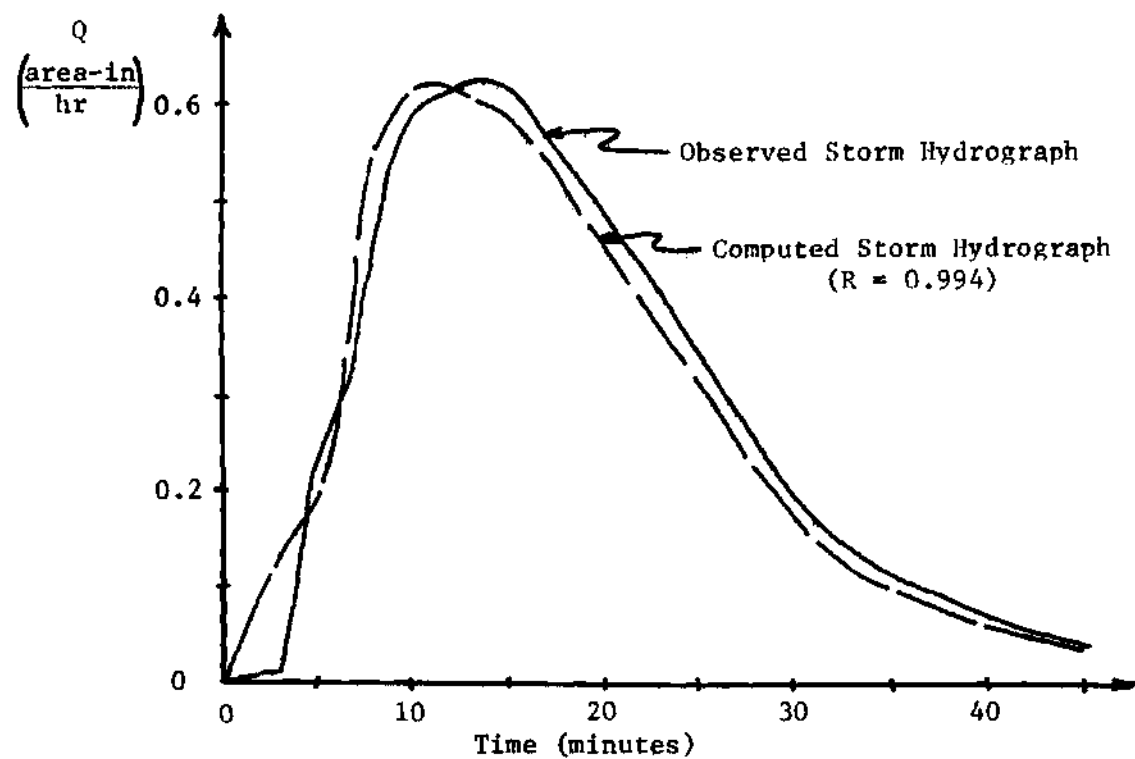


Figure 4-5. Nash Model Regeneration of Storm Event 8

theoretical basis for determining the number of reservoirs, the storage coefficient K was set equal to the time lag T_L and the value of n was determined using equation 4-9. The computed parameter values are given in Table 4-3.

Results

The correlation coefficients resulting from the hydrograph regeneration indicate that the Nash model is capable of comparatively good regeneration. The correlation coefficient for the regenerated storm hydrographs are given in Table 4-3. Of the twenty-two storm events the Nash model provided correlation coefficients greater than 0.98 for five events while only three storm events resulted in values less than 0.90. Figure 4-5 shows the regenerated hydrograph for storm event 8. Even for a comparatively high correlation coefficient of 0.994, the observed and regenerated hydrographs have noticeable differences. The peak discharges differ in magnitude by approximately 1 percent but the peak of the regenerated hydrograph occurs two minutes before the peak of the observed hydrograph.

Double Routing Model

The double routing model consists of two linear reservoirs in series. Each reservoir is governed by a storage coefficient K . The block diagram of the DR model is shown in Figure 4-6. The precipitation excess

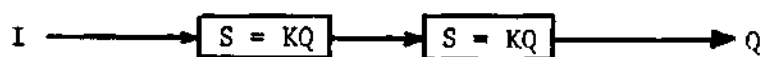


Figure 4-6. Block Diagram Representation of Double Routing Model

input is routed through the first linear reservoir. The output from the first reservoir is used as the input to the second linear reservoir. The output from the second reservoir represents the direct runoff.

The DR model response function can be derived using the storage equation, equation 4-2, and the continuity equation, equation 4-3. Equation 4-16 is the transfer function of the double routing model.

$$Q(s) = \frac{(1/K)^2}{(s + 1/K)^2} \quad (4-16)$$

The inverse Laplace transform of equation 4-16 yields the following response function of the DR model

$$h(t) = t e^{-t/K} / K^2 \quad (4-17)$$

The double routing model is a special case of the Nash model. Thus, by setting $n = 2$ in equation 4-13, the response function of the DR model can be determined.

Derivation of Model Parameter

Holtan and Overton (9) suggested that the storage coefficient could be estimated by one-half the time lag T_L . The model response function would then be

$$h(t) = 4 t e^{-2t/T_L} / T_L^2 \quad (4-18)$$

Table 4-3. Regeneration for Nash Model

Storm Event	Storage Coefficient (K)	Number of Reservoirs (n)	Correlation Coefficient (R)
1	8.617	1.386	0.903
2	2.864	1.238	0.953
3	11.474	1.291	0.972
4	15.646	1.503	0.816
5	4.372	1.368	0.935
6	46.042	1.800	0.969
7	14.994	1.235	0.975
8	10.844	1.271	0.994
9	27.469	1.183	0.911
10	14.168	1.273	0.944
11	4.633	1.208	0.981
12	5.187	1.258	0.889
13	10.156	1.279	0.777
14	9.686	1.348	0.941
15	64.637	1.163	0.969
16	28.176	1.531	0.901
17	4.640	1.132	0.985
18	10.299	1.237	0.966
19	6.626	1.077	0.933
20	13.271	1.279	0.941
21	11.566	1.263	0.980
22	11.651	1.036	0.904

It was also suggested by Holtan and Overton (9) that the storage coefficient could be estimated from the recession limb of the observed hydrograph. This seems reasonable if the storage coefficient is assumed only to represent storage depletion. For this study, the storage coefficient was determined using the objective function, equation 4-9, which minimizes the sum of the squares of the differences between the observed and computed hydrographs.

Results

The model parameters computed using equation 4-12 and the resulting correlation coefficients are given in Table 4-4. The double routing model consistently provided higher correlation coefficients than the other models investigated and only three correlation coefficients were less than 0.900. The DR model provided correlation coefficients greater than 0.98 for seven storm events and an additional two storm events resulted in correlation coefficients greater than 0.975. Figure 4-7 shows the observed and computed storm hydrographs for storm event 8. The double routing model provides a correlation coefficient of 0.981 for storm event 8. The model reproduces the peak in time but in magnitude there is almost a five percent difference. The rising limb of the observed storm hydrograph is accurately reproduced, but considerable differences exist in the recession limb.

Double Routing with Feedback Model

The block diagram representation of the double routing with feedback (DRWF) model is given in Figure 4-8. The model consists of two

Table 4-4. Regeneration for Double Routing Model

Storm Event	Storage Coefficient (K)	Correlation Coefficient (R)
1	4.645	0.937
2	1.796	0.930
3	6.489	0.975
4	9.095	0.840
5	2.554	0.958
6	13.714	0.934
7	6.127	0.934
8	6.356	0.981
9	11.059	0.895
10	5.423	0.944
11	2.530	0.981
12	2.773	0.920
13	4.404	0.790
14	5.373	0.977
15	22.279	0.937
16	13.714	0.928
17	2.484	0.986
18	5.518	0.986
19	3.584	0.983
20	6.604	0.985
21	6.354	0.995
22	4.160	0.916

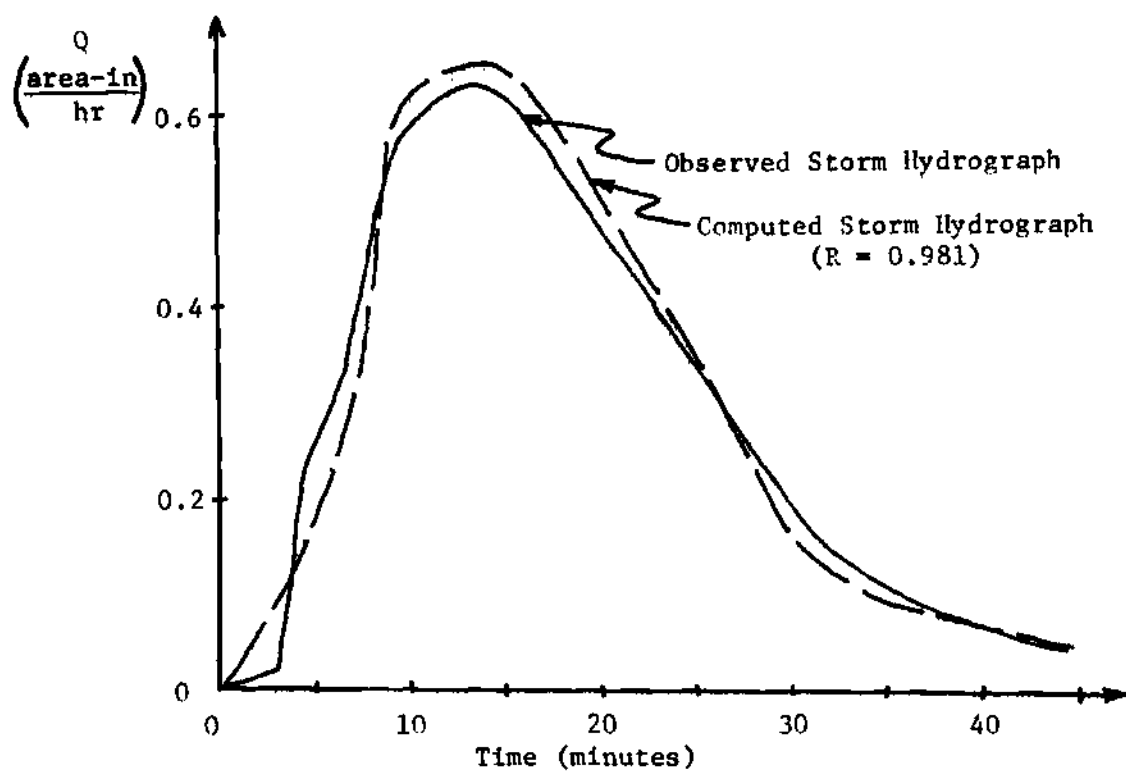
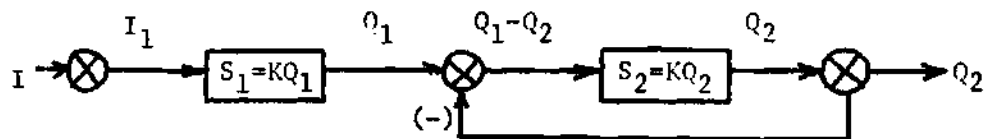


Figure 4-7. Double Routing Model Regeneration of Storm Event 8



I = System Input	S_1 = Storage in First Reservoir
I_1 = Input to First Reservoir	S_2 = Storage in Second Reservoir
Q_1 = Output from First Reservoir	K = Storage Coefficient
Q_2 = Output from Second Reservoir	

Figure 4-8. Block Diagram Representation of the DRWF Model

linear reservoirs each regulated by a storage coefficient K and a feedback loop around one of the storage elements. For the configuration shown in Figure 4-8, the input to the model is routed through the first reservoir. The input to the second reservoir is the difference between the output from the first reservoir and the output from the second reservoir. The transfer function of the SLR model is identical to the transfer function of the first reservoir in the DRWF. The input to the second reservoir is then given by

$$I_2 = Q_1 - Q_2 \quad (4-19)$$

Using the storage equation, equation 4-2, and the continuity equation, equation 4-3, the following differential equation can be derived to represent the DRWF model

$$Q_1 - 2Q_2 = K \, dQ_2/dt \quad (4-20)$$

Taking the Laplace transform of equation 4-20 and substituting equation 4-6 into the result yields the transfer function of the DRWF model

$$h_2(s) = (1/K)^2 / [(s + 1/K) (s + 2/K)] \quad (4-21)$$

The system response function of the DRWF model is

$$h(t) = t(e^{-t/K} - e^{-2t/K}) / K^2 \quad (4-22)$$

and is derived by finding the inverse Laplace transform of equation 4-21.

Derivation of Model Parameter

The value of the storage coefficient was determined using the objective function of equation 4-9. The computed parameter values are given in Table 4-5.

Results

The correlation coefficients for the regenerated storm hydrographs are given in Table 4-5. The correlation coefficient for five of the twenty-two storm events was less than 0.900. But only six events had correlation coefficients greater than 0.95 and not one correlation coefficient exceeded 0.98 which indicates that for those events analyzed the DRWF model is not capable of regenerating storm hydrographs as well as the DR model.

Linear Channel-Linear Reservoir Model

In addition to linear storage elements, linear systems can include

Table 4-5. Regeneration for DRWF Model

Storm Event	Storage Coefficient (K)	Correlation Coefficient (R)
1	5.059	0.900
2	1.722	0.942
3	6.666	0.943
4	9.692	0.721
5	2.628	0.939
6	17.260	0.907
7	7.932	0.918
8	6.064	0.968
9	14.127	0.867
10	7.225	0.945
11	2.671	0.971
12	3.068	0.893
13	5.914	0.767
14	5.871	0.932
15	29.704	0.931
16	18.807	0.929
17	2.572	0.977
18	5.866	0.959
19	3.509	0.979
20	7.030	0.949
21	6.565	0.969
22	5.229	0.889

linear time delay elements. In hydrologic systems theory the time delay element is called a linear channel. The time delay element, or linear channel, serves only as a time delay and does not alter the distribution of the function being routed through it. The linear channel-linear reservoir model consists of a linear storage element in series with a linear time delay element.

Dooge (5) divided the watershed into sub-basins of equal travel time to the gage point. Using the contours, or isochrones, of these sub-basins, an area-distance diagram, length of the contours versus the distance from the gaging station, was derived. The area-distance diagram can be converted to an area-time diagram if the distance-time relationship is known or can be assumed. For the cases presented herein distance was assumed to be proportional to time. The time-area-concentration diagram is determined by dividing the ordinates of the area-time diagram by the total area of the watershed. The time-area-concentration diagram $A(t)$ is defined by

$$A(t) = \begin{cases} (1/A) \, dA/dt & 0 \leq t \leq T \\ 0 & \text{otherwise} \end{cases} \quad (4-23)$$

where A is the total area of the basin and has the property

$$\int_0^{\infty} A(\tau) d\tau = \int_0^{T_c} A(\tau) d\tau = 1 \quad (4-24)$$

where T_c is the time of flow from the most remote part of the basin.

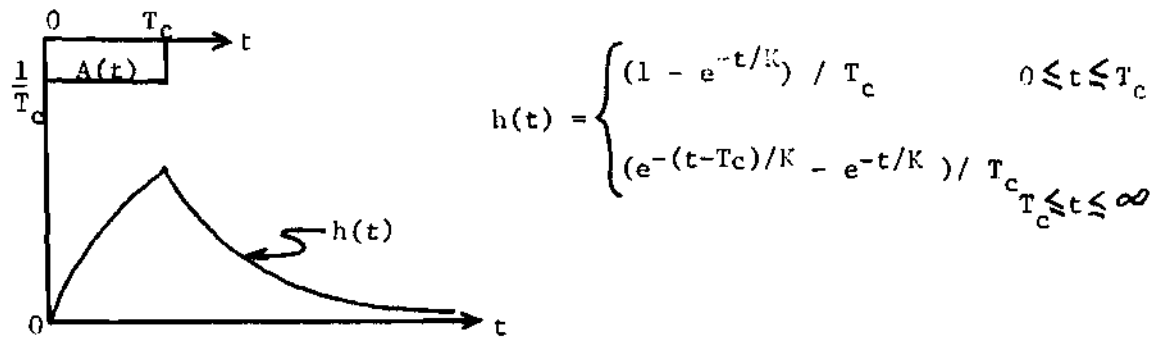
If a time-area-concentration diagram is routed through a linear reservoir with storage coefficient K , the resulting model response function is

$$h(t) = \int_0^{t \wedge T_c} (1/K) e^{-(t-\tau)/K} A(\tau) d\tau \quad (4-25)$$

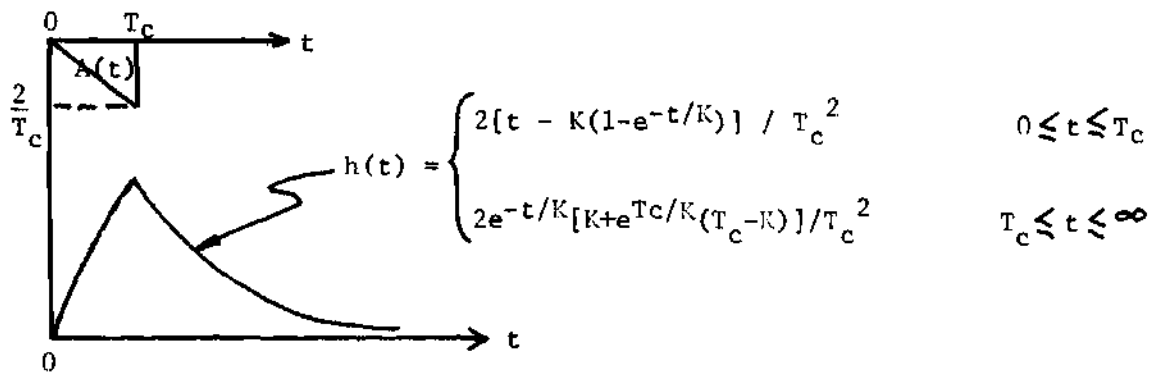
O'Kelly (6) and Dooge (5) investigated such linear conceptual models. Though each watershed has a characteristic time-area-concentration diagram it is difficult to determine. Based on the assumption that the watershed smoothes the input function, O'Kelly (6) replaced the true time-area-concentration diagram with various geometric shapes. O'Kelly and other investigators (27, 29) have used rectangular, triangular and parabolic shapes.

For this study, a rectangular (LCLR-R) and two triangular shaped (LCLR-LT and LCLR-RT) time-area-concentration diagrams were investigated. The system response functions for the three diagrams are given in Table 4-6. Each model response function $h(t)$ is a function of the storage coefficient K , the time of concentration T_c and time t . Sarma (29) observed four inherent characteristics of the LCLR models:

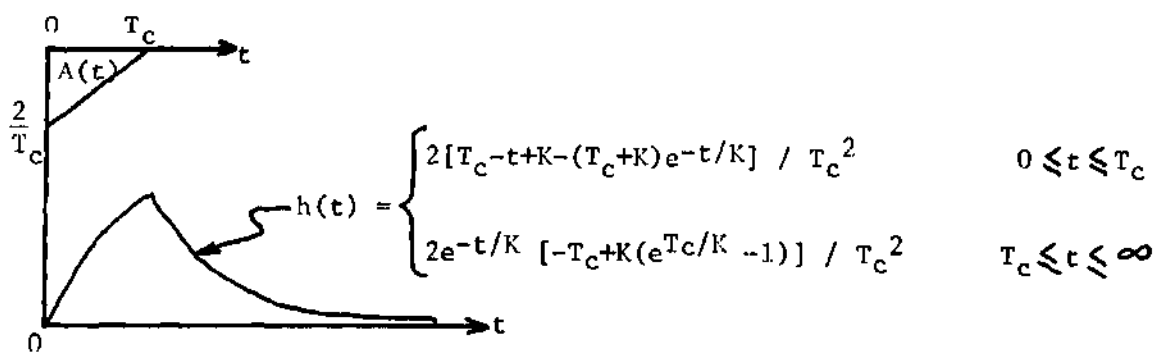
1. the shape of the system response function changes with the ratio K/T_c ;
2. the peak of the system response functions for the three LCLR models investigated herein differ little for a given value of K/T_c ;



(a) LCLR-R Model



(b) LCLR-RT Model



(c) LCLR-LT Model

Table 4-6. System Response Functions of the LCLR Models

3. the magnitude of the peak discharge of the system response functions increase for decreasing values of K/T_c ;
4. the time-to-peak of the three LCLR model response functions decrease with decreases in the ratio K/T_c .

Derivation of Model Parameters

The model response functions depend on the value of the storage coefficient K and the time of concentration. The time lag T_L was used as an estimate of the storage coefficient. The time of concentration was estimated by minimizing the sum of the squares of the deviations, equation 4-9, between the computed and observed hydrographs.

The time of concentration, defined as the time required for the runoff due to an instantaneous input to arrive at the gage point from the most remote part of the basin, is difficult to measure for large basins. Snyder (35) suggested using the time from the end of the excess rainfall to the point of inflection on the recession limb of the storm hydrograph. Clark (36) suggested using the time from the end of the excess rainfall to the time at which the rate of discharge decrease is greatest with respect to the discharge at that time. A preliminary investigation as part of this study indicated that neither the Snyder nor the Clark estimates of T_c would provide good results. In some instances, the computed times of concentration were negative. Sarma (29) also noted some inconsistencies when using these methods of estimating T_c .

Results

Table 4-7 lists the computed values of T_c and the correlation coefficients for the three LCLR models investigated in this study. The values of the storage coefficients, which are equal to T_L , are given in Table 4-1. In general, the results indicate that the LCLR models investigated herein are not capable of accurately regenerating the observed storm hydrographs. The correlation coefficient values indicate that no one of the three LCLR models is more capable of superior regeneration than any of the other LCLR models. Each model resulted in seven storm events with correlation coefficients with less than 0.90, and only for two storm events did the correlation coefficient exceed 0.98.

Comparative Evaluation of Conceptual Models

One means of comparing the conceptual models investigated herein is by the computed correlation coefficients. In Chapter VII the models will be compared through sensitivity analysis. Table 4-8 lists the correlation coefficients for six of the models investigated herein. The SLR_1 model with the storage coefficient set equal to the time lag T_L was not included since an analysis of Table 4-1 indicates that it, in general, does not provide output regeneration as good as the SLR_2 model, which uses equation 4-9 to determine the storage coefficient. Also, the LCLR-R and LCLR-LT models were not included in Table 4-8 because the three LCLR models provide almost identical results.

Table 4-9 summarizes the ranks of the correlation coefficient. The highest correlation coefficient is given a rank of one. Progressively lower ranks are associated with correspondingly lower correlation

Table 4-7. Regeneration for LCLR Models

Storm Event	K*	LCLR-R		LCLR-LT		LCLR-RT	
		T _c	R	T _c	R	T _c	R
1	8.617	1.167	0.795	1.121	0.778	1.207	0.815
2	2.864	0.853	0.953	0.893	0.953	0.819	0.953
3	11.474	1.023	0.919	1.014	0.917	1.035	0.921
4	15.646	1.136	0.540	1.097	0.529	1.172	0.555
5	4.372	0.887	0.871	0.916	0.871	1.140	0.923
6	46.042	1.860	0.954	1.876	0.954	1.841	0.954
7	14.994	1.566	0.948	1.639	0.948	1.460	0.948
8	10.844	0.944	0.967	0.958	0.967	0.932	0.967
9	27.469	1.923	0.858	1.927	0.858	1.916	0.858
10	14.168	1.316	0.959	1.366	0.959	1.249	0.959
11	4.633	1.031	0.979	1.055	0.978	0.987	0.978
12	5.187	1.079	0.866	1.058	0.860	1.103	0.874
13	10.156	12.000	0.900	15.037	0.919	10.000	0.897
14	9.686	1.031	0.853	0.993	0.850	1.069	0.860
15	64.637	3.000	0.955	3.171	0.955	2.851	0.955
16	28.176	2.223	0.930	2.511	0.930	2.000	0.930
17	4.640	0.971	0.982	1.005	0.982	0.943	0.982
18	10.299	1.026	0.936	1.018	0.935	1.038	0.935
19	6.626	0.953	0.993	0.975	0.993	0.932	0.993
20	13.271	1.041	0.872	1.003	0.868	1.075	0.880
21	11.566	0.983	0.940	0.996	0.940	1.016	0.941
22	11.651	3.851	0.937	3.839	0.925	3.823	0.942

*The value of the storage coefficient is common to all three LCLR models

Table 4-8. Summary of Correlation Coefficients for Six Models

Storm Event	SLR ₂	SLRWF	DR	DRWF	Nash	LCLR-RT
1	.738	.622	.937	.900	.903	.815
2	.985	.953	.930	.942	.953	.953
3	.921	.830	.975	.943	.972	.921
4	.553	.418	.840	.721	.816	.555
5	.728	.655	.958	.939	.935	.923
6	.753	.693	.934	.907	.969	.954
7	.674	.589	.934	.918	.975	.948
8	.972	.893	.981	.968	.994	.967
9	.653	.604	.895	.867	.911	.858
10	.717	.960	.944	.945	.944	.959
11	.979	.879	.981	.971	.981	.978
12	.817	.737	.920	.893	.889	.874
13	.499	.487	.790	.767	.777	.897
14	.834	.759	.977	.932	.941	.860
15	.757	.740	.937	.931	.969	.955
16	.555	.553	.928	.929	.901	.930
17	.972	.915	.986	.977	.985	.982
18	.925	.864	.986	.959	.966	.938
19	.995	.948	.983	.979	.993	.993
20	.844	.771	.985	.949	.941	.880
21	.933	.860	.995	.969	.980	.941
22	.750	.705	.916	.889	.904	.942

Table 4-9. Comparison of Regeneration by Rank

Rank	SLR ₂	SLRWF	DR	DRWF	Nash	LCLR-RT
1	2	1	11	0	6	3
2	0	1	4	4	9	6
3	2	0	4	8	5	1
4	1	0	2	7	2	11
5	16	0	0	3	0	1
6	1	20	1	0	0	0

coefficients. The lowest correlation corresponds to a rank of six. When two models have the same correlation coefficient values they are listed as having the same rank. The model exhibiting the next lower correlation is given the rank it would have received if the two models of equal correlation had not had identical correlation. For example, in storm event 3, the SLR and LCLR-RT models resulted in identical correlations of 0.921. Since the DR, Nash and DRWF provided better correlation, the LCLR-RT and SLR models have a rank of 4. Thus, no model has a rank of 5. The SLRWF model, with the lowest correlation, is given a rank of 6.

Table 4-9 indicates that for eleven of the twenty-two storm events, the DR model had the best, or equaled the best, correlation. The Nash model also provided good correlation and ranked "one" for six storm events. For storm event 11 the DR and Nash model provided identical correlations of 0.981. The Nash model ranked second to the DR model. The Nash model had a rank of 2 for nine storm events. For eleven of the twenty-two storm events, the LCLR-RT model ranked 4. The SLR₂ and SLRWF models provided comparatively poor regeneration. The SLR₂ model ranked 5 for sixteen storm events and in all except three cases, the SLRWF model provided the worst correlation. To use the "rank" system as a means of comparative evaluation can be misleading. For example, for storm event 2 the DR model ranked 6 with a correlation coefficient of 0.930. But in five of the twenty-two storm events the highest correlation was equal to or less than the 0.930 value. Thus, although the "rank" system provides a means for comparing the output regeneration capability of conceptual models, it is necessary to look at the individual values of the correlation

coefficients to determine the quality of regeneration.

Intuitively, one would expect the two-parameter models, each model having two degrees of freedom, to fit better than the models having one parameter, and thus, one degree of freedom. But it is evident from Table 4-8 and Table 4-9 that the two-parameter models were not, in general, capable of providing better regeneration than the one-parameter models. Such results occur because the value of one of the parameters of the two-parameter models is set prior to optimization of the other parameter value. This reduces the flexibility of the two-parameter models.

The figures presented in this chapter were selected to purposely show the regeneration for various correlation values. It is evident that a comparatively high correlation may not indicate an acceptable level of regeneration. For example, even with a correlation of 0.969 (see Figure 4-2), the computed peak discharge is at least forty percent greater than the observed storm hydrograph peak. This is unacceptable regeneration for any hydrologic purpose. But for eleven of the twenty-two storm events the model having the highest correlation has a correlation coefficient equal to or less than 0.969. Thus, in general, for storm events and watersheds similar to those investigated herein, the conceptual models investigated in this study are not capable of adequate output regeneration.

Unique Parameter Values for a Watershed

Past investigations (28, 29) have concluded that the storm-to-storm variation of computed model parameter values is of such significance

that a unique parameter value for a given watershed is not possible. That is, regeneration of several storm events using a parameter value averaged from the parameter values computed for the individual storm events has not provided acceptable output regeneration. Ten storm events from five watersheds were used to determine if the use of average watershed parameter values resulted in a significant reduction in the quality of output regeneration.

The average parameter value was computed for the two storm events on each of five watersheds. For the Nash model both the storage coefficient K and the number of storage elements n were averaged. The average parameter values were then used to regenerate the ten storm hydrographs. Table 4-10 lists the correlation coefficients and Table 4-11 lists the standard error estimates for both the individual and averaged parameter values. In general, the standard error values indicate that the averaged watershed parameter values are not capable of providing output regeneration which is better than that resulting from the optimized parameter values. The average standard error for the five models defined by the optimized parameter values was 0.507. Use of the averaged parameter values resulted in an average standard error of 0.551. The correlation coefficients resulting from use of the optimized parameter values exceeded 0.9 for 52 percent of the cases and had an average value of 0.872. The correlation coefficients resulting from use of the averaged parameter values exceeded 0.9 for 38 percent of the cases and had a mean value of 0.816. The DR model provided, in general, the best output reproduction when the response function was defined by the averaged parameter value.

Table 4-10. Correlation Coefficients Resulting from
Joint Parameter Regeneration

Storm Event	SLR		SLRWF		DR		DRWF		Nash	
	I*	J**	I	J	I	J	I	J	I	J
1	0.738	0.651	0.622	0.447	0.937	0.823	0.900	0.675	0.903	0.746
2	0.980	0.918	0.953	0.980	0.930	0.797	0.942	0.883	0.953	0.854
9	0.653	0.410	0.604	0.334	0.895	0.773	0.867	0.747	0.911	0.874
10	0.717	0.944	0.960	0.923	0.944	0.936	0.945	0.943	0.944	0.898
11	0.979	0.982	0.879	0.970	0.981	0.954	0.971	0.969	0.981	0.951
13	0.499	0.454	0.487	0.330	0.790	0.652	0.767	0.580	0.777	0.677
19	0.995	0.968	0.948	0.995	0.983	0.921	0.979	0.978	0.993	0.943
20	0.844	0.800	0.771	0.665	0.985	0.952	0.949	0.849	0.941	0.887
21	0.933	0.888	0.860	0.668	0.995	0.986	0.969	0.944	0.980	0.970
22	0.750	0.858	0.705	0.662	0.916	0.957	0.899	0.921	0.904	0.919

*Correlation coefficient for optimized parameter values

**Correlation coefficient for averaged parameter values

Table 4-11. Standard Error Values Resulting from
Joint Parameter Regeneration

Storm Event	SLR		SLRWF		DR		DRWF		Nash	
	K*	L**	K	L	K	L	K	L	K	L
1	0.468	0.510	0.648	0.679	0.258	0.388	0.571	0.613	0.368	0.449
2	0.097	0.187	0.192	0.256	0.202	0.269	0.256	0.300	0.145	0.226
9	0.820	0.850	0.918	0.931	0.779	0.790	0.903	0.907	0.805	0.812
10	0.608	0.736	0.632	0.867	0.764	0.776	0.895	0.900	0.799	0.824
11	0.177	0.199	0.604	0.665	0.173	0.266	0.665	0.715	0.212	0.388
13	1.498	1.499	1.532	1.534	1.478	1.481	1.523	1.526	1.491	1.492
19	0.060	0.183	0.315	0.352	0.136	0.217	0.330	0.357	0.071	0.201
20	0.031	0.035	0.048	0.050	0.010	0.022	0.040	0.042	0.022	0.027
21	0.178	0.233	0.373	0.429	0.055	0.126	0.330	0.333	0.111	0.123
22	0.515	0.525	0.601	0.603	0.503	0.508	0.601	0.601	0.537	0.537

*Standard error for optimized parameter values

**Standard error for averaged parameter values

The Nash, SLR, DRWF and SLRWF models provided progressively poorer output reproduction. Since the relationship between the parameter values is not linear an increase in the standard error is not necessarily accompanied by a decrease in the correlation coefficient.

In order to determine if the average decrease in correlation (from 0.872 to 0.816) and the average increase in standard error (from 0.507 to 0.551) is hydrologically significant, two storm hydrograph characteristics were selected for comparison. The average percent error in the magnitude of the peak discharge

$$E_q = \sum_{j=1}^M \left(\sum_{i=1}^N |Q_{po} - Q_{pc}| / Q_{po} \right) / (M \times N) \quad (4-26)$$

where M and N are the number of models and number of storm events included in the analysis, respectively, and Q_{po} and Q_{pc} are the observed and computed peak discharges, respectively, and the average percent error in the time of the peak discharge

$$E_t = \sum_{j=1}^M \left(\sum_{i=1}^N |t_{po} - t_{pc}| / t_{po} \right) / (M \times N) \quad (4-27)$$

were determined for both the averaged and optimized parameter values.

E_t and E_q were used as a means of estimating the effect of using the averaged parameter values. Values of E_q of 31 percent and E_t of 27 percent resulted when the output generated using the optimized parameter values was compared with the observed output. Comparison of the output

generated using the averaged parameter values with the observed output produced values of E_q and E_t of 24.5 percent and 30 percent, respectively. The comparison of E_q and E_t values indicate that the changes in correlation and the standard error are not significant. Of the ten storm events analyzed only two did not occur during the period from June 16 to July 17. Thus, the watershed conditions and storm type might be similar for the storm events included in the analysis. Such similarity could be responsible for the apparent lack of hydrologic difference between using the optimized and averaged parameter values. But the correlation coefficient and the standard error measure the difference between observed and computed storm hydrographs over the entire time distribution of the hydrograph. The values of E_q and E_t depend only in the differences at the storm hydrograph peaks. Since the model response functions are more sensitive at the peak they provide better regeneration of the peak discharge (see Chapter VII for a complete discussion of sensitivity). Thus, the values of E_q and E_t should provide a more favorable indication of the ability of averaged parameter values to predict output than would either the correlation coefficient or the standard error.

Figure 4-9 shows that the SLRWF model defined by the optimized parameter value reproduced the rising and recession limbs more accurately than the same model defined by the averaged parameter value. Both the optimized and average parameter values resulted in a twelve percent error in reproducing the magnitude of the observed peak discharge but the time-to-peak occurred one minute sooner than the

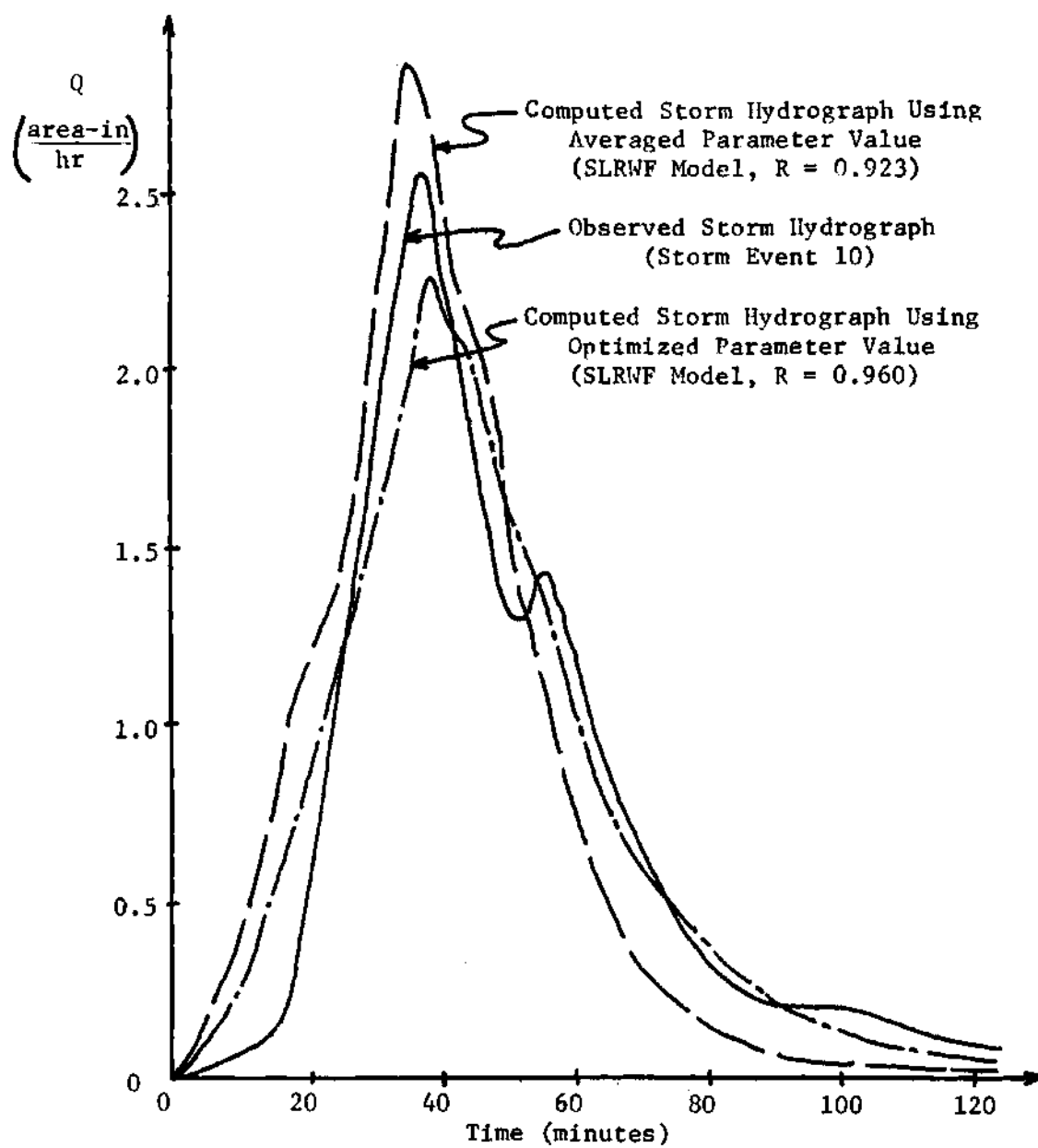


Figure 4-9. Regeneration Using Averaged Parameter Values

observed peak when the averaged parameter value was used.

Analysis of Results

The poor correlation between the observed storm hydrographs and the model-generated storm hydrographs indicates that the conceptual models investigated are not capable of consistently providing good estimates of the hydrologic response of watersheds. The functional representation of the model limits the ability of a response function to represent the hydrologic response of a watershed. Such a limitation could account for the inadequate regeneration provided by the conceptual models used in this study. Furthermore, the fact that no one model provided consistently better regeneration of observed storm hydrographs indicates that each observed storm hydrograph dictates which model is most capable of providing accurate reproduction of that observed hydrograph. The effect of the constraining shape of the model response functions will be investigated in Chapter V.

One objective of this study was to investigate the feasibility of using averaged model parameter values for each watershed. The results from the analysis of ten storm events indicated that averaged parameter values are not capable of providing adequate storm hydrograph regeneration and that the averaged parameter values provide lower correlation ($R=0.816$) than the optimized parameter values ($R=0.872$).

CHAPTER V

FACTORS AFFECTING THE DERIVATION OF THE SYSTEM RESPONSE FUNCTION OF SELECTED CONCEPTUAL MODELS

The purpose of a model is prediction. Such predictions are potentially limited in two ways. First, the mathematical structure of a model can effectively limit the flexibility of the model. Once the mathematical form of the model has been selected, parameters of the model must be evaluated. There are a number of factors which influence the process of parameter evaluation. These factors represent a limitation in the utilization of the associated model. The purpose of this chapter is to discuss the effect of data error and the nature of the process which is being modeled on model formulation and parameter evaluation.

The Watershed and Conceptual Model Response Functions

A specific conceptual model has a response function with a specific characteristic shape. This can be a disadvantage. For example, the single linear reservoir model has a response function which peaks at time $t = 0$ and decreases exponentially. The parameter of the model fixes the magnitude and distribution of the response function ordinates. If the model response function (MRF) does not provide a good approximation of the watershed response, then it is unlikely that the model will provide accurately regenerated storm hydrographs. Thus, it is important when selecting a model to choose a model flexible enough to provide a good approximation to a variety of possible watershed responses.

The Distribution of Precipitation Excess

The time distribution of precipitation excess affects the model parameters computed from rainfall and runoff data. This has been demonstrated by Dooge (37), and Laurenson and O'Donnell (38). In order to determine the effect of precipitation distribution on four specific models, three patterns of precipitation excess and the associated values of model parameters were investigated.

Types and Magnitude of Data Error

Error introduced into rainfall and runoff data will effect the computed model parameters. Both the type and magnitude of the data error are important. Data error can appear in both precipitation and streamflow data. Additional error can be introduced in the separation of rainfall losses from the total rainfall or in the separation of direct runoff from the total streamflow.

Precipitation data error can result from faulty chronometers or the shrinking and swelling of the recording chart on the analog recorders. Error can appear in precipitation data computed from several recording gages if the precipitation distributions are not properly synchronized or if the point rainfall measurements do not accurately represent the areal distribution of rainfall. Error contained in precipitation data will be transmitted to the computed precipitation excess distribution. Additionally, misrepresentation of the rainfall loss function can cause significant variation in the computed model parameters.

Error in the runoff data can result from inaccurate recording devices, errors in the stage-discharge curve, and in the separation of

direct runoff from the total flow. Factors which influence the stage-discharge relationship include the presence of ice, backwater from a nearby stream and a shifting control. Furthermore, extrapolation of the rating curve above measured flows can induce error into the streamflow data.

Lack of synchronization between the rainfall and runoff data can induce error into the computed model parameters. Faulty chronometers on either the precipitation or streamflow recording gages will cause such lack of synchronization. Detection of synchronization error would be difficult for larger basins in which the time interval between the start of precipitation and the start of runoff is relatively large.

Experimental Design

An experiment was designed to measure the effect of a number of factors on the parameters of four conceptual models. Factors included in the study are variation in the hydrologic response of the watershed (i.e., the effect of model formulation), variation in the time distribution of precipitation excess, and the introduction of error into the precipitation excess data. Each of these factors will be discussed in more detail in the following sections, and the effect of each factor and the interrelationships between factors will be investigated. For such an investigation, it was necessary to use artificial data since the true hydrologic response of a watershed cannot be determined and data error usually cannot be detected and adjusted objectively in data collected from watersheds.

Watershed Response Functions

Different watersheds have response functions of different shapes. For example, watershed A may have a quicker hydrologic response, and thus peak sooner than watershed B. Also, the recession curves of the two watersheds might differ significantly. For this study, two general shapes were investigated. It is assumed that both watershed response functions are linear and time-invariant. Both artificial watershed response functions are smoothly varying and single-peaked with a time-to-peak approximately twenty-five percent of the time base of the response function. It was desirable to use an analytical expression to represent the true (assumed) hydrologic response of the watershed. A series of exponential terms would provide the necessary shape, but since the response functions of the models investigated were composed of exponentials, such expressions were avoided to prevent biasing the results. A series of sine functions will provide a reasonable shape for unit hydrographs (39). The general equation used to represent both watershed response functions is

$$y(t) = \sum_{i=1}^n A_i \sin (i \pi t/B) \quad 0 \leq t \leq 20 \quad (5-1)$$

where A_i controls the magnitude of the i^{th} sine function, B controls the period of the sine functions, and n is the number of sine functions used to define $y(t)$. The parameter values used to define the two watershed response functions included in the experimental design are given in Table

5-1. The functions are shown in Figure 5-1. Response function I_2 is characterized by a relatively high peak and a rapid recession while response function I_1 has a relatively flat peak and a slow recession. The area enclosed by each response function was adjusted to unity.

Distribution of Precipitation Excess

The effect of the time pattern of precipitation excess on the response functions of the models was investigated using three shapes of rainfall excess hyetographs. The time patterns investigated, Figure 5-2, were (1) early peaked, P_1 , (2) late peaked, P_2 , and (d) double peaked, P_3 . Each had a volume of 10.5 volume units and a time base of ten time units. The early peaked pattern has an initial ordinate of 1.5 units and each successive ordinate is decreased by 0.1 units. The late peaked pattern has an initial ordinate of 0.6 units and the ordinates increase linearly to a value of 1.5 units. The double peaked pattern of precipitation excess is symmetrical and the largest ordinates of the pattern are 1.7 units.

Data Error Types

Rainfall and runoff data can contain many types of data error simultaneously. For this study, two types of data error were investigated. Both errors, a uniform loss error and a rainfall distribution error, were introduced independently into the distribution of precipitation excess and not the streamflow data.

Uniform loss function data error. Losses, including infiltration, interception, evapotranspiration and depression storage, are often

Table 5-1. Watershed Response Function Parameters

$$Q(t) = \sum_{i=1}^n A_i \sin(1\pi t/B)$$

Parameter	I_1	I_2
n	5	3
B	25	20
A_1	6	5
A_2	5	4
A_3	2	1
A_4	1	-
A_5	0.5	-

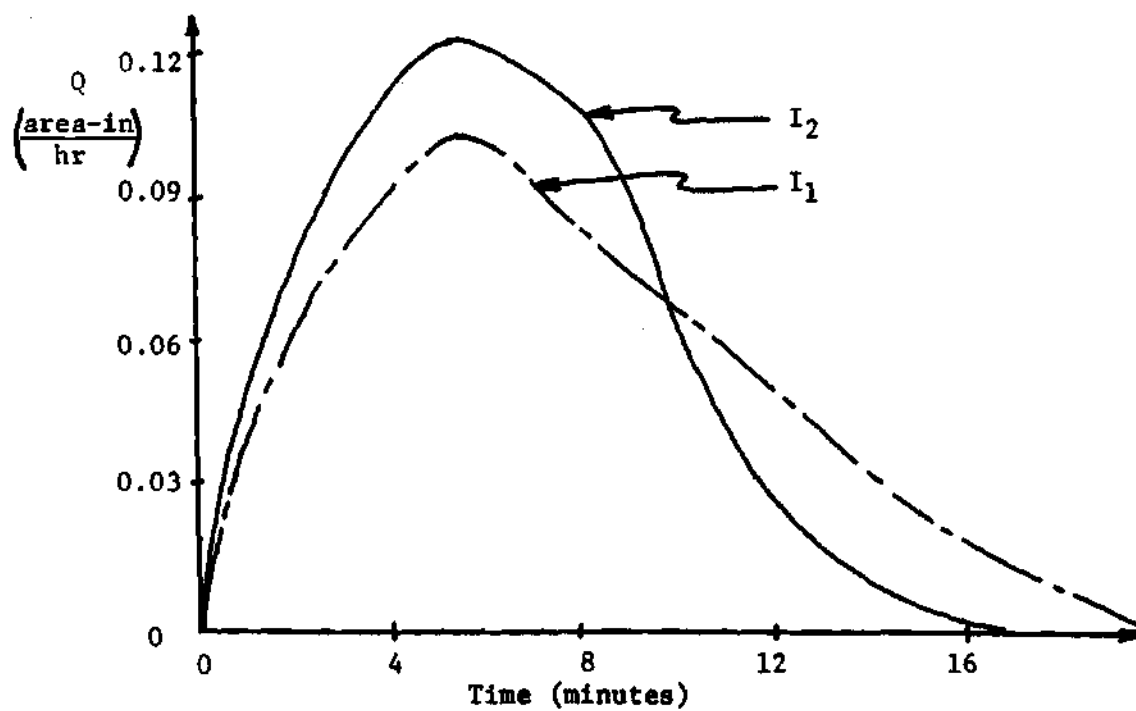
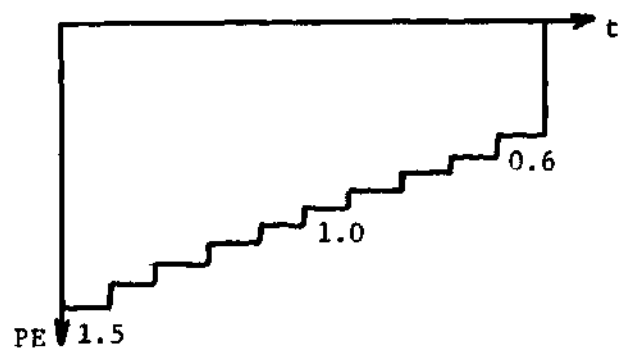
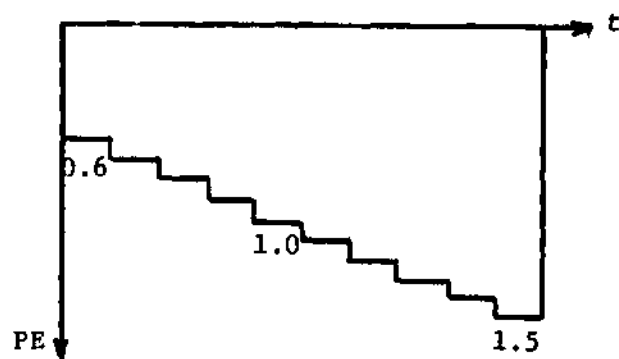


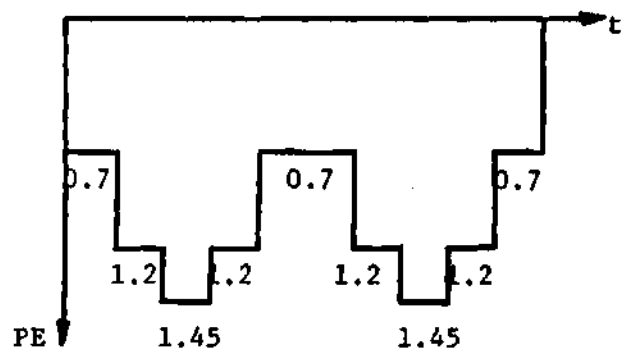
Figure 5-1. Watershed Response Functions



(a) Early Peaked



(b) Late Peaked



(c) Double Peaked

Figure 5-2. True Precipitation Excess Distributions

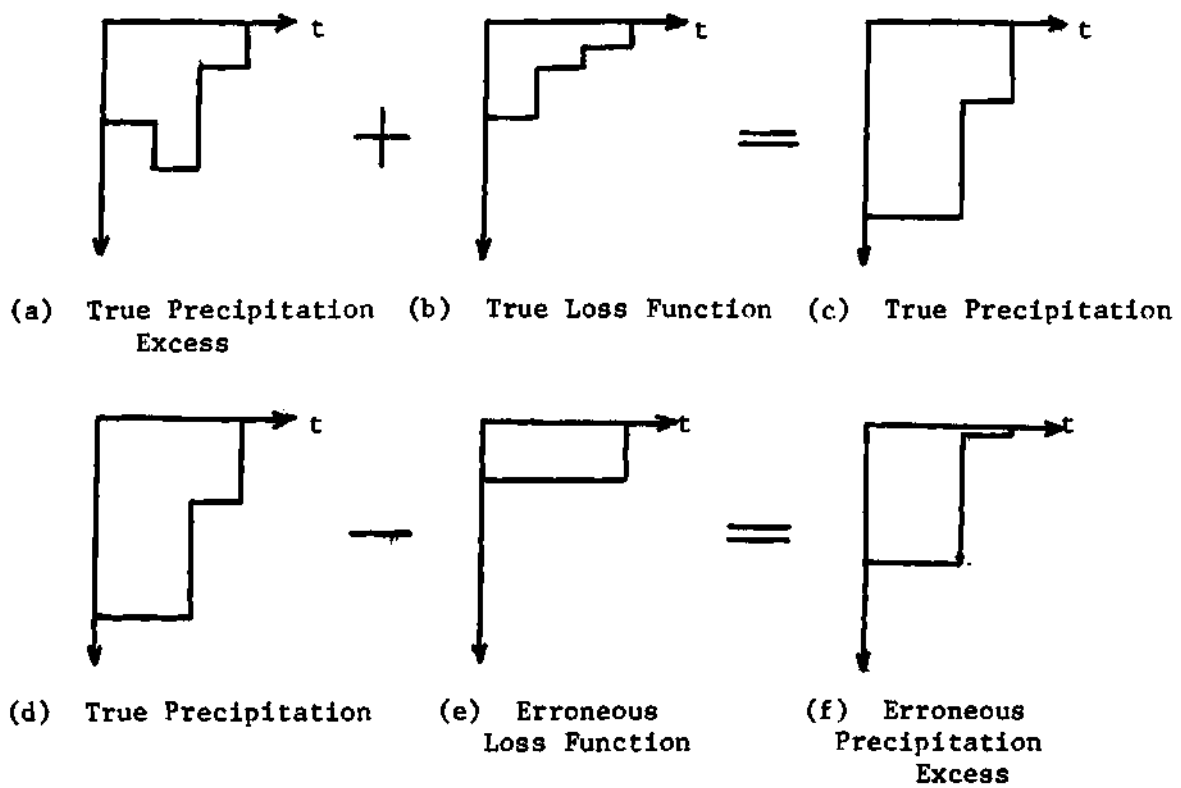


Figure 5-3. Introduction of a Uniform Loss Function Data Error

estimated using a uniform loss function (25). Laboratory and field measurements (24) have indicated that losses are greater at the beginning of a storm than at the end. Thus, use of the uniform loss rate may underestimate precipitation excess volumes at the end of the storm and overestimate the volumes at the beginning of the storm.

The procedure for studying the potential effect of such data error involved the addition of a time-varying loss function to each of the three "true" precipitation excess patterns, and subsequent subtraction of a uniform loss function, having a volume equal to the time varying loss function, from the computed true precipitation pattern, see Figure 5-3. Thus, three erroneous precipitation excess patterns, one corresponding to each of the three true precipitation excess patterns, were studied. Negative ordinates in the computed precipitation excess patterns were set equal to zero and the volume was adjusted to equal the volume of true precipitation excess. The true loss function was represented by a decaying exponential of the form

$$L(t) = f_c + (f_o - f_c)e^{-Kt} \quad (5-2a)$$

where f_o is equal to the initial infiltration rate, f_c is equal to the ultimate infiltration rate and K is the decay rate. The values of the true loss function were set at $f_c = 0.2$, $f_o = 0.4$, and $K = 0.1$, thus

$$L(t) = 0.2 + 0.2e^{-0.1t} \quad 0 \leq t \leq 10 \quad (5-2b)$$

The form of equation 5-2 was proposed by Horton (24). The volume of losses was approximately 5.73 units.

Rainfall distribution error. Error in the volume and distribution of rainfall can result from faulty recording instruments or by representing areal rainfall intensities by point rainfall measurements. Such error could be uniformly, randomly, or proportionately distributed in the measured rainfall. This type of error could result from an increase or reduction in the intensity of the storm as the storm moves from a gaging station located outside the watershed boundary to the watershed. The change in intensity could be distributed uniformly, proportionately or randomly.

For this study the rainfall distribution data error, applied independent of the uniform loss data error, was assumed to be distributed in the measured precipitation in proportion to the rainfall intensity. Specifically, the erroneous distributions of precipitation were determined by multiplying each ordinate of the true precipitation distribution by $1 + \alpha$, where α is the rainfall distribution data error constant. Two values of α , 0.10 and 0.25, were investigated. Positive values of α will increase the absolute difference between ordinates of the precipitation distribution. The distribution of erroneous precipitation excess was determined by subtracting the loss function from the erroneous precipitation distribution. Since the volume of precipitation excess must equal the volume of runoff it was necessary to increase the volume of losses by an amount equal to the change in volume of precipitation due to the introduction of data error. Since the data error was introduced to

investigate the potential effect on the output of errors in the time distribution of precipitation, the change in the volume of losses was distributed uniformly with time. Thus, the value of f_c and f_o in equation 5-2a were increased by a value $\Delta V/10$ where ΔV was the change in precipitation due to the introduction of the data error. In order to maintain the change in the shape of the precipitation distribution caused by the introduction of data error, the decay rate K , equation 5-2a, was not changed. A change in the value of K would, by itself, cause a change in the distribution of precipitation excess and thus, any change in the output could not result entirely from the introduction of data error. This technique of adjusting the loss function is not necessarily rational from a hydrologic viewpoint but was used to show the effect of introducing a proportional error into the precipitation data. If the distribution of the losses were also changed then one would not be able to distinguish between the effect of the data error and the error resulting from the change in the loss function.

Conceptual Models

The experimental design will include the following four conceptual models: [1] the single linear reservoir model, [2] the Nash model, [3] the double routing model, and [4] the linear channel-linear reservoir model with a rectangular time-area-concentration distribution. A rectangular time-area-concentration distribution was selected for use in the LCLR model because it provided output regeneration as well as any of the other LCLR models (Chapter IV) and because it is more easily programmed.

Experimental Procedure

In this study all combinations of the factors discussed in the previous paragraphs have been included in the analysis. Since conceptual models rigidly constrain the shape of the response function it was important to consider the error in the fitting of the conceptual models as well as the error induced by using erroneous data. It would not be necessary to compute the fitting error for methods such as the harmonic series (39) and least squares (34) which do not constrain the shape of the system response function (38), and thus, have relatively small fitting error in comparison to the fitting error of conceptual models.

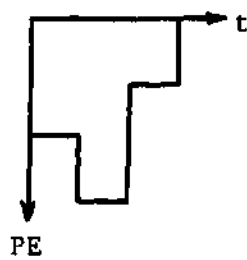
The following procedure, see Figure 5-4, was used for this experiment:

- [1] establish a true precipitation excess distribution;
- [2] establish a true loss function;
- [3] compute the true distribution of precipitation, [1] + [2];
- [4] establish the true watershed response functions, I_1 and I_2 ;
- [5] compute the true time distribution of direct runoff by convolving [1] and [4];
- [6] compute the true model parameters for each of the four conceptual models using the true distributions of precipitation excess [1] and direct runoff [5];
- [7] compute the true model response functions using the parameters computed in [6], select a means of comparison, and compare the true watershed response function [4] with the true model response functions;

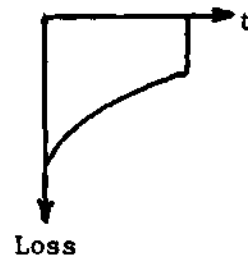
- [8] introduce data error into the distribution of true precipitation or precipitation excess;
- [9] convolve the distribution of erroneous precipitation excess [8] with the true system response function [4] to determine the erroneous storm runoff distribution;
- [10] compute the erroneous model parameters for each of the four conceptual models from the distributions of erroneous precipitation excess [8] and the erroneous storm runoff distribution [9];
- [11] compute the erroneous model response functions using the parameters computed in [10]; using the same method of comparison that was used in [7], compare each of the four erroneous model response functions with the true watershed response function [4].

In step [9] the distribution of erroneous precipitation excess was convolved with the true watershed response function to determine the erroneous storm runoff distribution. This procedure was used because it enabled the fitting error to be distinguished from the error introduced into the storm runoff distribution by the presence of data error. The response function computed in step [7] is free from the error introduced into the data in step [8], and thus a comparison of the true [7] and erroneous [10] response functions will indicate the effect of data error.

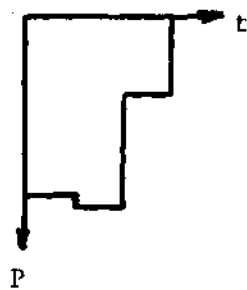
The true storage coefficient for the two single-parameter models (SLR and DR) was determined by minimizing the sum of the squares of the deviations between the computed storm hydrograph and the true time



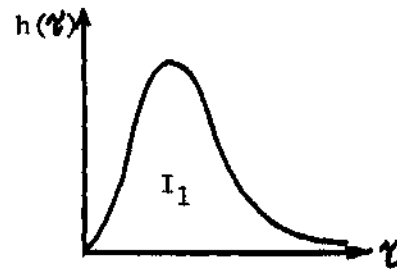
Step [1] True Precipitation Excess Distribution



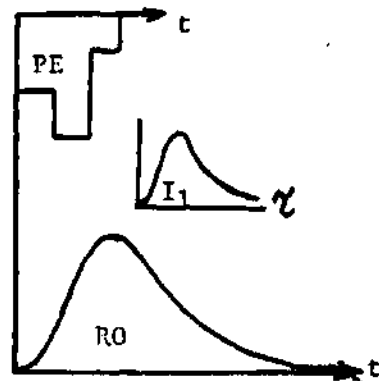
Step [2] True Loss Function



Step [3] True Precipitation Distribution [1]+[2]



Step [4] True Watershed Response Function I_1

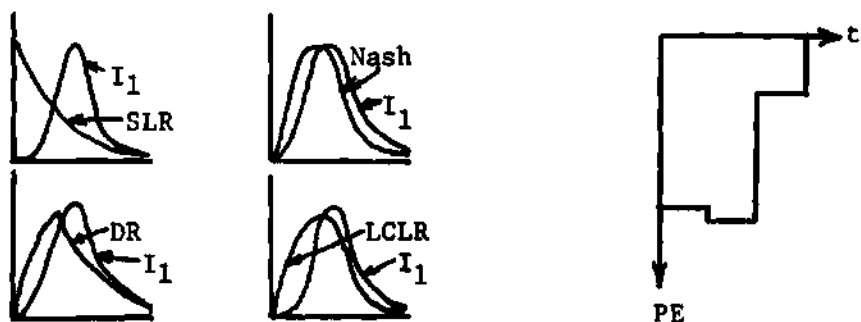


Step [5] Distribution of True Runoff

<u>Model</u>	<u>Parameter(s)</u>
SLR	K
Nash	K and n
DR	K
LCLR	K and T_c

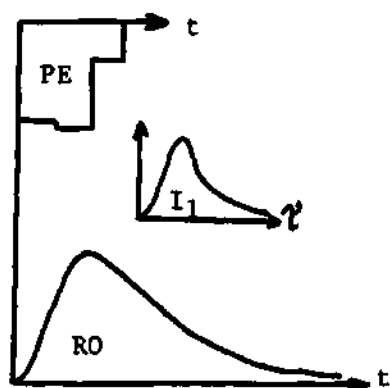
Step [6] Compute True Model Parameters

Figure 5-4. Experimental Procedure



Step [7] Generate and Compare True Model Response Functions with I_1 (or I_2)

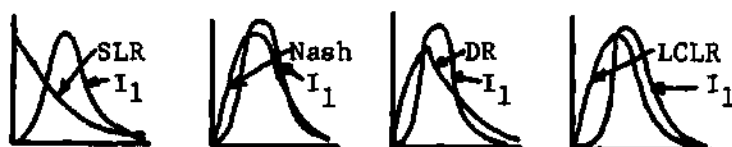
Step [8] Compute Erroneous Precipitation Excess



Model	Parameter
SLR	K
Nash	K and n
DR	K
LCLR	K and T_c

Step [9] Distribution of Erroneous Runoff

Step [10] Compute Erroneous Model Parameters



Step [11] Generate and Compare Erroneous Model Response Functions with I_1 (or I_2)

Figure 5-4. Experimental Procedure (cont'd)

distribution of direct runoff [5]. Similarly, the erroneous storage coefficient was determined by minimizing the sum of the squares of the deviations between the storm hydrograph computed using the erroneous precipitation excess [8] and the true time distribution of direct runoff [5]. The time interval T_L between the centers of mass of precipitation excess and runoff was used as the storage coefficient for the Nash model and the number of reservoirs n was then determined by minimizing the sum of the squares of the deviations. In the LCLR model the time of concentration was optimized using the "sum of squares" objective function after having equated the storage coefficient to the difference in centers of mass of rainfall excess and direct runoff. By using the sum of the squares of the deviations as an objective function for each model, consistency in the computational procedure was provided.

Three objective functions were used to compare the true and erroneous model response functions [7] and [10] with the watershed response function [4]. Comparison of the true model response function [7] with the watershed response function [4] serves as a measure of the fitting error. Comparison of the erroneous model response function [10] with the watershed response function [4] estimates the combined effect of fitting and data error. The three objective functions used were the sum of the absolute deviations as a percentage of the peak, the sum of the squares of the deviations as a percentage of the peak, and the sum of the squares of the deviations. All such objective functions characterize the overall fitting ability. Other objective functions which concentrate on the reproduction of the peak, in magnitude and/or time, could have been used. Although the values of the three objective

functions differ in magnitude, they lead to the same conclusions. Thus, the sum of the squares of the deviations was used for comparison of factor effects.

Results

The results of the experiment will be summarized in tables of experimental error. Each value in the table represents the total error as measured by the sum of the squares of the deviations between either the true or erroneous model response functions and the true watershed response function. When comparing the true model response function with the true watershed response function the total error will be indicative of the inability of the model to fit the true watershed response function and will be referred to herein as the fitting error. The total error when comparing the erroneous model response function with the true watershed response function is the sum of the fitting error and the effect of the error introduced into the data. In some cases, the introduction of error into the data will result in a lower total error than for the data that is free from data error. This occurs when the constraining shape of the conceptual model more easily adapts to the erroneous data set than to the set of data that is free from data error.

The individual effect of each experimental factor, shape of precipitation distribution, shape of the true watershed response function, etc., as measured by the total error are given in Table 5-2. In general, it is easier to draw conclusions from tables expressing the averaged effect of two factors than tables, such as Table 5-2, showing multifactor effects. To show the interaction effect of two factors, such as the

Table 5-2. Total Error Distribution

Model	PE Pattern	No Data Error Included			
		Watershed Response Function			
		I_1		I_2	
SLR	Early	.024195		.038197	
	Late	.024195		.038197	
	Double	.024233		.038292	
Nash	Early	.006922		.016614	
	Late	.005874		.015036	
	Double	.006454		.015984	
DR	Early	.001474		.006714	
	Late	.001474		.006714	
	Double	.001478		.006751	
LCLR-RT	Early	.001713		.005701	
	Late	.000896		.005430	
	Double	.000964		.005533	

Model	PE Pattern	Uniform Loss Function Data Error Included			
		Watershed Response Function and Difference			
		I_1	E_{11}^*	I_2	E_{12}^*
SLR	Early	.024135	-60	.038096	-101
	Late	.024257	62	.038298	101
	Double	.024233	0	.038290	-2
Nash	Early	.006912	-10	.016570	-44
	Late	.005959	85	.015190	154
	Double	.006668	214	.016339	355
DR	Early	.001470	-4	.006692	-22
	Late	.001478	4	.006737	23
	Double	.001478	0	.006750	-1
LCLR-RT	Early	.001708	-5	.005715	14
	Late	.000900	4	.005434	4
	Double	.001241	277	.005606	73

* E_{ij} = difference between total error and true error ($\times 10^{-6}$)
 i : subscript for data error type
 j : subscript for shape of true watershed response function

Table 5-2. Total Error Distribution (cont'd)

Model	PE Pattern	Rainfall Distribution Error, $\sigma=0.25$			
		Watershed Response Function and Difference			
		I_1	E_{21}^*	I_2	E_{22}^*
SLR	Early	.024042	-153	.037947	-250
	Late	.024093	-102	.038029	-170
	Double	.024158	-75	.038173	-119
Nash	Early	.006863	-59	.016458	-156
	Late	.005743	-131	.014786	-250
	Double	.006498	44	.016040	66
DR	Early	.001463	-11	.006660	-54
	Late	.001467	-7	.006677	-37
	Double	.001474	-4	.006732	-19
LCLR-RT	Early	.001614	-99	.005722	21
	Late	.000893	-3	.005425	-5
	Double	.000968	4	.005564	31

Model	PE Pattern	Rainfall Distribution Error, $\sigma=0.10$			
		Watershed Response Function and Difference			
		I_1	E_{31}^*	I_2	E_{32}^*
SLR	Early	.024134	-61	.038096	-101
	Late	.024160	-35	.038139	-60
	Double	.024204	-29	.038246	-46
Nash	Early	.006904	-18	.016559	-55
	Late	.005824	-50	.014945	-91
	Double	.006482	28	.016024	40
DR	Early	.001470	-4	.006692	-22
	Late	.001471	-3	.006702	-12
	Double	.001476	-2	.006744	-7
LCLR-RT	Early	.001709	-4	.005712	11
	Late	.000895	-1	.005428	-2
	Double	.000918	-46	.005548	15

* E_{ij} = difference between total error and true error ($\times 10^{-6}$)
 i : subscript for data error type
 j : subscript for shape of true watershed response function

shape of the precipitation excess distribution and the different conceptual models, the total error for all other factors are averaged. Unfortunately, use of the averaged total error effects can lead to erroneous conclusions. Several examples of this possibility will be presented in the discussion.

Figure 5-5 shows the flat-peaked watershed response function I_1 and the true model response functions for the four conceptual models. Since data error is not involved, the total error represents the inability of the model to represent the given watershed response function. Use of the DR model results in the lowest fitting error even though the LCLR model provides a better estimate of the true peak discharge.

It should be emphasized that the experimental procedure was designed to investigate two objectives. Of primary importance was the investigation of the potential adequacy of the models used herein to represent the hydrologic response of a watershed. The identification of factors which influence model parameter evaluation was of secondary importance. It is immediately evident from Table 5-2 that the constraining shape of the model response functions is responsible for the inability of the model to adequately represent the hydrologic response and that the presence of error in the data is not, in general, responsible for large deviations in the computed model parameters. For example, the largest change in total error is 0.000355 (for M2, P3, E1, I2) which is only two percent of the total error (0.016339). Thus, it is only necessary to consider the details of the experimental procedure (as given in Table 5-2) when examining the problem of parameter evaluation.

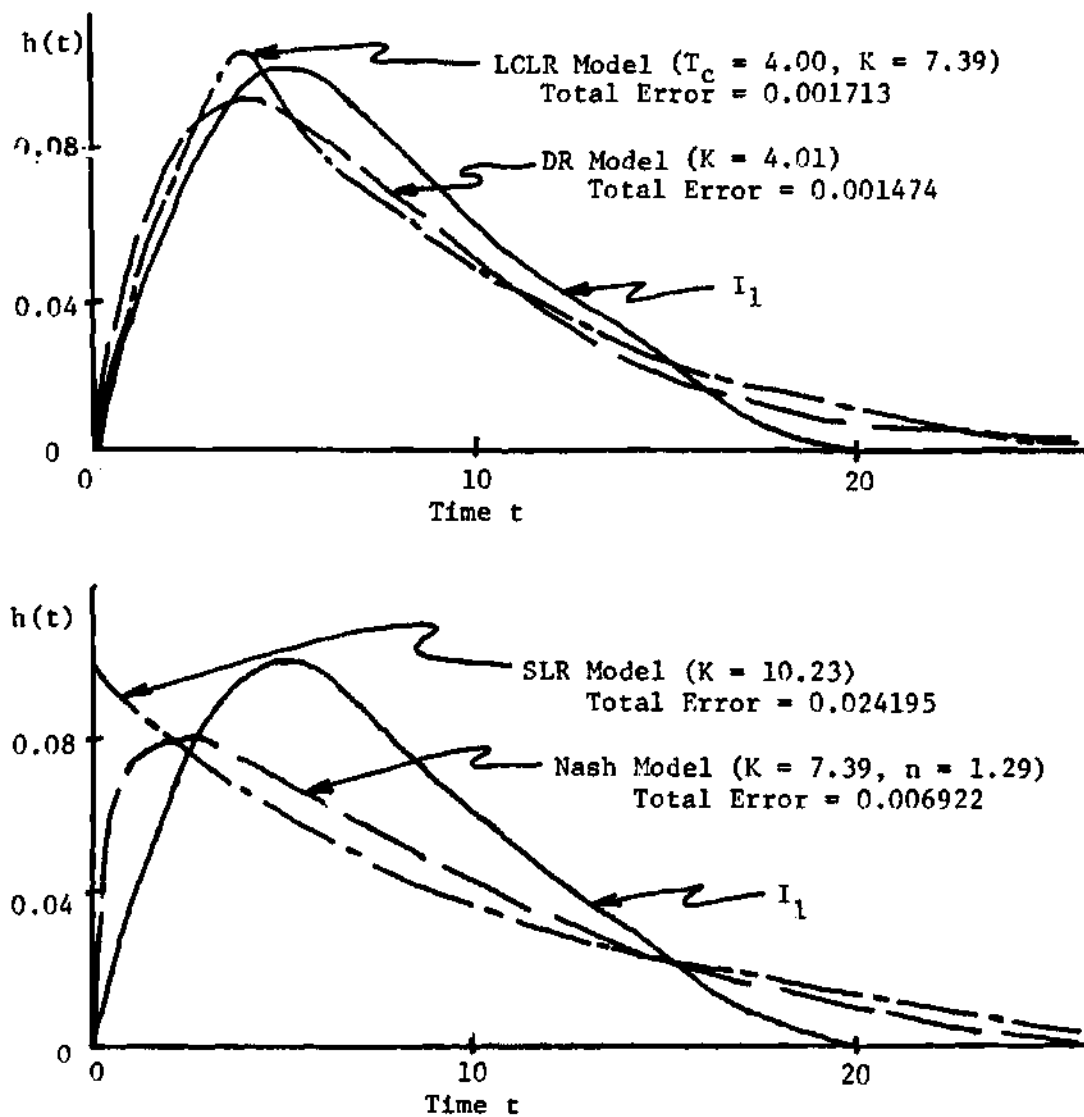


Figure 5-5. Comparison of Model Response Functions and Watershed Response Function I_1

Two-Factor Comparison of Conceptual Models and True System Response Function Shapes

Table 5-3 shows the average total error for variation in the shape of the true watershed response functions and the different conceptual models. Thus, Table 5-3 cannot be used to estimate the effects of variation in the types of data error or in the shape of the precipitation excess distribution. Table 5-3 also shows the variation in total error due to changes in magnitude of the rainfall distribution error proportionality constant α .

The mean total error due to the inability of the true model response function to fit the true watershed response function is, for all four conceptual models, greater for the higher peaked watershed response function (I_2). It should be emphasized that such a conclusion should not readily be extended to other conceptual models and other watershed response function shapes. The results also indicate that the SLR model provides the poorest fit while the DR and LCLR models have a significantly smaller error when they are used to reproduce the true watershed response.

For the combined data error ET_{12} , which is one-half the sum of the errors for E_1 and E_2 , the total error is decreased for all conceptual models except the Nash model when using the flat-peaked true watershed response function. But for the sharp-peaked true watershed response function I_2 the total error increases for all models except the SLR model. The absolute change in total error, $|\Delta E|$, is always greater when fitting the high-peaked true watershed response function which indicates that, in general, the conceptual models are more sensitive to data error when the

Table 5-3. Averaged Effects : Models Versus Watershed Response Function

Model	True Fitting Error		ET12:Average Total Error for Uniform Loss Function Data Error and Rainfall Distribution Error ($\alpha=0.25$)			
	Watershed Response Functions		Watershed Response Functions			
	I_1	I_2	I_1	ΔE^*	I_2	ΔE^*
SLR	.024208	.038229	.024153	-55	.038139	-90
Nash	.006417	.015870	.006441	24	.015897	27
DR	.001475	.006726	.001472	-3	.006810	84
LCLR-RT	.001191	.005555	.001175	-16	.005578	23

Model	True Fitting Error		ET13:Average Total Error for Uniform Loss Function Data Error and Rainfall Distribution Error ($\alpha=0.10$)			
	Watershed Response Functions		Watershed Response Functions			
	I_1	I_2	I_1	ΔE^*	I_2	ΔE^*
SLR	.024208	.038229	.024178	-21	.038194	-35
Nash	.006417	.015870	.006458	31	.015938	68
DR	.001475	.006726	.001474	-1	.006720	6
LCLR-RT	.001191	.005555	.001228	37	.005574	19

* ΔE is the difference between the total error and the true fitting error ($\times 10^{-6}$).

high-peaked response function I_2 is being modeled. The conclusions for ET12, the mean effect of introducing both types of data error with $\alpha=0.25$, are the same as those resulting from ET13, where $\alpha=0.10$. The only exception to the conclusions for ET12 is that the change in total error, ΔE , for the LCLR model is approximately twice as large for the response function I_1 (+37) as it is for the response function I_2 (+19). This results from the large total error, see Table 5-2, caused by the introduction of the uniform loss data error E1 in combination with the double peak precipitation excess pattern P3.

Two Factor Interaction Effects Between Conceptual Models and Type of Data Error

Table 5-4 gives the average total error when considering the variation in types of data error and conceptual models. Thus, the variation in total error due to the affect of different precipitation excess patterns and watershed response functions (I_1 and I_2) are averaged. It should be apparent that variation in either the precipitation excess patterns or the watershed response function will influence the total error values expressed in Table 5-4 but that individual variations of these factors will not be discernible.

The total error values of Table 5-4 indicate that the poorest fit occurs with the SLR model (total error = 0.031218). A total error of 0.003373 for the LCLR model is approximately one-tenth of the error for the SLR model. The Nash model provides a fit having a total error of about one-third of the SLR total error value.

The introduction of the uniform loss function data error E1 into

Table 5-4. Averaged Effects : Models Versus Data Error

Model	Fitting Error	Uniform Loss Error	ΔE_1^*	Rainfall Error ($\alpha=0.25$)	ΔE_2^*	Rainfall Error ($\alpha=0.10$)	ΔE_3^*
SLR	.031218	.031218	0	.031074	-144	.031163	-55
Nash	.011147	.011273	126	.011065	-82	.011123	-24
DR	.004095	.004101	6	.004080	-15	.004093	-2
LCLR-RT	.003373	.003434	61	.003365	-8	.003368	-5

* ΔE_1 is the difference between the averaged total error and the averaged true fitting error($\times 10^{-6}$).

Table 5-5. Averaged Effects : Models Versus PE Distribution

Model	PE Pattern	True Fitting Error	Combined Data Error ($\alpha=0.25$)	ΔE_1^*	Combined Data Error ($\alpha=0.10$)	ΔE_2^*
SLR	Early	.031196	.031055	-141	.031115	-81
	Late	.031196	.031169	-27	.031214	18
	Double	.031262	.031214	-48	.031243	-19
Nash	Early	.011768	.011701	-67	.011736	-32
	Late	.010455	.010420	-35	.010480	25
	Double	.011219	.011386	167	.011378	159
DR	Early	.004094	.004071	-23	.004081	-13
	Late	.004094	.004091	-3	.004097	3
	Double	.004115	.004108	-7	.004112	-3
LCLR-RT	Early	.003707	.003690	-17	.003711	4
	Late	.003163	.003164	1	.003164	1
	Double	.003248	.003345	97	.003328	80

* ΔE is the difference between the average combined data error and the average true fitting error ($\times 10^{-6}$).

the data induces change in the total error. Table 5-4 indicates that such data error has no affect ($\Delta E = 0$) when using the SLR model, a slight affect ($\Delta E = 0.000006$) on the DR model and a more significant influence on the LCLR and Nash models. To conclude that such data error has no effect on the SLR model would be highly erroneous. The total error values of Table 5-2 show that for the early-peaked precipitation pattern the total error decreases, the total error increases when using the late-peaked pattern and little change results when the double peaked pattern is used. This example indicates the importance of considering the effect of the individual factors before making conclusions from the averaged total error values of Tables 5-3 and 5-4.

The results for the rainfall distribution data error (E2 and E3) differ significantly from those of the uniform loss data error E1. For E2 and E3 the SLR model is, in general, more affected by such data error than are the other models. The Nash model is also highly sensitive to such data error while the DR and LCLR models are, on the average, less sensitive. As expected, the larger value of α , the rainfall distribution proportionality constant, induces larger changes in the total error.

Two Factor Comparison of Conceptual Models and the Precipitation Excess Patterns

The total error values of Table 5-5 can be used to estimate the average effect of data error types and the different watershed response shapes on the conceptual models and for variation in the distribution of precipitation excess. The total error values lead to conclusions similar to those previously discussed. Specifically, the DR and LCLR models

provide better estimates of the true watershed response function than does the Nash and SLR models. Also, the effect of data error is considerably less than the error due to the inability of the conceptual models to fit the true watershed response function.

The total error values indicate that the conceptual models are consistently less sensitive to data error when the late-peaked precipitation excess pattern is used. Furthermore, the Nash and LCLR models are more sensitive (larger ΔE values) to data error when the double-peaked precipitation excess pattern is used while the SLR and DR models are more sensitive to data error when the early-peaked precipitation excess pattern is used. The SLR and DR models are more sensitive to parametric variation in the rising limb of the model response functions and thus, they are more affected by data error when using the early peaked precipitation-excess pattern. The reasons for the results derived from Table 5-5 will be more apparent after model sensitivity has been discussed (Chapter VII).

In general, the DR model is less affected by the introduction of error into the data. The greater adjustability of the DR response function minimizes the effect of data error. This is a favorable result for users of the DR model, especially since the fitting error when using the DR model is relatively small when compared with that of the other models investigated.

Introduction of error into the data and the use of the early-peaked precipitation excess pattern resulted, in all cases, in a reduction in total error. This indicates that the erroneous storm hydrograph

provides model parameters which produce a model response function more similar to the true watershed response function. That is, the effect of the constraining shape is less noticeable for the erroneous data. The double-peaked precipitation excess pattern results in, for two of the four conceptual models, increased total error. In these cases, the introduction of error into the data emphasizes the constraining effect of the conceptual models.

Summary of Results

Four factors were identified which were considered important in the derivation of the response functions of four conceptual models. The experimental design which investigated various levels of these factors produced the following general conclusions concerning parameter evaluation and model formulation.

First, the effect of data error is considerably less than the error imposed by the constraining shape of the conceptual model. For example, the method of abstracting precipitation losses has little influence on the level of regeneration obtained from the use of such models. This should be expected of conceptual models because the data error is just a perturbation of the data and the constraining effect will dominate the data error effect when the shape of the model response function is not the same as the shape of the watershed response function.

Second, the output from conceptual models is less sensitive to data error when the precipitation excess pattern is characterized by a late peak. The rising limbs of the model response functions are more sensitive (model sensitivity will be discussed in detail in Chapter VII)

to parametric variation and thus, precipitation excess patterns characterized by early peaks will stress the sensitivity of the rising limbs.

Third, the model response functions are more sensitive to data error when the watershed response function is relatively sharp-peaked. Sharp-peaked response functions have smaller values of the storage coefficient and thus, the sensitivity will be increased. Thus, the error introduced into the data will, as will be shown in detail in Chapter VII, have more effect on the output.

Fourth, the LCLR and DR models provide better estimates of the watershed response functions than the other models investigated herein. The less sensitive SLR model provides poorer estimates of the true watershed response function. The DR and LCLR response functions provided better fits of the watershed response functions investigated. For other watershed response functions the SLR and Nash models might provide the better approximation.

Fifth, because the DR and LCLR models provide a better fit of the hydrologic response of the watersheds, the introduction of error into the data does not affect the parameter values of the models as much as for the SLR and Nash models. Thus, the overall change in output for the DR and LCLR models is less than that resulting from the use of the SLR and Nash models.

The above results are based on the averaged total error values of Tables 5-3, 5-4, and 5-5. Thus, the results will not always be valid for every level of each factor involved in the experimental design. Exceptions to the general conclusions have been discussed and are apparent

from the total error values of Table 5-2. It should also be emphasized that these conclusions are based on the analysis of artificial data and for the levels of the factors used. Thus, quantitative conclusions are not drawn.

The reasons for the stated conclusions have often been explained in terms of model sensitivity. At this point it should suffice to state that the more sensitive the model output is to variation in its parameters, the more likely it is that a better fit will be provided. The topic of model sensitivity, as mentioned previously, will be discussed in detail in Chapter VII.

The Importance of Considering the Shape Characteristics of Conceptual Model Response Functions

The results of the experimental design showed that the DR model provided the best estimate of the assumed hydrologic response functions. The analysis of hydrologic data (see Chapter IV) showed that the DR model did not always provide the best estimates of actual hydrologic responses. Other investigations (29) have shown that the SLR and Nash models provided better regeneration of observed storm events than the DR model. Since from the analysis of real and artificial data it is apparent that no one model consistently provides superior regeneration it would be beneficial to investigate the cause of such results.

Insight into the potential ability of various linear models to represent hydrologic responses of different shapes can be gained by examining the ability of two models (SLR and DR) to represent four artificial-data watershed response functions (see Figure 5-6). The values of

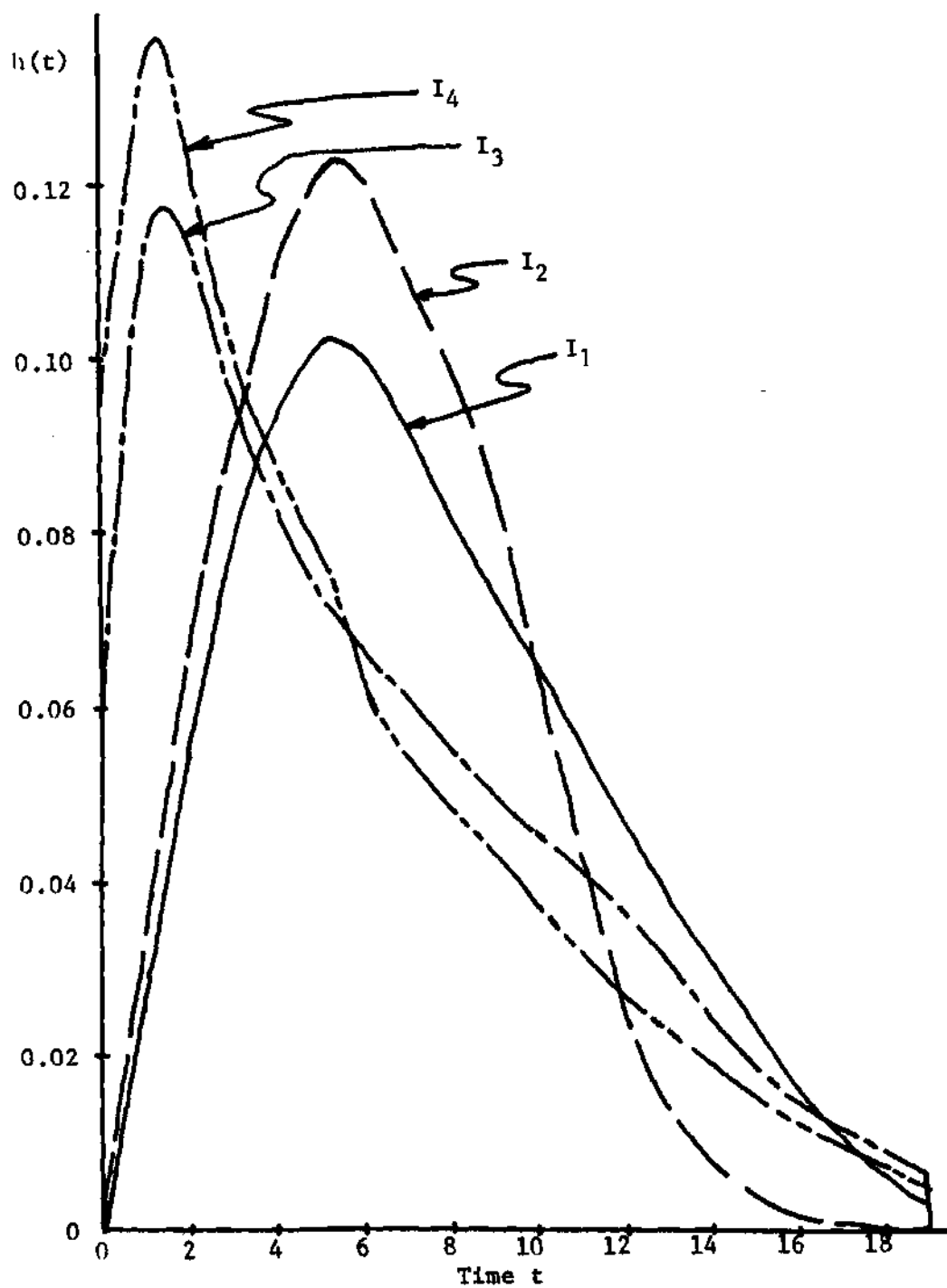


Figure 5-6. Comparison of Watershed Response Functions

the model parameters were determined by fitting the response function to artificial data using the first six steps of Figure 5-4. As with step 7 of Figure 5-4 the resulting model response functions were compared to the watershed response functions. The sum of the squares of the deviations between the computed output and assumed true output was used to indicate the level of output reproduction; the resulting values are given in Table 5-6.

As shown by the values of Table 5-6 the SLR model provides a better estimate of response functions characterized by a small time-to-peak, such as with watershed response functions I_3 and I_4 . The DR model provides better estimates of response functions I_1 and I_2 which are characterized by a comparatively longer time-to-peak. When compared with rural watersheds an urban watershed has a shorter time-to-peak and thus the SLR model should provide a better estimate of the watershed response. Since the watersheds used by Sarma (29) had a comparatively higher percentage of impervious area and thus a correspondingly shorter time-to-peak the SLR model should have been expected to provide better estimates of the watershed response than the DR model. When compared with the SLR model the DR model consistently provided better estimates of the hydrologic response for the rural watersheds examined in this study. Since the hydrologic response of a watershed varies with storm characteristics and watershed conditions (e.g., antecedent moisture, vegetal cover) the DR model should not be expected to provide better regeneration than the SLR model for all storm events analyzed. Thus, it is apparent that the characteristics of the actual hydrologic response of a watershed determines which model will provide the best estimate.

Table 5-6. Model Regeneration Capability

Model	Assumed Watershed Response Function			
	I_1	I_2	I_3	I_4
SLR	0.024233*	0.038292	0.004793	0.002349
DR	0.001478	0.006751	0.010382	0.017798

*Values represent the sum of the squares of the deviations between the watershed response functions and model response functions.

CHAPTER VI

PREDICTION OF CONCEPTUAL MODEL RESPONSE FUNCTIONS

Hydrologists, hydraulic engineers and others have for many years been concerned with prediction of streamflow for ungaged areas. These studies usually involve the development of a rainfall-runoff model, the derivation of the model parameters by data analysis and an attempt to define a mathematical relationship between the resulting model parameters and storm and watershed topographic characteristics. Using computed storm and topographic characteristics for the ungaged watershed, the mathematical relationship is used to estimate the model parameter value or values.

The above general procedure was followed in this study. The parameter values for the conceptual models discussed in Chapter IV were computed using the rainfall excess and direct runoff data collected for twenty-two storm events on sixteen watersheds. Prior to developing prediction equations, factor analysis (40,41), a multivariate statistical technique (see Appendix H), was used to analyze the intercorrelations between the twenty-six topographic characteristics and the parameters of the models. Components regression (41, 42, 43) (see Appendix I), another multivariate statistical technique, was used to determine the coefficients of a prediction model relating topographic and storm characteristics to the model parameters.

Factor Analysis of Topographic Characteristics and Model Parameters

A factor analysis of each set of model parameters and the twenty-six topographic characteristics, discussed previously in Chapter III, was performed in an attempt to reduce the number of characteristics to a manageable number. Since eleven of the variables represented basin slope and an additional eleven represented the shape of the basins, high parameter intercorrelations should be expected. For a set of highly intercorrelated variables, one or two variables might be able to effectively represent in a prediction equation the intended characteristic just as efficiently as the use of all the variables. For example, the use of S_{10-85} (see Appendix J for the definition of all topographic parameters) to represent basin slope might provide predicted model parameters which are capable of regeneration equal to that obtained when using S_w , S_T , S_j , S_L , etc., to estimate the model parameters. Thus, factor analysis, by identifying the characteristic intercorrelations, can lead to a reduction in the data needed to predict the model parameters.

A factor analysis was performed using the optimized model parameters of each model, see Chapter IV, and the twenty-six topographic parameters. In each case the matrix of correlation coefficients indicated that the computed parameters for each of the conceptual models were not highly correlated with any of the twenty-six topographic parameters. The time lag T_L , which was used to represent the storage coefficient in the SLR, Nash and LCLR models, was best correlated with the basin area A , the length parameters L_L , L , L_{cm} , L_{cal} , and L_{ca} , and the shape factor F_s , which is the ratio of A to L . The correlation for these parameters

ranged from 0.91 to 0.94 while the correlation coefficients between T_L and the remaining parameters did not exceed 0.65. The matrix of correlation coefficients for the DR and DRWF models were very similar. The area A , shape factor F_s and the five length parameters mentioned above had correlations between 0.82 and 0.87 while the remaining correlation coefficients, when using the storage coefficient for the DR and DRWF models, did not exceed 0.65. The remaining model parameters, K for the SLR and SLRWF models, n for the Nash model and T_c for the three LCLR models, which were all computed using the objective function of equation 4-12 were poorly correlated with the twenty-six topographic parameters. For these six model parameters the slope ratio R_s had the highest correlation coefficients, but none of the correlation coefficients exceeded 0.60. No correlation coefficient in the matrix of correlation coefficients for the three T_c parameter values exceeded 0.15. Since the correlation coefficients were, in general, low, the prediction equations were not expected to provide parameter estimates capable of acceptable output regeneration. The factor loadings (see Appendix H) indicate that the basin area A , the shape parameter F_s and the length parameters L , L_{cm} , L_{cal} , L_{ca} , and L_L provide essentially the same information while nine of the eleven slope parameters set up an additional item of information. Similar results were found in a study by the TVA (44). They found the basin area to be the primary physiographic characteristic with all other characteristics being highly correlated with the area. Sarma (29) in a study of Indiana watersheds found the area to be the only physiographic characteristic needed for use with storm characteristics to predict the model parameters.

Conceptual Model Parameter Prediction Equations

In order to use the models to predict runoff for future storm events and on ungaged watersheds, it is necessary to estimate the model parameter values. It was shown in Chapter IV that a unique parameter value which provided good hydrograph prediction for each storm could not be determined for a watershed because the parameter values varied significantly from storm to storm. Furthermore, it should be expected that the storage coefficient would be a function of storm characteristics and the conditions of the watershed since the storage coefficient represents a time interval related to the delaying action of the watershed. Thus, parameter values computed from topographic parameters were not expected to provide good storm hydrograph regeneration. But in spite of the poor expectations for good results, prediction equations were developed which related topographic characteristics to the model parameters of each model investigated. The results indicate the potential reduction in storm hydrograph regeneration for parameter values computed from prediction equations compared to the regeneration resulting for optimized parameter values.

Since previous studies (29, 44, 45), have indicated that the basin area was the only significant physiographic characteristic, a linear regression equation of the model parameters on the area was used to predict the value of the model parameter. A correlation coefficient measuring the relationship between the area A and the model parameter was computed for each model, see Table 6-1. Three models, SLR_1 , DR and DKWF, resulted in comparatively high correlation ($R > 0.8$) while the

Table 6-1. Correlation Coefficients for Prediction Equations

Model	Parameter	$P=f(A)^*$	$P=f(A,L,S_{10-85})^*$	$P=f(A,V_p,S_d)^*$
SLR ₁	K	0.911	0.944	0.925
SLR ₂	K	0.189	0.264	0.387
SLRWF	K	0.103	0.257	0.411
DR	K	0.822	0.873	0.921
DRWF	K	0.828	0.871	0.947
Nash	K	0.910	0.944	0.925
	n	0.157	0.356	0.519
LCLR-R	K	0.910	0.944	0.925
	T _c	0.090	0.104	0.200

*Definitions for watershed and storm characteristics

L : basin length

A : basin area

S₁₀₋₈₅ : slope parameter

V_p : volume of precipitation excess

S_d : duration of precipitation excess

P : predicted parameter value

remaining models had correlation coefficients less than 0.20. Since the value of the storage coefficient K for the Nash and LCLR-R models was set equal to the value of K for the SLR_1 model, the resulting correlation coefficients are the same. But the correlation coefficients for the Nash parameter n and the LCLR-R parameter T_c were less than 0.2. In this study, the predicted parameter values from the individual regression equations were not used for storm hydrograph regeneration because other prediction equations developed herein provided better correlation between the optimized and predicted parameter values.

The factor analysis performed using the model parameters and physiographic parameters indicated that the model parameters were moderately related to the basin area and length L , a fact reported by others (46). The relationship between the model parameters and slope parameters was less significant. Using components regression, see Appendix I, prediction equations were determined which related A , L and S_{10-85} to the individual model parameters. As expected, because of the relatively small intercorrelations between the model parameters and the two parameters L and S_{10-85} and the high intercorrelation between A , L and S_{10-85} , the addition of L and S_{10-85} into the prediction equation increased the correlation only slightly. The largest increase in correlation for those models having relatively high correlation was an increase, see Table 6-1, from 0.822 to 0.873 for the DR model. The resulting components regression equations for the DR, DRWF and SLR, are given in Table 6-2. The coefficients of the prediction equation indicate that watersheds having a large area or length will result in large values

Table 6-2. Model Parameter Prediction Equations

Model	Prediction Equation	R^2	Equation
DR	$K = 6.72 + 0.9 \times 10^{-7} A + 4.76 \times 10^{-4} L - 31.42 S_{10-85}$	0.7665	6-1
DRWF	$K = 7.51 + 1.2 \times 10^{-7} A + 6.78 \times 10^{-4} L - 34.54 S_{10-85}$	0.7609	6-2
SLR ₁	$K = 12.94 + 3.0 \times 10^{-7} A + 1.69 \times 10^{-3} L - 61.47 S_{10-85}$	0.8914	6-3

Table 6-3. Watershed and Storm Characteristic Values

Storm Event	Area (acres)	V_p (area-in)	S_d (minutes)
1	110900	0.3898	16
2	110900	0.2158	10
3	98400	0.4172	15
4	84200	0.5071	24
5	164300	0.0442	2
6	49600000	0.6565	50
7	349000	0.4818	20
8	349000	0.2379	25
9	3220000	1.5447	40
10	3220000	1.5447	64
11	183100	0.5595	20
12	192000	0.3613	10
13	183100	0.7839	6
14	160300	0.2404	16
15	90900000	0.4327	90
16	2848000	0.0813	165
17	545000	0.0882	8
18	10820	0.4425	17
19	10760	0.4742	15
20	10760	0.0581	19
21	10690	0.5022	18
22	10690	0.1414	29

of K while basins with steep slopes will have comparatively small K values. Thus, from a hydrologic viewpoint, the coefficients are rational. The inclusion of the basin length L in the prediction equation was not expected to add any significant new information since the factor analyses indicated that L was strongly related to the area A. It was reported by Sarma (29) that Wu (45) demonstrated that for rural watersheds in Hawaii having areas less than twenty square miles the average values of the time lag, defined as the average time from the beginning of rainfall excess to the peak of direct runoff hydrograph, are a function only of the basin area and that the mean slope was not influential in determining the computed model parameters. Sarma (29) showed that for watersheds having areas less than twenty square miles the inclusion of the slope in a prediction equation involving the basin area and an urbanization factor increased the correlation coefficient from 0.927 to 0.929. Sarma (29) derived, using multiple regression analysis, an equation for the prediction of the time lag T_L

$$T_L = 0.803 A^{0.512} (1 + U)^{-1.433} \quad (6-4)$$

where A is the basin area in square miles, U is the fraction of the basin that is impervious and T_L is the time lag in days. The equation, which was derived using both urban and rural watersheds, provided poor storm hydrograph regeneration of the storm events on Indiana watersheds and thus was considered by the author to be inadequate.

In this study attempts to predict model parameter values computed from physiographic characteristics did not result in good correlation.

Since model parameter values computed through the analysis of rainfall excess and direct runoff data varied greatly from storm to storm, the volume and duration of precipitation excess were the storm characteristics selected to represent the storm. The storm duration S_d and volume of precipitation excess V_p values, in addition to the basin areas, are given in Table 6-3. Using A , V_p and S_d , a components regression equation was derived to estimate the model parameters. As with the equations using the physiographic characteristics, only the DR, DRWF and SLR_1 model parameters provided correlation above 0.6. For all models examined use of the storm characteristics increased the correlation over that found when using only physiographic characteristics, see Table 6-1. The resulting components regression prediction equations for the DR, DRWF and SLR_1 models are given in Table 6-4. The prediction equation coefficients indicate that basins with larger areas will have larger storage coefficients. Similarly, for storms of long duration the model parameters, which represent the delaying action of the watershed, will be correspondingly larger. Thus, the coefficients seem rational. The parameters computed using the components regression equations of Table 6-4 were used for the storm hydrograph regeneration of the twenty-two storm events. The resulting correlation coefficients measuring the level of regeneration are given in Table 6-5. The correlation coefficients indicate that the DR model provided the highest correlation in fourteen of the twenty-two cases investigated, the DRWF model ranked second for nineteen storm events and the SLR_1 model had the poorest correlation in sixteen cases. Prediction equations, equations 6-5b, 6-6b and 6-7b,

Table 6-4. Model Parameter Prediction Equations

Model	Prediction Equation	R ²	Equation
DR	$K = 3.41 + 1.4 \times 10^{-7} A + 1.03 V_p + 0.059 S_d$	0.8497	6-5a
DR	$K = -13.07 + 0.96 \ln A - 0.48 \ln V_p + 2.45 \ln S_d$	0.6895	6-5b
DRWF	$K = 3.12 + 1.9 \times 10^{-7} A + 1.69 V_p + 0.089 S_d$	0.8966	6-6a
DRWF	$K = -20.20 + 1.36 \ln A - 0.75 \ln V_p + 3.48 \ln S_d$	0.7351	6-6b
SLR ₁	$K = 3.91 + 3.7 \times 10^{-7} A + 4.45 V_p + 0.220 S_d$	0.8602	6-7a
SLR ₁	$K = -44.15 + 2.91 \ln A - 0.84 \ln V_p + 7.50 \ln S_d$	0.7024	6-7b

using a logarithmic transformation of the variables A , V_p and S_d resulted in lower correlation than the use of equations 6-5a, 6-6a and 6-7a (see Table 6-4).

The correlation coefficients for the regenerated hydrographs determined using the data-optimized model parameters are also listed in Table 6-5. For the SLR_1 model the components regression parameters result in correlation comparative to those for the optimized parameter values. For ten of the twenty-two storm events the components regression parameters resulted in higher correlation than did the optimized parameter values. Although the correlation coefficients were higher for these ten storm events, the error sum of squares were also higher when the averaged parameter values were used. Both estimators are single-valued estimators of the regeneration and thus, provide contrasting estimates of the regeneration. Since the error sum of squares was used as the criteria for determining the optimal parameter values the use of averaged parameter values will always result in a higher error sum of squares. Figure 6-1 shows the observed, regenerated and predicted storm hydrographs for storm event 19.

For the DR model the parameters derived from the components regression prediction equation resulted in higher correlation than that obtained using the data optimized parameters for only five of the twenty-two storm events. Whereas, the components regression prediction equation for the SLR_1 model provided fairly good prediction results, the correlation obtained using the DR model prediction equation indicates that the loss in regeneration capability is of such magnitude that the use of such an

Table 6-5. Prediction Equation Regeneration Comparison

Storm Event	SLR ₁ Model		DR Model		DRWF Model	
	R ₁ [*]	R ₂ ^{**}	R ₁ [*]	R ₂ ^{**}	R ₁ [*]	R ₂ ^{**}
1	0.643	0.672	0.937	0.940	0.900	0.883
2	0.969	0.936	0.930	0.592	0.942	0.805
3	0.856	0.808	0.975	0.937	0.943	0.872
4	0.425	0.271	0.840	0.561	0.721	0.422
5	0.601	0.679	0.958	0.873	0.939	0.961
6	0.877	0.859	0.934	0.941	0.907	0.923
7	0.749	0.633	0.934	0.878	0.918	0.813
8	0.925	0.909	0.981	0.985	0.968	0.960
9	0.713	0.603	0.895	0.747	0.867	0.710
10	0.956	0.970	0.944	0.923	0.945	0.931
11	0.951	0.978	0.981	0.869	0.971	0.918
12	0.758	0.825	0.920	0.811	0.893	0.900
13	0.549	0.551	0.790	0.809	0.767	0.677
14	0.701	0.735	0.977	0.957	0.932	0.874
15	0.829	0.837	0.937	0.935	0.931	0.928
16	0.901	0.898	0.928	0.928	0.929	0.929
17	0.944	0.973	0.986	0.878	0.977	0.968
18	0.893	0.885	0.986	0.980	0.959	0.940
19	0.984	0.994	0.983	0.939	0.979	0.979
20	0.794	0.656	0.985	0.922	0.949	0.816
21	0.889	0.863	0.995	0.978	0.969	0.928
22	0.859	0.830	0.916	0.957	0.889	0.922
Average R	0.807	0.789	0.941	0.879	0.922	0.871

*R₁ : Correlation coefficient using optimized parameter values
(average R = 0.890)

**R₂ : Correlation coefficient using predicted parameter values
(average R = 0.846)

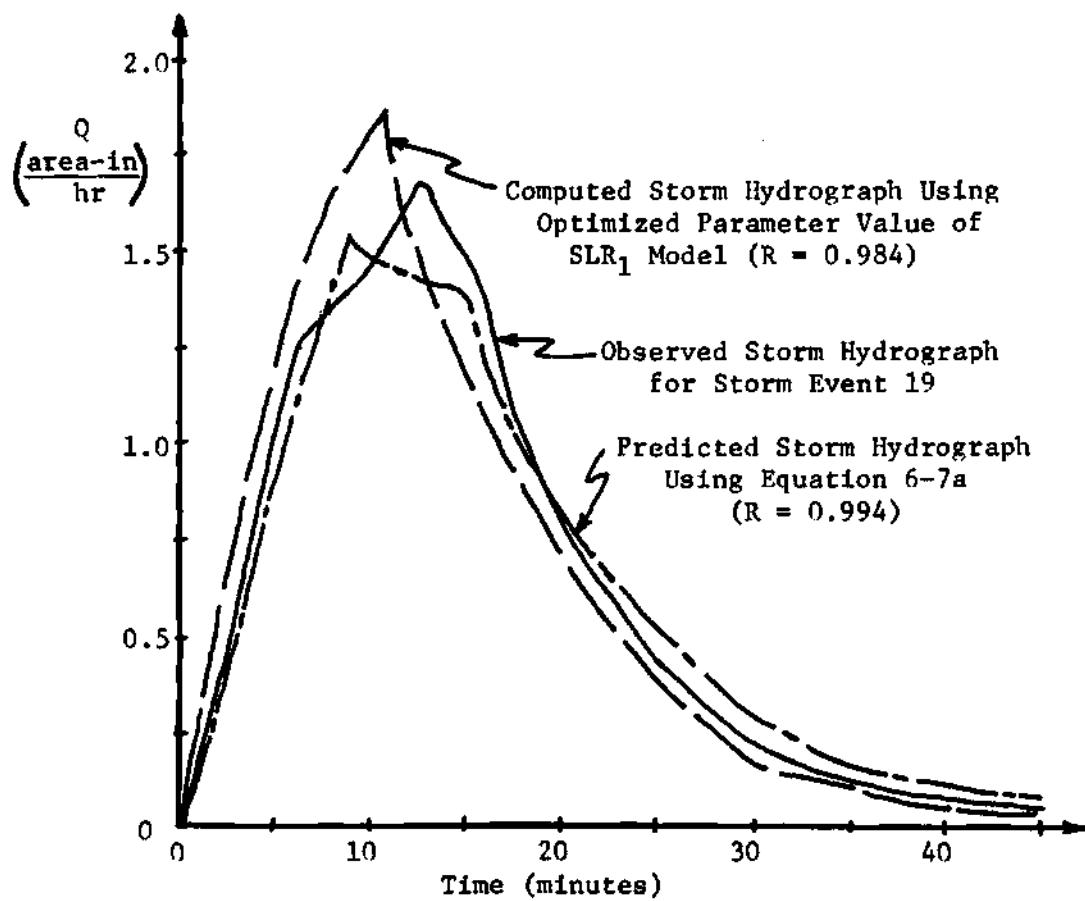


Figure 6-1. Regeneration Using Predicted Parameter Value

equation on ungaged watersheds would be risky. The loss in regeneration capability might be partially the result of the comparatively low correlation (0.921) between the observed and predicted model parameters.

The components regression prediction equation, equation 6-6a, for the DRWF model did not provide parameter values which resulted in acceptable regeneration. The predicted parameter values resulted in correlation coefficients greater than those obtained using the optimized parameter values for only four of the twenty-two storm events. The correlation coefficients for the optimized parameter values exceeded those obtained using the predicted parameter values by 0.300 in ten of the twenty-two cases examined. The DRWF model, when compared with the other models, had the highest correlation (0.947) between the predicted and optimized parameter values and thus, better regeneration when using the predicted parameter values was expected. The regeneration of the optimized DRWF model parameter values was comparatively low. Thus, the prediction equation, which was derived using parameter values that did not provide good regeneration, should not be expected to provide parameter values capable of good storm hydrograph regeneration.

Parameter Prediction for Ungaged Watersheds

Having derived prediction equations which can be used to estimate the parameters for the DR, DRWF and SLR_1 models, it is necessary to examine the capability of the prediction equations for the estimation of parameter values on ungaged watersheds. For this purpose, four storm events (discussed in Chapter III) were collected from watersheds not used in the derivation of the prediction equations. Using the ϕ index

method, the volumes of observed precipitation and runoff were used to estimate the distribution of precipitation excess. The basin area and the volume and duration of precipitation excess were then used to compute the model parameters. The resulting parameters were then used to predict storm hydrographs. The level of regeneration was again measured by the correlation coefficient. Also, the observed storm hydrograph and the computed distribution of precipitation excess were used to derive the model parameters, and subsequently, correlation coefficients were computed as a measure of the regeneration. The correlation coefficients for both the optimized parameters and predicted parameter values are given in Table 6-6. For the DR and DRWF models the predicted parameter values always resulted in poorer storm hydrograph regeneration than that provided by the optimized parameter values. For two storm events, E1 and E3, the reduction in correlation, when using the prediction equations for the DR and DRWF models exceeded 0.300. As with the results for the storm events used in the derivation of the prediction equations, the SLR_1 model prediction equation provides regeneration comparable to that obtained using the optimized parameter values.

Analysis of Prediction Equations

A primary objective of this study was to determine the adequacy of linear conceptual models for the representation of the rainfall-runoff process. A test of the adequacy of a model is the ability of the model to predict streamflow for ungaged areas. But if the parameter values derived from the analysis of data do not accurately reproduce the observed output data then prediction equations derived from such parameter values cannot be expected to provide computed parameter values capable

Table 6-6. Regeneration for Ungaged Watersheds

(a) Correlation Coefficient Using Data
Optimized Parameter Values (average R = 0.833)

Model	Storm Event			
	E ₁	E ₂	E ₃	E ₄
SLR ₁	0.905	0.785	0.464	0.380
DR	0.972	0.976	0.936	0.910
DRWF	0.971	0.965	0.863	0.866
Average R	0.949	0.909	0.754	0.719

(b) Correlation Coefficient Using
Predicted Parameter Values (average R = 0.644)

Model	Storm Event			
	E ₁	E ₂	E ₃	E ₄
SLR ₁	0.829	0.922	0.031	0.659
DR	0.591	0.844	0.440	0.854
DRWF	0.659	0.920	0.188	0.786
Average R	0.693	0.885	0.220	0.766

of adequate prediction of storm runoff on ungaged watersheds. The results of the data analysis in Chapter IV (see Table 4-7) indicate that the model response functions defined by optimized parameter values were not indicative of the hydrologic response of the watershed. Thus, the optimized parameter values were not expected to provide prediction equations capable of producing computed parameter values which adequately reproduced observed storm events or storm events on ungaged basins.

Use of the optimized parameter values for the SLR_1 , DR and DRWF models resulted in an average correlation of 0.890 for the twenty-two storm events. Use of the parameter values predicted from equations 6-5a, 6-6a and 6-7a resulted in an average correlation of 0.846 for the twenty-two storm events. The reduction in correlation of 0.044 indicates that use of the prediction equations for predicting parameter values for storm events used in the development of the prediction equations does not result in a significant decrease in potential regeneration.

An average correlation coefficient of 0.833 resulted from the use of data optimized parameter values for the SLR_1 , DR and DRWF models and four storm events not included in the development of the prediction equations. Equations 6-5a, 6-6a and 6-7a, which were then used to predict model parameter values for the four storm events E1, E2, E3 and E4, provided an average correlation of 0.644. Thus, as indicated by the reduction in the average correlation coefficient from 0.833 to 0.644, the prediction equations are not capable of providing adequate parameter values for storm events not included in the development of the equations.

CHAPTER VII

SENSITIVITY ANALYSIS

In Chapter V an analysis of artificial data indicated that the largest source of error in the regeneration of observed storm hydrographs was the constraining shape of the conceptual model response function. The ability of a response function to represent the hydrologic response of a watershed is reflected in the sensitivity of the parameters which define the response function. A function called the sensitivity function will be developed and used as a measure of the ability of the model response function to represent the actual hydrologic response of a watershed. The sensitivity function can also be used to compute the change in model output resulting from the uncertainty involved in the estimation of the model parameters.

The Sensitivity Function

The response functions of the models investigated herein, such as equation 4-17 for the DR model, can be represented by the differential equation form

$$f(\dot{y}, y, K_1, K_2, \dots, K_n; t) = f(x) \quad (7-1)$$

where x and y are the input and output, respectively, \dot{y} is the first derivative of the output with respect to time, t represents time and K_i , $i = 1, 2, \dots, n$, are the model parameters. The solution of the differ-

ential equation, equation 7-1, is given by

$$y = f(K_1, K_2, \dots, K_n ; t) \quad (7-2)$$

For the case of a single parameter model, the solution is

$$y = f(K ; t) \quad (7-3)$$

The solution to the differential equation represents the response function. Equation 7-3 corresponds to the expression for the response function of the DR model given by equation 4-17. Since the computed storm hydrograph, generated by convolving the response function of equation 7-3 with the precipitation excess, will probably differ from the observed storm hydrograph, it would be of interest to examine the effect of varying the storage coefficient K on the model response function, and thus, the computed storm hydrograph. The change in the response of a model Δy for a small change in K can be estimated by dividing the difference in the solutions for the parameter values $K + \Delta K$ and K by the change in the parameter value ΔK ,

$$\frac{\Delta y}{\Delta K} = \frac{y(K + \Delta K ; t) - y(K ; t)}{\Delta K} \quad (7-4)$$

In the limit as ΔK approaches zero,

$$\lim_{\Delta K \rightarrow 0} \frac{y(K + \Delta K ; t) - y(K ; t)}{\Delta K} \rightarrow \frac{dy(K ; t)}{dK} = \dot{y}(K ; t) \quad (7-5)$$

$\$ (K ; t)$ is the sensitivity of the solution 7-3 to variation in the parameter K . It is a function of both time and the value of the model parameter and is called the sensitivity function. Thus, sensitivity is the change in the response of a model for a small change in the model parameter.

For a dynamic system in steady-state the solution, or response, does not depend on time and the sensitivity function is

$$\$_s(K_1, K_2, \dots, K_n) = \text{static parametric sensitivity function (7-6)}$$

Steady-state response functions are important in electronic systems, but the hydrologist is most often interested in the transient response of the watershed, and thus, the dynamic, or time-dependent, sensitivity function is of primary importance. Since the model response varies with changes in the model parameters, as well as with time, the sensitivity function is dynamic as well as parametric. Thus, the dynamic parametric sensitivity function

$$\$_p(K_1, K_2, \dots, K_n ; t) = \text{dynamic parametric sensitivity function (7-7)}$$

is used when steady-state conditions do not exist. If the sensitivity of a model for a specified level of parameter values is of interest then the dynamic sensitivity function

$$\$_d(K_{01}, K_{02}, \dots, K_{0n} ; t) = \text{dynamic sensitivity function (7-8)}$$

is used. In the dynamic sensitivity function K_{01} represents the specified value of the i^{th} parameter. For multi-parameter models the response function is dependent on the values of all the model parameters. In estimating the sensitivity of the response function to variation in any one parameter, it should be emphasized that the values of the other parameters will, in general, influence the resulting value of the sensitivity functions.

The sensitivity functions of equations 7-6, 7-7 and 7-8 can be represented by vector spaces. The value of the static sensitivity function depends on n parameter values. Thus, to represent the static sensitivity function a set of $n + 1$ coordinate axes, one for each of the n model parameters and one for the value of the sensitivity function, will be required. The value of the sensitivity function at specific values of all parameters defines a surface in an $n + 1$ vector space. A sensitivity surface can also be defined for the dynamic parametric sensitivity function $\$p$. The $\$p$ surface would require $n + 2$ coordinate axes, one for each of the n model parameters, one for time (t) and one for the value of the sensitivity function. The dynamic sensitivity function $\$d$ only requires a two-dimensional space because the n model parameter values are pre-determined. Thus, one coordinate axis is used for time and the other axis is used for the value of $\$d$.

The Sensitivity Equation

The sensitivity functions can be used to estimate the change in output for changes in the model parameter values. If an analytical expression of the model response function is available, and if this expression

can be differentiated or the higher derivatives estimated, then the incremented solution $y(K + \Delta K ; t)$ can be estimated by a Taylor series equation

$$y(K + \Delta K ; t) = y(K ; t) + \frac{\partial y}{\partial K} \Delta K + \frac{1}{2!} \frac{\partial^2 y}{\partial K^2} \Delta K^2 + \dots \quad (7-9)$$

Equation 7-9 can be used to estimate the solution for small variations in the parameter K .

If the change in the model parameter is small then the values ΔK^2 , ΔK^3 , ... will be much smaller than ΔK , for $\Delta K \ll 1$, and equation 7-9 can be approximated by

$$y(K + \Delta K ; t) \approx y(K ; t) + \frac{\partial y}{\partial K} \Delta K \quad (7-10)$$

The value of the first term of the truncated series can be used as an estimate of the truncation error of equation 7-10. Estimates of the truncation error were not made for this study.

For multi-parameter models the linearized sensitivity equation is

$$y(K_1 + \Delta K_1, \dots, K_n + \Delta K_n; t) = y(K_1, \dots, K_n; t) + \sum_{i=1}^n \frac{\partial y}{\partial K_i} \Delta K_i \quad (7-11)$$

The partial derivatives $\partial y / \partial K_i$, $i=1, 2, \dots, n$, are the sensitivity functions for the n model parameters. The second order terms of the truncated series for the multi-parameter Taylor series expansion can be used to estimate the truncation error. The second order terms include

the main, ΔK_i^2 , and interaction, $\Delta K_i \cdot \Delta K_j$, $i \neq j$, elements.

Sources of Parametric Error

In order to use the sensitivity equation to estimate the potential change in the model solution, equation 7-2, it is necessary to know the solution of the equation for the nominal parameter values, the dynamic sensitivity functions S_d and the expected parametric error. Three sources of parametric variation for any given model were investigated in Chapter V. These sources are (1) data error, (2) the inability of the model response function to represent the watershed response, and (3) the distribution of precipitation excess.

The Sensitivity Functions of the Conceptual Models

The system response function of a model is the output resulting from a unit impulse input. Since the model output will depend on the values of the parameters it is reasonable to consider the effect of parametric error on the system response function. The effect of parametric error for other input functions can be easily determined for linear conceptual models by using the convolution integral. For small magnitudes of parametric error, sensitivity analysis provides a more convenient alternative for estimating parametric error effects than the determination of the model system response function.

Each conceptual model has a sensitivity function with a characteristic shape, but the magnitude of the sensitivity function ordinates will vary with changes in the values of the model parameters. Since model regeneration capability and parametric error are influenced by sensitivity it is important to consider the corresponding ordinates of the sensitivity

and system response functions. For example, if the peak of the system response function is of primary importance then for better regeneration of the peak discharge a model with higher sensitivity at the system response function peak might be preferable. The following paragraphs of this section will discuss the characteristic shape of the sensitivity functions and correspondence between ordinates of the system response function and sensitivity function of the linear conceptual models investigated herein. A comparison of the various models will not be made in this section since comparisons of sensitivity should be made on the basis of optimized model parameters and not for arbitrarily selected parameter values. It is necessary to use optimized parameter values because both the model response function and sensitivity function depend on the model parameter values. The structure of the sensitivity functions will be discussed for each of the conceptual models. The implications of the structures will be made after each structure has been discussed separately.

Single Linear Reservoir Model

The sensitivity function S_p of the single linear reservoir model is given by

$$S_1(K;t) = (t - K)e^{-t/K} / K^3 \quad (7-12)$$

Like the model response function, the sensitivity function is a function of the storage coefficient K and time t . At $t = 0$, $S_1(K;t)$ has its largest absolute value of $1/K^2$ (see Figure 7-1). $S_1(K;t)$ is negative at

$t = 0$ and increases in value to zero at $t = K$ and continues to increase to a relative maximum of e^{-2}/K^2 at $t = 2K$. From time $t = 2K$ the ordinates decrease and approach zero asymptotically. The model output becomes less sensitive to parametric error as the value of K increases. Also, for increases in the storage coefficient the relative peak at $t = 2K$ occurs sooner in time and the recession approaches zero quicker. These characteristics are apparent from Figure 7-1. Since the model response function and S_1 both peak at $t = 0$, the peak of the model would be more influenced by parametric error than would other ordinates of the model response function.

Single Linear Reservoir with Feedback Model

For unity feedback around a single linear reservoir the sensitivity function is given by

$$S_2(K;t) = (2t - K)e^{-2t/K} / K^3 \quad (7-13)$$

Figure 7-2 shows that the model response function is maximum at $t = 0$. The absolute value of the sensitivity function is also maximum at $t = 0$ with a value of $-1/K^2$. S_2 increases from $t = 0$ to zero at $t = K/2$ and continues to increase to a relative maximum of $(3e^{-4})/K^2$ at $t = K$. From time $t = K$, S_2 decreases asymptotically to zero. Model sensitivity decreases with increases in the storage coefficient. Although the timing and magnitudes differ, the SLR and SLRWF models have sensitivity functions of similar shape.

Double Routing Model

The sensitivity function of the double routing model is given by

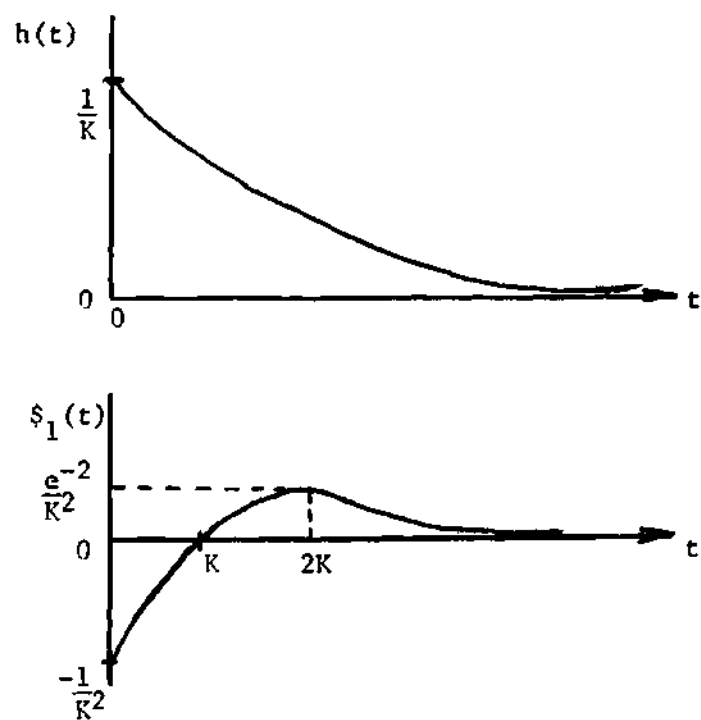


Figure 7-1. Sensitivity Functions : SLR Model

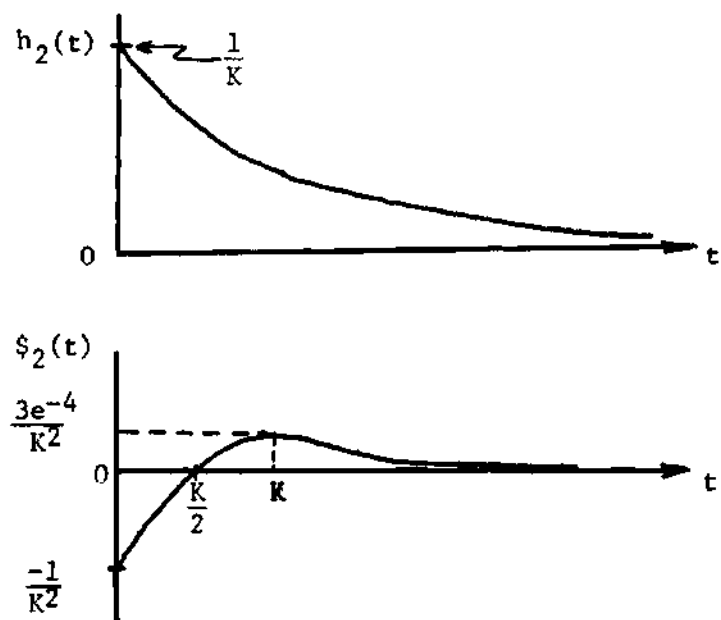


Figure 7-2. Sensitivity Functions : SLRWF Model

$$S_3(K;t) = [t(t - 2K)e^{-t/K}] / K^4 \quad (7-14)$$

Unlike the SLR and SLRWF models, the peak of the sensitivity function of the DR model does not occur at the same time as the peak of the model response function. S_3 is zero at $t = 0$. It decreases to an absolute maximum of approximately $-0.461 / K^3$ at $t = K(2 - \sqrt{2})$. From the maximum, the sensitivity increases in value to zero at $t = 2K$ and then increases to a relative maximum of approximately $0.1591 / K^3$ at $t = (2 + \sqrt{2})K$. For $t > (2 + \sqrt{2})K$ the sensitivity decreases asymptotically to zero. The sensitivity of the DR model at the peak of the model response function has a value of $-e^{-1}/K^2$. The sensitivity of the response function decreases for increases in the parameter K . The sensitivity function is shown in Figure 7-3.

Double Routing with Feedback Model

The sensitivity function of the DRWF model, as given by 7-15,

$$S_4(K;t) = [(t - K)e^{-t/K} - (2t - K)e^{-2t/K}] / K^3 \quad (7-15)$$

is shown in Figure 7-4. The sensitivity is zero at $t = 0$ and when $(t - K) / (2t - K) = e^{-t/K}$. Between the two points of zero sensitivity the maximum sensitivity of the DRWF model occurs. Empirical data has indicated that the point of maximum sensitivity occurs at approximately $t = 0.4 K$. For a given value of K the time of maximum sensitivity occurs at the time where the equality $(2K - t) = 4(K - t)e^{-t/K}$ is valid. This equality can also be used to compute the time of the relative maximum

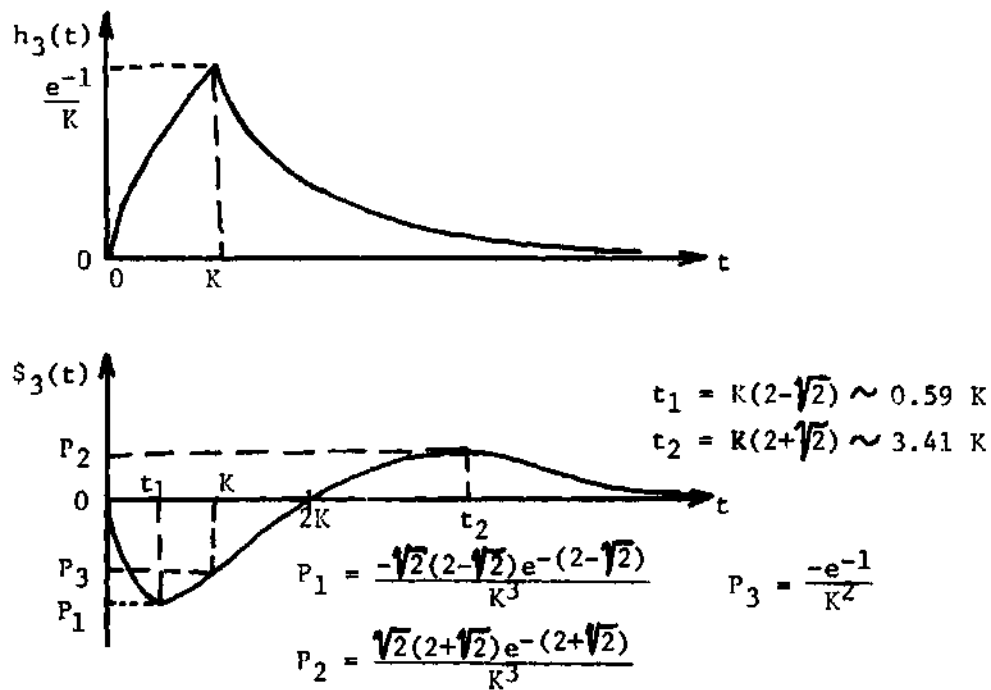


Figure 7-3. Sensitivity Functions : DR Model

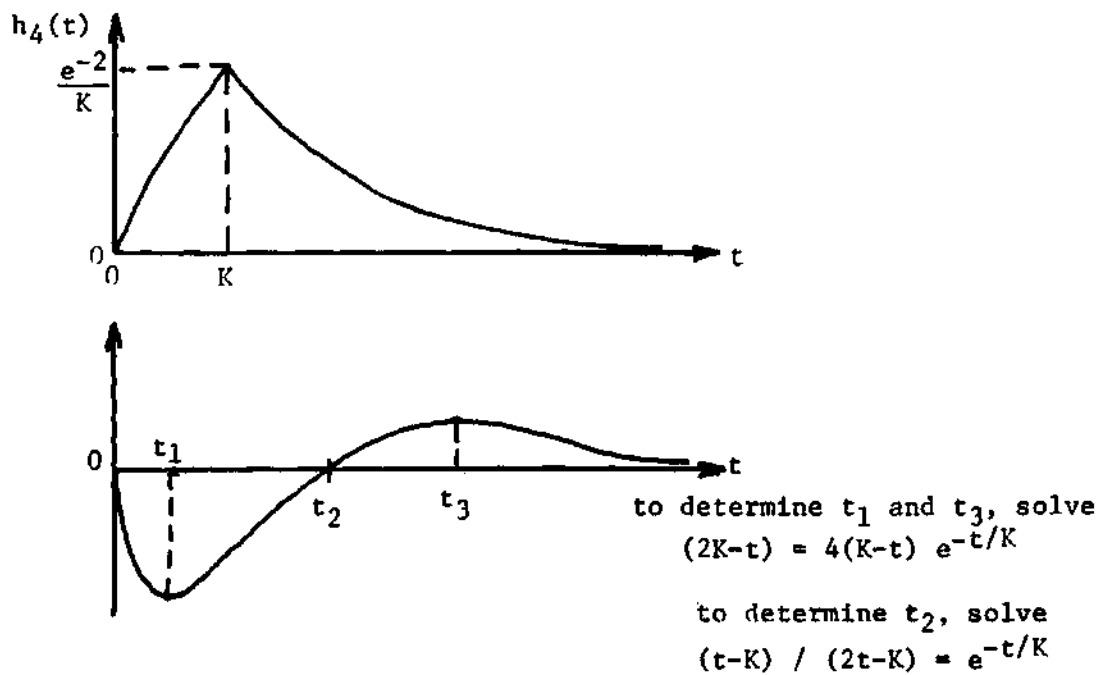


Figure 7-4. Sensitivity Functions : DRWF Model

sensitivity value which occurs after the second point of zero sensitivity. The magnitude of the two maximum sensitivity values can be computed from equation 7-15 once the time of maximum sensitivity has been determined.

Nash Model

The Nash model is a function of two parameters, K and n . Thus, there are two sensitivity functions for the Nash model. The sensitivity function (see Figure 7-5) for the storage coefficient K is

$$S_5(K, n; t) = \frac{t^{n-1} e^{-t/K} (t - nK)}{K^{n+2} \Gamma(n)} \quad (7-16)$$

where $\Gamma(n)$ is the gamma function. The sensitivity function S_5 is zero at $t = 0$ and decreases to an absolute maximum at $t_{\max} = K(n - \sqrt{n})$. The value of the sensitivity function increases to a value of zero at $t = nK$ and continues to increase to a relative maximum at $t = K(n + \sqrt{n})$. The value of the sensitivity function at either the absolute or relative maximum can be determined by substituting the values of K , n and t_{\max} into equation 7-16.

The sensitivity function (see Figure 7-5) for the parameter n is given by

$$S_6(K, n; t) = \frac{t^{n-1} e^{-t/K}}{K^n \Gamma(n)} [\ln_e t - \ln_e K - \frac{\Gamma'(n)}{\Gamma(n)}] \quad (7-17)$$

where $\Gamma'(n)$ is the derivative with respect to n of $\Gamma(n)$. The relative maximum occurs for the value of time when

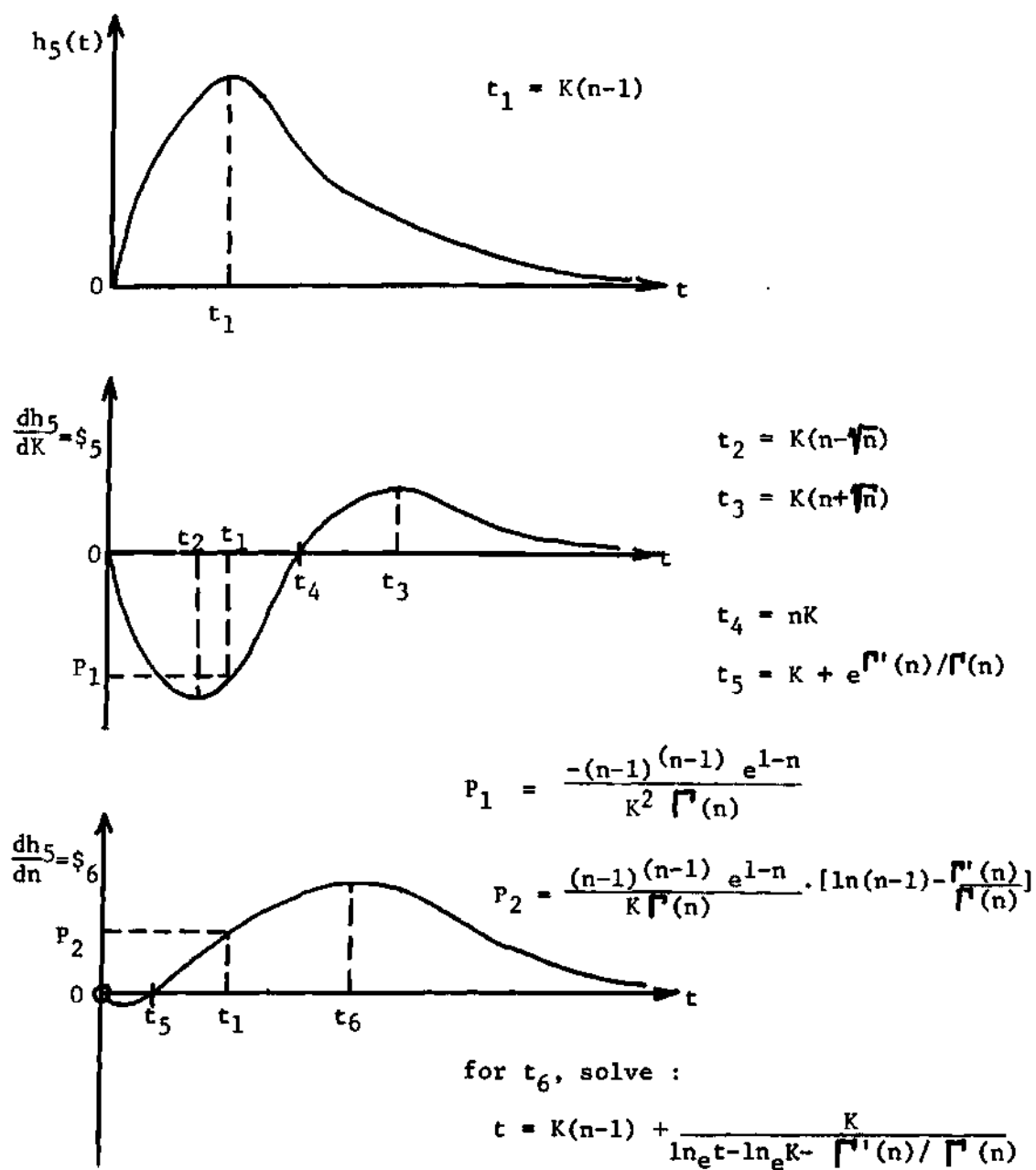


Figure 7-5. Sensitivity Functions : Nash Model

$$t = K(n-1) + \frac{K}{[\ln_e t - \ln_e K - \frac{\Gamma'(n)}{\Gamma(n)}]}, t > 0 \quad (7-18)$$

At time $t = 0$ the sensitivity function is indeterminate. The time at which the sensitivity is zero is when

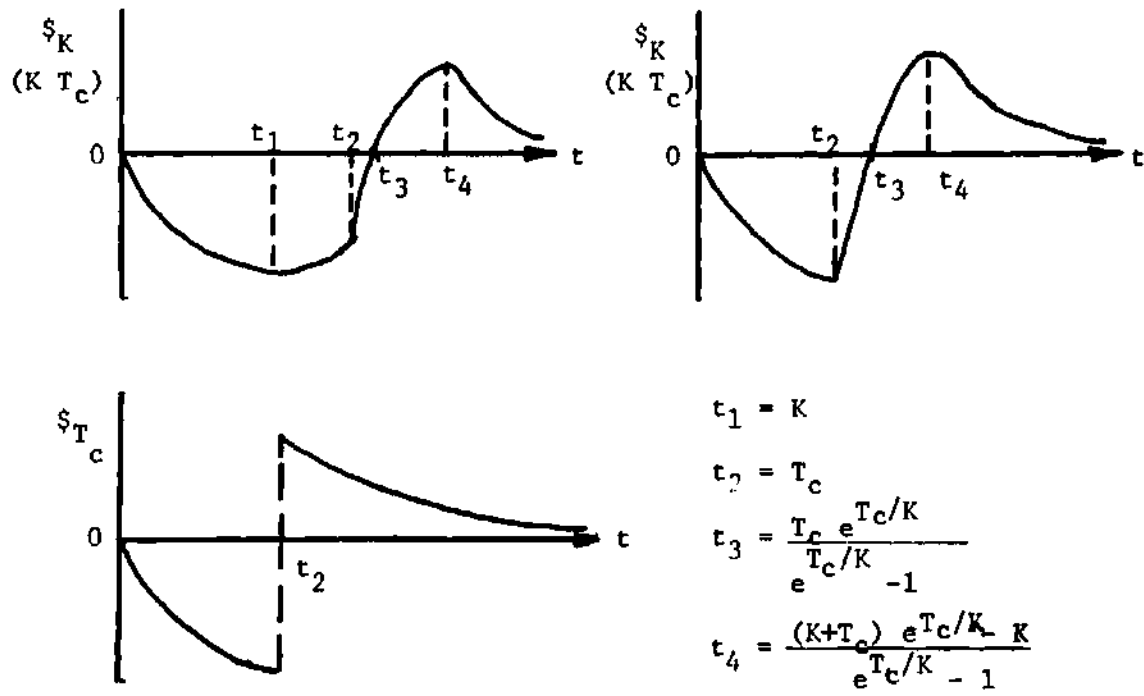
$$\ln_e t = \ln_e K + \frac{\Gamma'(n)}{\Gamma(n)} \quad (7-19)$$

Linear Channel-Linear Reservoir Models

The three LCLR models are a function of the parameters K and T_c . Thus, each model will have two sensitivity functions. The sensitivity functions for the three models are given in Figures 7-6, 7-7 and 7-8. The sensitivity function plots are all characterized by a discontinuity at $t = T_c$. This results from the discontinuity of time-area-concentration diagram at that point on the time scale. The sensitivity at any time t can be determined from the sensitivity functions given by equations 7-20 through 7-25.

The Sensitivity-Regeneration Capability Trade-Off

There is an inherent desire of every model builder to develop a model which is capable of a high degree of output regeneration. The ability of a model to regenerate observed output depends on the ability of the response function to conform to the shape of the hydrologic response. As the sensitivity of a model increases the model more easily adjusts to the shape of the hydrologic response and thus, the potential level of regeneration capability increases. The level of regeneration



$$S_K = \begin{cases} -t e^{-t/K} / T_c K^2 & 0 \leq t \leq T_c \\ [e^{-(t-T_c)/K} (t-T_c) - t e^{-t/K}] / T_c K^2 & T_c \leq t \leq \infty \end{cases} \quad (7-20)$$

$$S_{T_c} = \begin{cases} (e^{-t/K} - 1) / T_c^2 & 0 \leq t \leq T_c \\ [e^{-(t-T_c)/K} (T_c/K - 1) + e^{-t/K}] / T_c^2 & T_c \leq t \leq \infty \end{cases} \quad (7-21)$$

Figure 7-6. Sensitivity Functions : LCLR-R Model

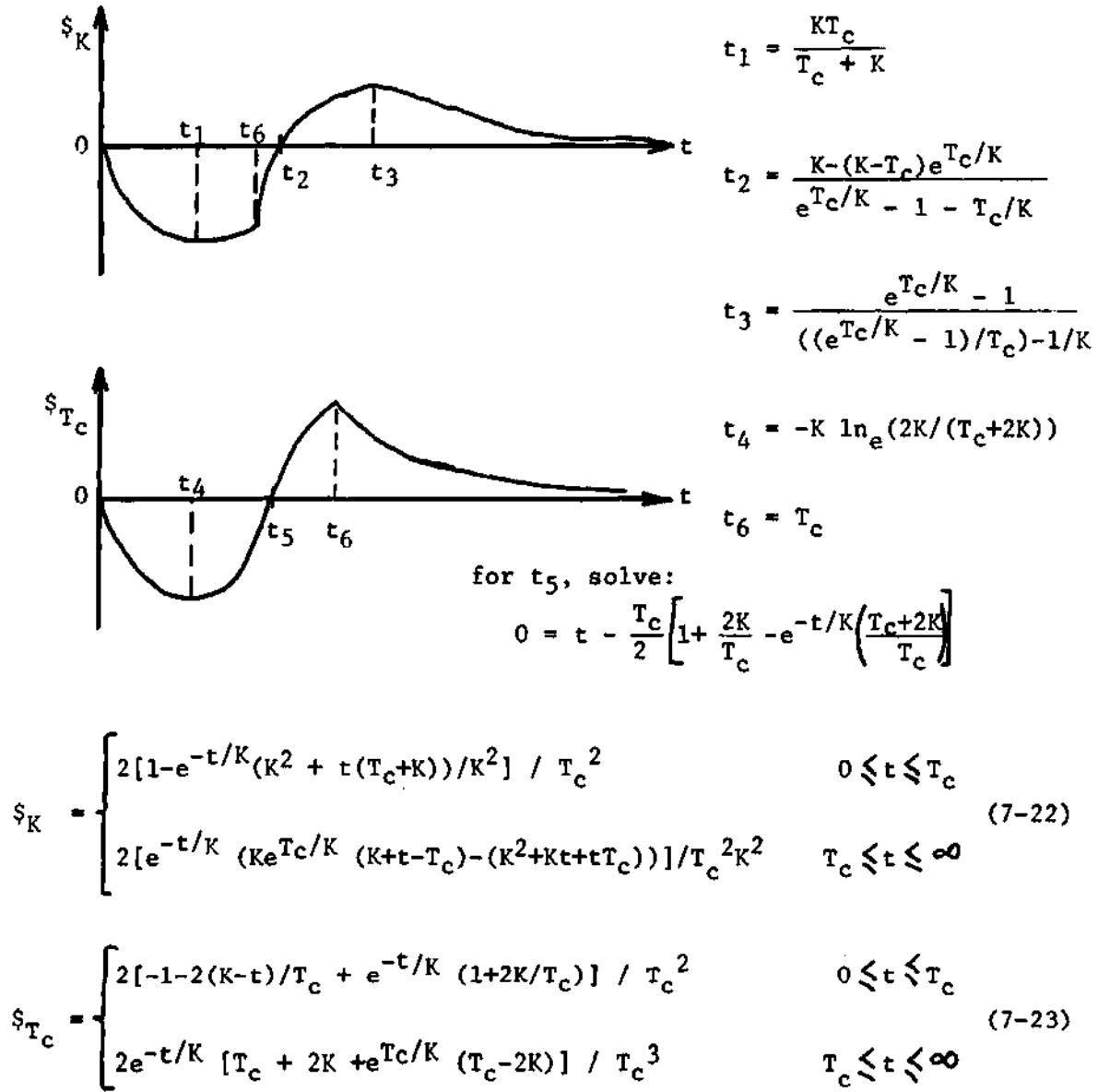


Figure 7-7. Sensitivity Functions : LCLR-LT Model

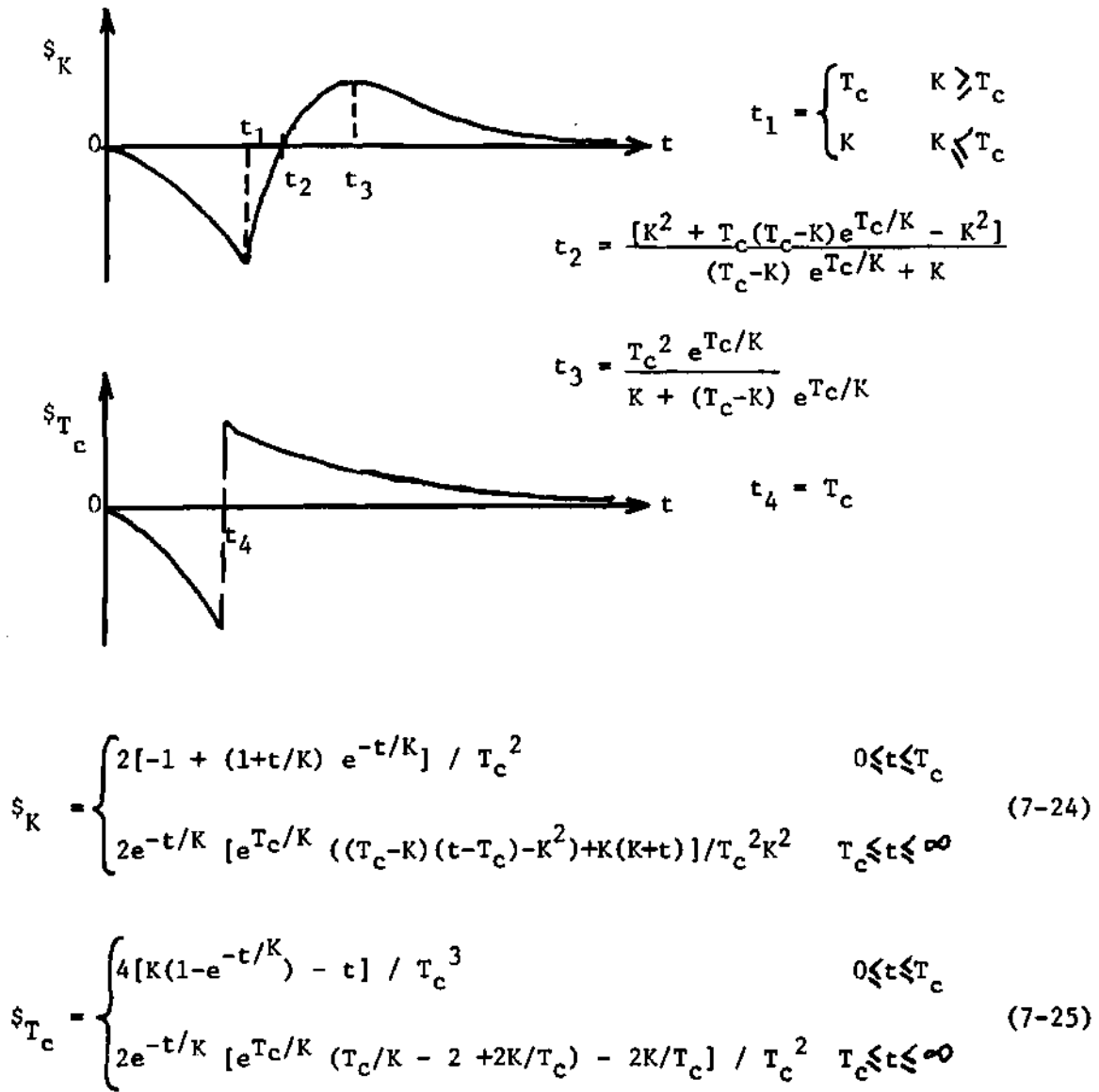


Figure 7-8. Sensitivity Functions : LCLR-RT Model

attained may be measured by the correlation coefficient. Unfortunately, as the sensitivity of a model is increased the potential error induced into the output by parametric error increases. This is evident from the sensitivity equation, equation 7-10. The change in output is given by

$$y(K+\Delta K;t) - y(K;t) = \frac{dy}{dK} \Delta K = \$ (K;t) \Delta K \quad (7-26)$$

For example, if two models M_A and M_B have sensitivity functions $\$_A$ and $\$_B$, where $\$_A > \$_B$, the change in output would be greater for model A if $\Delta K_A \geq \Delta K_B$. Thus, it is the product of the sensitivity function and the parametric error, $\$(K;t) \cdot \Delta K$, and not the individual terms, that is important. It should be emphasized that models with greater sensitivity are not necessarily accompanied by correspondingly less parametric error. Models that are more sensitive are also more adjustable and thus, more likely to provide better estimates of the true response of the watershed. If the model parameter is to be estimated by data analysis, parametric error can result from the sources discussed previously in this chapter. If the model parameter is to be estimated using a prediction equation based on topographic and storm characteristics, the standard error can be used as an estimate of the parametric error. Thus, in the selection of a model for use in estimating the hydrologic response of a watershed the potential effect of parametric error on the computed output must be weighed against the regeneration capability of the model. That is, a model which is more sensitive, and thus, potentially more capable of providing better regeneration of observed output, might not be preferred to

a model with lower sensitivity if the higher sensitivity is accompanied by relatively large expected parametric error.

Comparison of Conceptual Model Sensitivity

Since model sensitivity influences the regeneration capability of the model it is important to compare the sensitivity of the various models. The sensitivity functions cannot be compared on the basis of identical, arbitrarily selected model parameters. The comparison of sensitivity functions must be made using functions defined by model parameters which have been optimized for a given data set. That is, instead of comparing, for example, $\$_1(K_1 = 1; t)$ with $\$_3(K_3 = 1; t)$, where $\$_1(K; t)$ and $\$_3(K; t)$ are the sensitivity functions of the SLR and DR models, respectively, the comparison must be between $\$_1(K_1'; t)$ and $\$_3(K_3'; t)$, where K_1' and K_3' are the optimized model parameters.

In order to demonstrate the sensitivity-regeneration capability relationship, it is necessary to provide single-valued estimates of the sensitivity function and the regeneration capability. The sensitivity function should be used as a measure of sensitivity but it would be difficult to compare distributed functions. Three possible single-valued sensitivity estimators are: (1) the maximum ordinate of the sensitivity function, (2) the sensitivity at the peak of the model response function, and (3) the area under the sensitivity function between some specified times. Using the area enclosed by the sensitivity function between specified times might not lead to a distinction between uniformly and time-varying distributed sensitivity functions. The implications of the first two estimators can be compared using the sensitivity functions of

Figure 7-9. The peak of the sensitivity function S_A occurs simultaneously with the peak of the response function $h_A(t)$ while the peak of S_B occurs before the peak of the response function $h_B(t)$. If a hydrologist was only interested in estimating peak discharge then the sensitivity at the peak of the response function would probably be the preferred estimator. If the entire hydrograph were of importance then the peak sensitivity might be selected to represent the sensitivity function. When considering sensitivity functions which are explicitly expressed both sensitivity estimators, the absolute value of the maximum sensitivity and the sensitivity at the peak of the response function, will lead to similar conclusions since the shape of the sensitivity functions are characteristic of the model. That is, increases or decreases in sensitivity are apparent in all ordinates of the sensitivity functions.

In addition to selecting a single-valued estimator of the sensitivity function it is necessary to provide a single-valued estimator of the regeneration. In Chapter IV the correlation coefficient and the standard error of the estimate were defined and used to measure model regeneration capability. These two statistics will be used as regeneration estimators and compared with the single-valued sensitivity estimators.

Comparison of Single Parameter Conceptual Model Sensitivity

The sensitivity of the following four single-parameter conceptual models were compared: [1] SLR, [2] SLRWF, [3] DR, and [4] DRWF. For the storm events analyzed and discussed previously, the DR model consistently provided better output regeneration whether the regeneration was measured

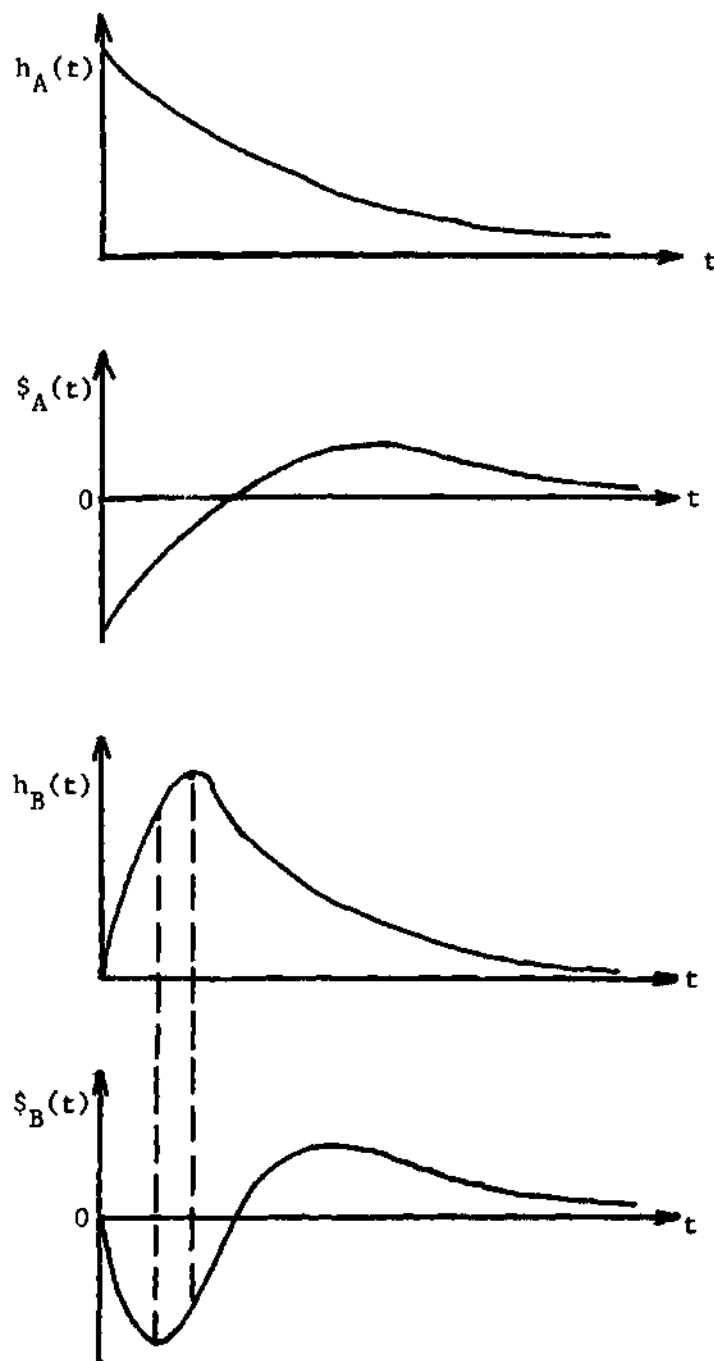


Figure 7-9. Comparison of Sensitivity Functions

by the correlation coefficient, Table 7-1, or the standard error of the estimate, Table 7-2. The regeneration was consistently less for the SLRWF model than for any other model whether measured by the standard error or correlation coefficient. The correlation coefficient criterion indicates that the DRWF model provides better regeneration than the SLR model, whereas use of the standard error to measure regeneration results in the opposite conclusion, see Table 7-2. When using the maximum ordinate of the sensitivity function to represent the sensitivity function, Table 7-3 indicates that the DR model is the most sensitive while the DRWF, SLR and SLRWF models are progressively less sensitive. For the twenty-two storm events, the ranking of the models on the basis of the correlation coefficients and the sensitivity estimates, using either the maximum sensitivity or the sensitivity at the peak of the response function, are identical. Because the square of the correlation coefficient equals the ratio of the explained sum of squares to the total sum of squares, it is invariant to the magnitude of the hydrographs. Therefore, when comparing data sets of different magnitudes the correlation coefficient provides a better means of comparing the regeneration of storm hydrographs enclosing equal volumes of runoff than does the standard error of the estimate, which is not invariant to magnitude.

For eleven of the twenty-two storm events analyzed the ranking of the correlation coefficients were identical to the ranking of the maximum sensitivity estimators, see Appendix L. For example, for storm event 3 the double routing model provided the highest correlation ($R = 0.975$) and the highest peak sensitivity ($|\dot{S}_p| = 0.00872$) while the DRWF ($R = 0.943$,

Table 7-1. Regeneration Capability Measured by Correlation Coefficient

Rank*	SLR	SLRWF	DR	DRWF
1	2	1	18	1
2	2	1	2	17
3	17	0	1	4
4	1	20	1	0

*Rank = 1 indicates highest correlation coefficient

Table 7-2. Regeneration Capability Measured by Standard Error

Rank*	SLR	SLRWF	DR	DRWF
1	5	0	17	0
2	16	3	2	2
3	1	2	3	15
4	0	17	0	5

*Rank = 1 indicates lowest standard error

Table 7-3. Rank of Sensitivity Estimates

Rank*	SLR	SLRWF	DR	DRWF
1	0	4	18	0
2	7	0	1	14
3	13	2	3	4
4	2	16	0	4

*Rank = 1 indicates highest sensitivity

$|\$p| = 0.00577$), SLR_2 ($R = 0.921$, $|\$p| = 0.00381$) and $SLRWF$ ($R = 0.830$, $|\$p| = 0.00235$) models provided progressively lower correlation and sensitivity. That is, the model having the highest sensitivity also had the highest correlation coefficient. There are three reasons why the remaining eleven storm events did not exhibit the same correspondence between sensitivity and regeneration capability. First, if the correlation coefficients of the various models differ significantly, for example, by about 0.05, then the models are not providing comparatively equal regeneration, and thus the sensitivity functions are not indicative of the true sensitivity. Second, it was shown in Chapter IV that a correlation coefficient of less than 0.95 indicated poor regeneration. Thus, the model parameter computed from data was not representative of the true value and both the model response function and sensitivity function were misleading. Third, the single-valued estimator of the sensitivity function may not adequately represent the time distribution of parametric sensitivity. Also, the correlation coefficient, a single-valued estimator of the regeneration, might not provide adequate representation of the output regeneration.

For cases with relatively equal correlation values it might be necessary to compare the entire sensitivity functions and computed output functions. The table in Appendix L indicates that the data analysis for storm events 7, 9, 10, 11, 13, 15, 16, and 22 resulted in significantly different correlation for the four models. For these cases the difference in correlation explains the lack of correspondence between sensitivity and regeneration.

Storm events 2, 8 and 19 have somewhat similar correlation coefficients but the highest correlation is not accompanied by the highest sensitivity. This results from the inability of the correlation coefficient to indicate that the greatest difference between the observed and computed storm hydrographs occurs in the region where the models are most sensitive. For observed storm hydrographs, such as storm events 2 (see Figure 7-10), 8 and 19, in which the constraining shape of the response function results in especially large deviations in the region of highest sensitivity, the higher level of regeneration will occur for the less sensitive models. For the model with the highest sensitivity the error in the parameter value due to the inability of the model response function to represent the hydrologic response of the watershed results in greater differences in computed storm hydrograph. The change in output could be computed using the sensitivity equation.

Comparison of Two-Parameter Model Sensitivity

The comparison of multi-parameter models is similar to single-parameter model comparison even though it is somewhat more difficult. As with the single-parameter models it is necessary to represent the sensitivity functions and level of regeneration with single-valued estimators. The correlation coefficient will be used to represent the level of regeneration while estimates of the sensitivity functions will be made using the maximum ordinate of the sensitivity function and the sensitivity at the peak of the model response function. It is also necessary to make the comparisons using sensitivity functions computed with optimized parameters and not parameter values selected arbitrarily. Also,

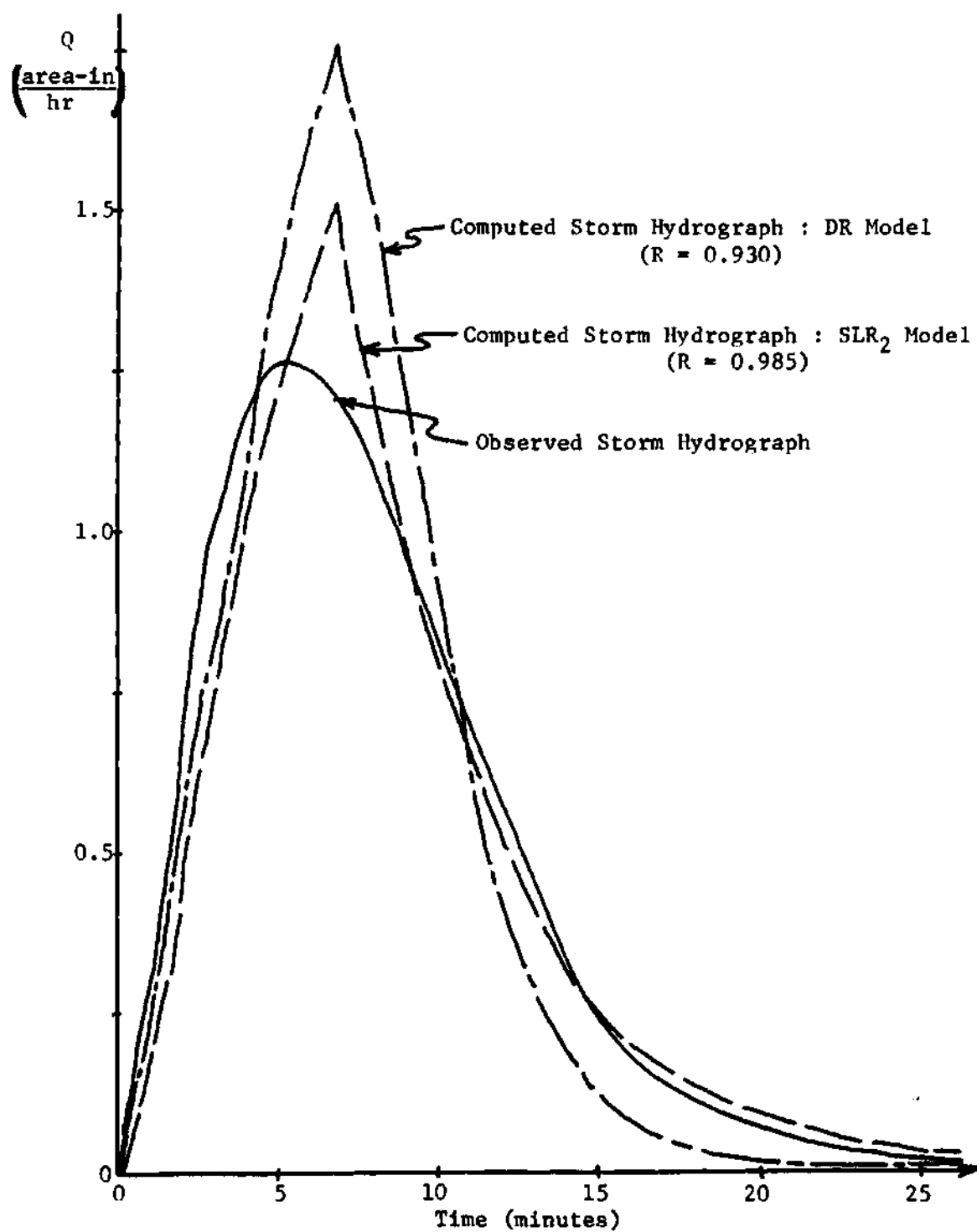


Figure 7-10. Regeneration of Storm Event 2

model comparison should be made only for data resulting in similar levels of regeneration. Comparison of the sensitivity of multi-parameter models is made difficult by the necessity to consider more than one sensitivity function for each model. Even though the comparison of the sensitivity function estimators of the most sensitive model parameters might be an acceptable means of comparing some models, in general, it will be necessary to consider the sensitivity functions of all model parameters, or at least those parameters having a level of sensitivity which noticeably affects the output.

The table in Appendix L lists the two sensitivity estimators and the correlation coefficients obtained from twenty-two storm events for the Nash model and two cases of the LCLR model. The LCLR-R and LCLR-LT models were used in the comparison of sensitivity. The two estimators, the correlation coefficient and the sensitivity at the peak of the model response function, appear to provide good representation of the output regeneration and the model sensitivity since for fifteen of the twenty-two storm events, high correlation is accompanied by high sensitivity. For example, Table 7-4, which was abstracted from Appendix L shows the correlation coefficient and the absolute value of the maximum ordinates of the sensitivity functions for three two-parameter models. For storm event 18 the Nash model provided higher correlation than either the LCLR-R or LCLR-LT models. The Nash model parameter n is the most sensitive parameter. The Nash model parameter K is more sensitive than the least sensitive parameter of both LCLR models. Thus, as expected, the highest correlation was accompanied by the highest sensitivity. But the

Table 7-4. Comparison of Two-Parameter Model Sensitivity
for Storm Event 18

Model	Correlation Coefficient	Parameter Sensitivity	
		Most Sensitive	Least Sensitive
Nash	0.966	0.03051 (n)	0.00578 (K)
LCLR-R	0.936	0.00816 (K)	0.00446 (T_c)
LCLR-LT	0.935	0.00828 (K)	0.00038 (T_c)

most sensitive parameter of the LCLR-R model is slightly less sensitive than the most sensitive parameter of the LCLR-LT model even though the LCLR-R model resulted in higher correlation. The correlation is higher for the LCLR-R model because the sensitivity of T_c is much greater than the sensitivity of the parameter T_c for the LCLR-LT model. That is, the comparatively higher sensitivity of the parameter T_c for the LCLR-R model offsets the slightly lower sensitivity of the parameter K for the same model. The results, thus, indicate the need to consider the sensitivity of both parameters and not just the most sensitive parameter. Two storm events, 5 and 13, have large differences in correlation, and thus, the sensitivity functions are not comparable. Five of the twenty-two storm events, 6, 10, 11, 16 and 22, do not have high sensitivity accompanied by high regeneration. As with the single-parameter models, the inability to accurately estimate the parameter values cause the more sensitive Nash model to have a lower correlation coefficient.

Inverse Sensitivity Analysis

Defining the Inverse Sensitivity Problem

The sensitivity equation,

$$y(K+\Delta K;t) = y(K;t) + \frac{dy}{dK} \Delta K + \frac{1}{2!} \frac{d^2y}{dK^2} \Delta K^2 + \dots \quad (7-9)$$

relates the change in output, parametric error, and the sensitivity functions. If the response function of a model is represented by an algebraic expression for which the differential can be found then the sensitivity

functions can be determined analytically; otherwise, a numerical method must be used to estimate the sensitivity functions. The allowable error in output is subjective and will differ for different model users and uses, but an allowable change in output can be set by the model user prior to using the model. The parametric error is an unknown quantity. Thus, the error must be estimated. If the parametric error could be expressed as a function of the sensitivity functions and the allowable change in output, then estimates of the allowable parametric error could be made using equation 7-27

$$\Delta K_i = f^{-1}(\xi_i, \Delta y) \quad (7-27)$$

where ξ_i is the sensitivity function of the i^{th} parameter, Δy is the allowable change in output, and ΔK_i is the unknown parametric error. Equation 7-9 is the direct sensitivity equation while equation 7-27 defines the inverse sensitivity equation.

Solving the Inverse Sensitivity Equation

The solution of the inverse sensitivity equation is complicated by two factors. First, there is no one-to-one correspondence between the change in output Δy and the corresponding changes in the model parameters ΔK_i . Only for single parameter models will a one-to-one correspondence between Δy and ΔK exist. Second, the determination of a solution to the inverse sensitivity equation requires the selection of an objective function. The objective function is necessary to provide an optimum set of ΔK_i values for the selected level of output error. As

with any optimization problem any number of objective functions could be used, and in all probability, the solutions from each would be different. Two common objective functions are the minimization of the absolute error and the minimization of the mean square error between the observed and computed solutions. The output or solution error Δy is the difference between the observed and incremented solutions. The minimization of the mean square error was used as an objective function for this study. The objective function in discrete form is

$$E_{\min} = \sum_{t=0}^T [y(K_1; t) - y(K_1 + \Delta K_1; t)]^2 \quad (7-28)$$

The linearized sensitivity equation, equation 7-8, can be used as an estimate of $\Delta y(K_1 + \Delta K_1; t)$ and thus, equation 7-28 becomes

$$E_{\min} = \sum_{t=0}^T [y(K_1; t) - (\frac{\partial y}{\partial K_1} \Delta K_1 + \cdots + \frac{\partial y}{\partial K_n} \Delta K_n)]^2 \quad (7-29)$$

A necessary condition for a relative minimum is the vanishing of the partial derivatives with respect to the model parameters, ΔK_1 . Thus,

$$\frac{\partial E}{\partial \Delta K_1} = 2 \sum_{t=0}^T [y(K; t) - \sum_{i=1}^n s_i \Delta K_i] \frac{\partial y}{\partial \Delta K_1} = 0 \quad (7-30)$$

$$\frac{\partial E}{\partial \Delta K_2} = 2 \sum_{t=0}^T [y(K; t) - \sum_{i=1}^n s_i \Delta K_i] \frac{\partial y}{\partial \Delta K_2} = 0$$

$$\begin{aligned} & \vdots \\ & \vdots \\ & \frac{\partial E}{\partial \Delta K_n} = 2 \sum_{t=0}^T [y(K;t) - \sum_{i=1}^n s_i \Delta K_i] \frac{\partial y}{\partial \Delta K_n} = 0 \end{aligned}$$

By algebraic manipulation of equations 7-30, a set of equations, called the normal equations, can be determined,

$$\sum_{t=0}^T (y(K;t) \cdot s_1) = \sum_{t=0}^T [(\sum_{i=1}^n s_i \Delta K_i) s_1] \quad (7-31)$$

$$\vdots$$

$$\sum_{t=0}^T (y(K;t) \cdot s_n) = \sum_{t=0}^T [(\sum_{i=1}^n s_i \Delta K_i) s_n]$$

The normal equations provide a one-to-one correspondence; that is, the number of equations and the number of unknown ΔK_i values are equal. The set of ΔK values are the optimized set of tolerable parameter values.

Application of Inverse Sensitivity Analysis

The user of any model is primarily interested in the ability of the model to regenerate existing data and the ability to predict the output of future events. The user of a model establishes the allowable level of output difference, the difference in computed and observed output functions which is considered acceptable. An output tolerance might be established for the peak of the storm hydrograph or for each ordinate

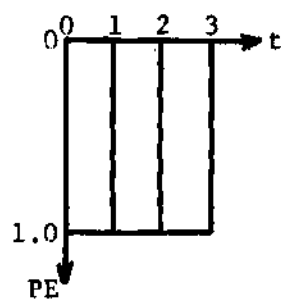
of the storm hydrograph.

The peak of the SLR model response function and its sensitivity function occur at $t = 0$. If, for example, the design storm and model response function, both detailed in Figure 7-11, were convolved, the design storm hydrograph would be as shown in Figure 7-11c. For a one parameter model the normal equation, equation 7-31, becomes $\Delta y = S \Delta K$. Solving for the parametric error yields $\Delta K = \Delta y / S$. Thus, if the sensitivity function and tolerable output variation are known the allowable parameter error can be determined. If the maximum solution error, Δy , has been specified as one percent of the storm hydrograph peak the allowable parametric error would be

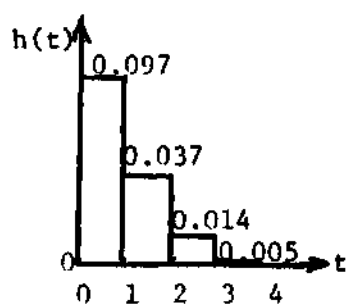
$$\Delta K = \frac{\Delta y}{S} = 0.01(0.148) / S_{\text{peak}} = 0.00148 / -0.0135 = -0.110$$

Since the peak of the model response function and its sensitivity function occur at the same time it is only necessary to check the output at the point of maximum sensitivity. For the given sensitivity function, Figure 7-12, the peak sensitivity was -0.0135. If tolerable limits were placed on the entire hydrograph it would be necessary to check the allowable parametric error for points on the hydrograph other than at the peak. To demonstrate that the output will be within the tolerance set at one percent of the peak requires a new parameter value to be defined as

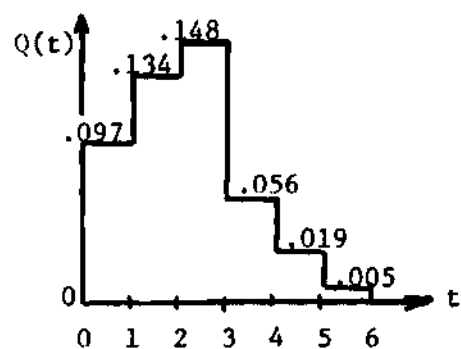
$$K' = K + \Delta K = 10.226 + (-0.110) = 10.116$$



(a) Design Storm Precipitation Excess



(b) Response Function



(c) Design Storm Runoff

Figure 7-11. Example : Inverse Sensitivity Analysis

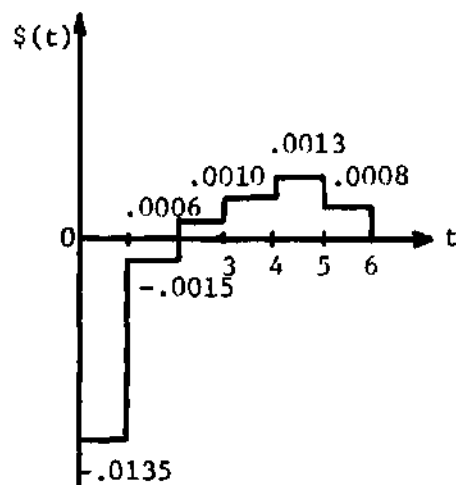
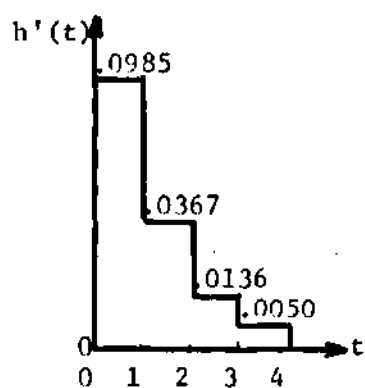
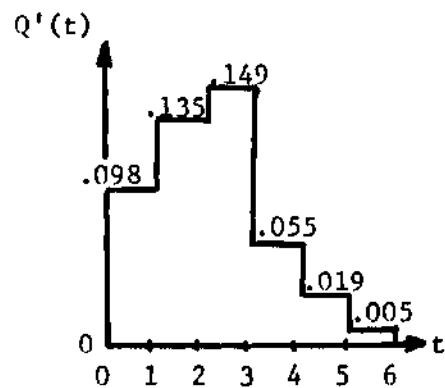


Figure 7-12. Sensitivity Function for Inverse Sensitivity Example



(a) Adjusted Response Function



(b) Adjusted Storm Runoff

Figure 7-13. Adjusted Storm Runoff for Inverse Sensitivity Example

The adjusted model response function, which is defined by K' , is shown in Figure 7-13a. The convolution of the design storm, Figure 7-11a, with the adjusted model response function yields the adjusted storm hydrograph, which is shown in Figure 7-13b. All ordinates in the adjusted storm hydrograph are within the allowable solution error of one percent or 0.00148 units. Thus, any parametric error greater than the computed value $|0.110|$ would produce an unacceptable storm hydrograph.

Unfortunately, for most models the peaks of the model response functions and sensitivity functions do not occur at the same time. In such cases, it is necessary to compute the parametric error, ΔK , at those points near the peaks of both the model response function and sensitivity functions, so that the solution error, Δy , can be compared with the specified tolerance.

CHAPTER VIII

DISCUSSION AND CONCLUSIONS

Adequacy of Linear Conceptual Models

One of the objectives of this study was to determine the adequacy of simple linear models to represent the hydrologic response of a watershed. The relatively poor regeneration and prediction results obtained from the analysis of twenty-six storm events seems to indicate that the linear models investigated herein are, in general, not capable of representing the response of a watershed. A primary consideration when using such models is the recognition of the constraining shape of the response functions. Response functions of models which are defined by one or two parameters cannot readily adapt to the time varying response of a small watershed such as those included in this study, and thus, exceptionally good regeneration (e.g., $R > 0.98$) should not be expected for the majority of storm events analyzed.

Past investigations (29) have indicated that simple linear conceptual models can provide acceptable regeneration. Such a conclusion naturally depends on what is considered acceptable. Sarma (29) considered the regeneration to be "good" when the correlation coefficient was less than 0.95 but at least 0.90. However, it has been demonstrated (see Figure 4-2) that a computed peak discharge forty-four percent greater than the observed peak discharge can result in a correlation coefficient of 0.969. For some design purposes such results might be

considered unacceptable and thus, recognition of what is considered acceptable or unacceptable must accompany any conclusions concerning the ability of such models to provide a good representation of the hydrologic response of a watershed.

Six types of conceptual models were involved in this study since past investigators have not been able to determine which conceptual model provides better estimates of the hydrologic response of watersheds. For the single parameter models investigated the same objective function (equation 4-9) was used to determine the model parameter value K . After setting the storage coefficient K equal to the time lag the objective function of equation 4-9 was used to determine the value of the remaining parameter of the two-parameter models. Such a procedure was used to provide a measure of consistency. Although the DR model provided the highest level of regeneration for fifty percent of the storm events investigated, in most cases the correlation was low enough that the DR model should not be considered superior to the other models investigated. The results of this study in conjunction with the results of other investigators lead to the conclusion that the shape of the hydrologic response of the watershed will dictate which model will provide the best regeneration and prediction. For example, the SLR model will provide better regeneration than the DR model when the time-to-peak is relatively small, such as that found for urban watersheds. Similarly, the DR model will provide better regeneration when the response of the watershed tends to delay the transformation of precipitation to runoff. In Chapter V the constraining shape of the conceptual model was found to be a very significant factor. Thus,

no one model should be expected to provide consistently better regeneration or prediction, but a model having the constraining shape which best conforms to the hydrologic response for a specified storm event will provide the best results. Thus, a comparative analysis of the adjustability of the model response functions might identify the conditions for which each model will provide the best results.

Prediction of Model Parameter Values

The results of this study (Chapter IV) indicate that averaged parameter values for watersheds are not capable of acceptable storm hydrograph regeneration and prediction. Such a conclusion was expected for the models investigated in this study. The model parameter K, which was common to each model included in this study, represents the time delaying action of a watershed. Naturally the condition of the watershed (i.e., the soil moisture content, the growth of the vegetal cover, etc) will vary considerably from storm to storm and thus the delaying action should be reflected in the values of the parameters. If it were possible to quantify the various watershed conditions then it might be possible to estimate parameter values capable of acceptable storm hydrograph regeneration.

In Chapter VI prediction equations were determined for the estimation of model parameter values. The basin area proved to be the only physiographic characteristic of importance although the addition of the parameters representing the slope and length of the watershed provided better correlation between the model parameter values computed from data and those computed using the prediction equation. The introduction into

the prediction equation of parameters (the volume and duration of precipitation excess) to characterize the storm further increased the correlation (above that obtained when using the area or the area, slope and length) but the parameter values obtained from the prediction equations were still not capable of adequate storm hydrograph regeneration. Factors which limit the potential of such prediction equations are the lack of precise data and again, the constraining shape of the response functions.

Sensitivity Analysis

In Chapter VII the following general considerations were discussed in detail: [1] the sensitivity of a model parameter varies with time over the duration of the response function; [2] the sensitivity of a specified model parameter depends on the value of the other parameters of the model; [3] the shape of the sensitivity function(s) of the conceptual models investigated herein are characteristic of the model; [4] the sensitivity of a model for an optimal solution to a given set of data is a measure of the level of regeneration obtained; [5] the sensitivity of a parameter is related to the change in output and the parametric error by the sensitivity equation.

Since the sensitivity function of each model parameter has a characteristic shape it is important to consider, when selecting a model, the relative timing between the ordinates of the response function and the sensitivity function. If the model parameters can be determined with little error, then it would be preferable to use a model, model A, for which the peaks of the response function and sensitivity functions occur

simultaneously. Such a model will provide a better estimate of the peak discharge. But since the peak of the sensitivity function occurs simultaneously with the peak of the response function the greatest potential for error in the output will also occur at the peak of the output.

When the potential error in the parameter value is small, the expected error in the output might be considered acceptable. But if the expected parametric error is comparatively large, then it might be preferable to use a model, model B, for which the peak of the sensitivity function occurs at a point on the time base far removed from the peak of the response function. In this case the model would probably not achieve the level of regeneration obtained using Model A. But the expected difference in the computed output at the peak when using Model B would be less than that for Model A. In both situations the sensitivity equation can be used to compute the change in output which would occur for the expected parametric error.

Unfortunately, the expected parametric error is difficult, if not impossible, to estimate. In Chapter VI it was demonstrated that model parameters computed using regression equations were not capable of adequate regeneration; that is, the predicted model parameter differed significantly from the optimized model parameter. Since the parametric error is very large, the sensitivity equation, which requires ΔK in equation 7-9 to be small, could not be used to estimate the change in output. Only in situations where the model parameter can be accurately estimated will the sensitivity equation be useful. But even when the expected parametric error is large it is important to consider the

correspondence between the shapes of the response function and sensitivity function.

The sensitivity of a model parameter varies both with time and the values of the other model parameters. The interactive nature of sensitivity can be misleading. Whenever the sensitivity of a specific parameter of a multi-parameter model is stated, it is important to specify the levels of the other parameters. For example, the sensitivity plots presented by Lichty (14) and Dawdy (11) indicate the change in the value of an objective function for various levels of changes in a specified parameter value. The sensitivity plots do not recognize either the parametric or dynamic nature of sensitivity. Such plots correspond to a static sensitivity coefficient in which only one of the n parameters of equation 7-6 are free to vary. Sensitivity plots which represent the sensitivity of a parameter for large changes in parameter values can also be misleading since they deviate considerably from the optimal solution. In Chapter VII it was shown that for cases where the computed solution differs significantly from the observed solution the sensitivity estimates are inadequate for comparing different models.

Conclusions

This study examined the potential adequacy of six linear conceptual models to represent the hydrologic response of watersheds. The analysis of Chapter IV showed that the observed storm hydrographs and computed storm hydrographs were not highly correlated. The analysis of artificial data in Chapter V indicated that the constraining shape of the model response functions was responsible for the poor correlation obtained in

Chapter IV. The sensitivity computations of Chapter VII provided a quantitative means of measuring the adjustment capability or constraining effect of a model. Since the parameters derived in Chapter IV did not provide good estimates of the hydrologic response of the watershed, the prediction equations developed in Chapter VI should not have been expected to provide good parameter estimates and thus, should not be used as an indication of the ability of the model to represent the watershed. The following statements summarize the specific findings of this study.

1. The simple linear models investigated herein do not appear to be capable of providing an acceptable degree of storm hydrograph regeneration and prediction (page 60).

2. The double routing model provided, in general, the best regeneration of observed storm hydrographs (page 52).

3. The introduction of a feedback element into a linear model reduces the adjustment capability of a model and thus provides poorer regeneration of observed storm hydrographs (page 51).

4. Model parameter values are not constant from storm to storm (page 54).

5. The regeneration performance of the single linear reservoir model can be increased over that obtained using the observed time lag as the storage coefficient by using an optimization scheme as was described in Chapter IV (page 49).

6. The basin area was the only significant physiographic characteristic. The slope and length of the basin are only slightly

significant and their use in prediction equations increased only slightly the correlation between the computed and predicted model parameter values. The use of storm characteristics increases the ability of prediction equations to estimate model parameters (pages 97, 99 and 102).

7. The sensitivity of model parameters is dynamic and parametric and both properties have important implications (page 113).

8. The shape of the sensitivity function of a model is characteristic of that model (page 116).

9. It has been shown that parameter sensitivity is related to the change in output and the change or error in a parameter by the sensitivity equation (pages 114-115).

10. It has been shown that the sensitivity of parameters can be used to compare the regeneration capability of different models (pages 124-139).

11. If only one parameter of a multi-parameter model is to be included in the optimization scheme then the most sensitive parameter should be selected for optimization (page 130).

CHAPTER IX

RECOMMENDATIONS

It is evident from this study that model parameter sensitivity analysis provides a means of analyzing the response functions of linear storage models. The linear storage models introduced in Chapter IV were selected for study in order to avoid problems which might come to light in the analysis of more complex models. In spite of the structural simplicity of the storage models, many problems concerning model parameter sensitivity remain unanswered. Such problems will require more extensive research not only with linear storage models but with models of a more complex structure.

Optimum Sensitivity

Part of the initial motivation into the examination of model parameter sensitivity was an attempt to define optimum sensitivity. There were two diverse avenues of thought into what was meant by optimum sensitivity.

First, if the hydrologic model were an exact duplicate of the watershed then the sensitivity of the model components would be identical to the sensitivity of the corresponding watershed processes. But since all models fail to precisely describe the prototype, the sensitivity of the individual model components will differ from the sensitivity of the corresponding watershed processes. But one would expect a correspondence

between model parameter sensitivity and the sensitivity of the watershed processes. Such correspondence would be a measure of the optimality of the model structure.

Second, the optimum sensitivity could be the level of sensitivity at which the effect of data error becomes more significant than the error introduced by the constraining shape of the model response function. For relatively insensitive models, such as the linear storage models investigated herein, the constraining shape of the response function was a more important factor in output reproduction than the effect of error in the data. Increasing the flexibility of a model results in a model with more potential for output reproduction. But data error has a more detrimental effect on output reproduction as the sensitivity of a model is increased. At the optimum level of sensitivity, further increases in the sensitivity would result in poorer regeneration due to the dominant effect of data error.

Both concepts of optimum sensitivity need further investigation. A solution to the problem first requires the development of a means for systematically varying the sensitivity of a model.

Parameter Sensitivity and Parameter Importance

The sensitivity of model parameters, as determined by equation 7-5, specifies the change in the response for a unit change in the parameter value. But a change of unity is not expected for each parameter value. For example, a parameter representing the percentage of impervious area in a watershed, and which is quantified by a value from zero to one, would not change by a value of one. In fact, for such a parameter

one might expect an error on the order of 0.01 when estimating the parameter value. Other parameter values, such as those determined in this study, vary from near zero to upwards of fifty. For parameters having such widely different magnitudes it is difficult to use the sensitivity values as a means of identifying the relative importance of the individual parameters. That is, the parameter with the highest sensitivity is not necessarily the most important parameter of the model. If parameter sensitivity is to be used as a measure of parameter importance, it will be necessary to provide standardized measures of sensitivity. The standardized sensitivity estimates could be used to rank the parameters of a model in the order of importance and also identify which parameters contribute little information and thus, could reasonably be eliminated from the model. This would be an important tool especially for the analysis of more complex models.

Comparison of Model Sensitivity

In Chapter VII the four one-parameter models were compared on the basis of sensitivity separately from the comparison of the two-parameter models. The procedure for comparing sensitivity and the regeneration capability of multi-parameter models, and especially models having a different number of parameters, is of considerable importance if sensitivity is to be used for the analysis of model structure. Use of single-valued estimates of sensitivity and regeneration result in a loss of information although such estimates are easier to compare than time or spatially distributed estimates. The multi-parameter sensitivity equation, equation 7-11, might be used in the comparison of model parameter

sensitivity.

Structural Analysis of Multi-parameter Models Using Parametric Sensitivity

In this study the derivative approach was used to derive sensitivity estimates for linear storage models. The same approach could be applied to the more complex hydrologic models and thus, replace the use of the numerical approach to the estimation of parametric sensitivity. The numerical method of computing sensitivity is seriously handicapped by the need to specify a criterion function. But when the response function of a model is not represented in a closed form, it might be difficult to derive a functional representation of the sensitivity of a parameter. In fact, it will probably be impossible to represent the sensitivity in a closed form. If parametric sensitivity estimates can be determined for complex models it will be especially important to derive standardized estimates of sensitivity and to develop a means of relating parameter importance to parametric sensitivity.

Summary

A few of the many aspects of sensitivity have been discussed throughout this study. Many of the potential uses of parametric sensitivity remain unknown. For example, sensitivity estimates of the model parameters could be incorporated into a procedure for determining the optimum values of the model parameters to a given set of data. Before sensitivity estimates are used in hydrologic analysis the properties of sensitivity, such as those discussed in the preceding paragraphs, must be more fully understood.

REFERENCES

1. Smith, R. L.: Application of Models in Urban Hydrology, Chapter 2 Appendix A in Urban Water Resources Research, a study by ASCE Urban Hydrology Research Council, September, 1968.
2. Amorocho, J., and W. E. Hart: A Critique of Current Methods in Hydrologic Systems Investigation, Transactions of American Geophysical Union, Vol. 45, No. 2, pp. 307-321, June, 1964.
3. McCuen, R. H.: Hydrologic Implications of Trend Surface Analysis, M. S. C. E. Thesis, Georgia Institute of Technology, November, 1969.
4. Zoch, R. T.: On the Relation Between Rainfall and Stream Flow, Monthly Weather Review, Vol. 62, pp. 315-322, 1934; Vol. 64, pp. 105-121, 1936; Vol. 65, pp. 135-147, 1937.
5. Dooge, J. C. I.: A General Theory of Unit Hydrograph, Journal of Geophysical Research, Vol. 64, No. 1, pp. 241-256, 1959.
6. O'Kelly, J. J.: The Employment of Unit Hydrographs to Determine the Flows of Irish Arterial Drainage Channels, Proceedings of the Institute of Civil Engineers, Vol. 4, pt. 3, pp. 365-412, 1955.
7. Nash, J. E.: The Form of Instantaneous Unit Hydrograph, International Association of Scientific Hydrology, Pub. 45, Vol. 3, pp. 114-121, 1957.
8. Nash, J. E.: A Unit Hydrograph Study, with Particular Reference to British Catchments, Proceedings of the Institute of Civil Engineers, Vol. 17, pp. 249-282, 1960.
9. Holtan, H. N., and D. E. Overton: Storage Flow Hysteresis in Hydrograph Synthesis, Journal of Hydrology, Vol. 2, pp. 309-323, 1964.
10. Overton, D. E.: Analytical Simulation of Watershed Hydrographs From Rainfall, Proceedings of the International Hydrology Symposium, Fort Collins, Colorado, Vol. 1, pp. 9-17, September, 1967.
11. Dawdy, D. R.: Considerations Involved in Evaluating Mathematical Modeling of Urban Hydrologic Systems, Chapter 6 of Appendix A, Urban Water Resources Research, A Study by ASCE Urban Hydrology Research Council, September, 1968.
12. Dantzig, G. B.: Linear Programming and Extensions, Princeton University Press, Princeton, New Jersey, 1963.

13. Dawdy, D. R., and T. O'Donnell: Mathematical Models of Catchment Behavior, Proceedings of the American Society of Civil Engineers, Journal of the Hydraulics Division, Vol. 91, No. HY4, pp. 123-137, July, 1965.
14. Lichty, R. W., D. R. Dawdy, and J. M. Bergmann: Rainfall-Runoff Model for Small Basin Flood Hydrograph Simulation, International Association of Scientific Hydrology, Pub. No. 81, pp. 356-367, Symposium of Tucson, 1968.
15. Vemuri, V., J. Dracup, R. Erdmann and N. Vemuri: Sensitivity Analysis Method of System Identification and its Potential in Hydrologic Research, Water Resources Research, Vol 5, No. 2, April, 1969, p. 341.
16. Tomovic, R.: Sensitivity Analysis of Dynamic Systems, McGraw-Hill Book Company, Inc., New York, 1963.
17. Crawford, N. H., and R. K. Linsley: Digital Simulation in Hydrology: Stanford Watershed Model IV, Technical Report No. 39, Department of Civil Engineering, Stanford University, California, July, 1966.
18. Rosenbrock, H. H.: An Automatic Method of Finding the Greatest or Least Value of a Function, Computer Journal, Vol. 3, pp. 175-184, 1960.
19. O'Donnell, T.: Methods of Computation in Hydrograph Analysis and Synthesis, Chapter 3 of Recent Trends in Hydrograph Synthesis, Committee for Hydrological Research T. N. O., The Hague, 1966.
20. DeCoursey, D. G. and W. M. Snyder: Computer-Oriented Method of Optimizing Hydrologic Model Parameters, Journal of Hydrology, Vol. 9, pp. 34-56, 1969.
21. Selected Runoff Events for Small Agricultural Watersheds in the United States, U. S. Department of Agriculture, Washington, D. C., January, 1960.
22. Hydrologic Data for Experimental Agricultural Watersheds in the United States 1956-59, Miscellaneous Publication No. 945, U. S. Department of Agriculture, Washington, D. C., November, 1963.
23. Hydrologic Data for Experimental Agricultural Watersheds in the United States 1960-61, Miscellaneous Publication No. 994, U. S. Department of Agriculture, Washington, D. C., May, 1965.
24. Horton, R. E.: The Role of Infiltration in the Hydrologic Cycle, Transactions of the American Geophysical Union, Vol. 14, 1933, pp. 446-460.

25. Linsley, R. K., M. A. Kohler, and J. L. Paulhus: Hydrology for Engineers, McGraw-Hill Book Company, Inc., New York, New York, pp. 204-208, 1958.
26. Minshall, N. E.: Predicting Storm Runoff on Small Experimental Watersheds, Proceedings of the American Society of Civil Engineers, Journal of the Hydraulics Division, Vol. 86, No. HY8, pp. 17-38, August, 1960.
27. Singh, K. P.: Nonlinear Instantaneous Unit Hydrograph Theory, Proceedings of the American Society of Civil Engineers, Journal of the Hydraulics Division, Vol. 90, No. HY2, pp. 313-347, March, 1964.
28. Blank, D., and J. W. Delleru: A Program for Estimating Runoff from Indiana Watersheds, Part I Linear System Analysis in Surface Water Hydrology and its Applications to Indiana Watersheds, Technical Report No. 4, Purdue University Water Resources Research Center, Lafayette, Indiana, August, 1968.
29. Sarma, P. B. S., J. W. Delleur, A. R. Rao: A Program in Urban Hydrology, Part II, Technical Report No. 9, Purdue University, Water Resources Research Center, Lafayette, Indiana, October, 1969.
30. Snedecor, G. W., and W. G. Cochran, Statistical Methods, 6th Edition, Iowa State University Press, Ames, Iowa, 1968.
31. Nash, J. E.: Systematic Determination of Unit Hydrograph Parameters, Journal of Geophysical Research, Vol. 64, No. 1, pp. 111-115, January, 1959.
32. Eagleson, P. S., R. Nejlja, F. March: The Computation of Optimum Realizable Unit Hydrographs from Rainfall and Runoff Data, Hydro-Dynamic Laboratory Report, No. 84, M. I. T., Cambridge, Massachusetts, September, 1965.
33. Delleur, J. W. and E. B. Vician: Discussion on the paper "Time in Urban Hydrology" by G. E. Willeke, Proceedings of the American Society of Civil Engineers, Journal of the Hydraulics Division, Vol. 92, No. HY5, pp. 243-251, September, 1966.
34. Snyder, W. M.: Hydrograph Analysis by the Method of Least Squares, Proceedings of the American Society of Civil Engineers, No. 793, 1955.
35. Snyder, F. F.: Synthetic Flood Frequency, Proceedings of the American Society of Civil Engineers, Journal of the Hydraulics Division, Vol. 84, No. HY5, pp. 1808-1--1808-22, October, 1958.
36. Clark, C. O.: Storage and the Unit Hydrograph, Transactions of the American Society of Civil Engineers, Vol. 110, pp. 1419-1446, 1945.

37. Dooge, J. C.: Analysis of Linear Systems by Means of Laguerre Functions, Journal of the Society for Industrial and Applied Mathematics, No. 3, pp. 396-408, 1965.
38. Laurenson, E. M. and T. O'Donnell: Data Error Effects in Unit Hydrograph Derivation, Proceedings of the American Society of Civil Engineers, Journal of the Hydraulics Division, Vol. 95, No. HY6, Paper No. 6887, November, 1969.
39. O'Donnell, T: Instantaneous Unit Hydrograph Derivation by Harmonic Analysis, International Association of Scientific Hydrology, Pub. No. 51, pp. 546-557, 1960.
40. Harman, H. H.: Modern Factor Analysis, University of Chicago Press, Chicago, Illinois, 1967.
41. Kendall, M. G.: A Course in Multivariate Analysis, Hafner Publishing Company, New York, 1968.
42. Snyder, W. M.: Some Possibilities for Multivariate Analysis in Hydrologic Studies, Journal of Geophysical Research, Vol. 6, No. 2, p. 721, February, 1962.
43. Cooley, W. W. and P. R. Lohnes: Multivariate Procedures for the Behavioral Sciences, J. Wiley & Sons, Inc., New York, 1962.
44. Bradshaw Creek--Elk River: A Pilot Study in Area-Stream Factor Correlation, Tennessee Valley Authority, Research Paper No. 4, Knoxville, Tennessee, April, 1964.
45. Wu, I. P.: Flood Hydrology of Small Watersheds--Evaluation of time Parameters and Determination of Peak Discharge, paper presented at the winter meeting of the American Society of Agricultural Engineers, Chicago, Illinois, December, 1968.
46. Hack, J. T.: Studies of Longitudinal Stream Profiles in Virginia and Maryland, U. S. Geological Survey Professional Paper 294-B, 1957.
47. Derusso, P. M., R. J. Roy, C. M. Close: State Variables for Engineers, John Wiley & Sons, Inc., New York, 1967.
48. Distefano, J. J., A. Stubberud, and I. Williams: Feedback and Control Systems, Schaum's Outline Series, McGraw-Hill Book Co., New York, 1967.

APPENDIX A

THE LAPLACE TRANSFORM

Time dependent functions, $f(t)$, and frequency dependent functions of the complex variable s , $F(s)$, can be transformed by the Laplace and inverse Laplace transforms. Such transforms are useful because operations in the time domain are often simpler when performed in the frequency domain.

The Laplace transform is defined by

$$\mathcal{L}[f(t)] = F(s) = \lim_{\substack{T \rightarrow \infty \\ \epsilon \rightarrow 0}} \int_{\epsilon}^T f(t)e^{-st}dt = \int_{0^+}^{\infty} f(t)e^{-st}dt \quad 0 < \epsilon < T \quad (\text{A-1})$$

The lower limit of integration is denoted by 0^+ and is useful when considering functions which are discontinuous at $t = 0$. All time functions considered in this study are Laplace transformable.

Once the solution has been determined in the s domain, it is necessary to transform the solution to the time domain. The inverse Laplace transform is defined by

$$\mathcal{L}^{-1}[F(s)] = f(t) = \frac{1}{2\pi j} \int_{c-j\omega}^{c+j\omega} F(s)e^{st}ds \quad (\text{A-2})$$

where $j = \sqrt{-1}$.

There are many techniques which can be used to simplify the contour integrations of equations A-1 and A-2. Tables of Laplace and inverse Laplace transforms are extremely useful for simple functions. Table A-1 contains elementary transforms, some of which will be used in this study.

Table A-1. Table of Laplace Transforms

Function	$f(t)$	$F(s)$	
Unit Impulse	1	$1/s$	$s > 0$
Unit Ramp	t	$1/s^2$	$s > 0$
Polynomial	t^n	$n!/s^{n+1}$	$s > 0$
Exponential	e^{at}	$1/(s-a)$	$s > a$

There are several properties of transforms which are important to this study of linear conceptual models. First, the Laplace and inverse Laplace transforms are linear. Thus, $a \cdot f_1(t) + b \cdot f_2(t)$ has the equivalent transform of $a \cdot F_1(s) + b \cdot F_2(s)$.

The second property of importance herein states that the Laplace transform of the time derivative of the time function $f(t)$ is given by

$$\mathcal{L}[df(t) / dt] = s F(s) - f(0^+) \quad (A-3)$$

where $f(0^+)$ is the initial value of $f(t)$.

Third, the integration

$$\int_0^t F(u)G(t-u) du \quad (A-4)$$

has the equivalent transform operation

$$f(s)g(s)$$

(A-5)

APPENDIX B

SYSTEM REPRESENTATION

After the characteristics which are to be modeled have been selected, a task often more difficult than selecting an appropriate mathematical form, it is necessary to characterize the relationships between the various components of the system. A block diagram is a convenient means of representing the cause and effect relationship between the model components. A block diagram consists of blocks, arrows and summing points. Arrows are used to indicate the flow of information or matter. It is important to understand that an arrow does not necessarily indicate the flow of a physical material although this is often the case. Blocks are used to represent components or mathematical operations that must be performed on the input function. Summing points, usually represented by small circles, are used to add or subtract two or more pieces of information. Input of information to a component of a model is represented by an arrow with an arrowhead pointing into the block. Output of information from a model component is represented by an arrow with the arrowhead pointing away from the block or summing point.

For example, the block diagram of Figure B-1 would be used to represent the precipitation-total runoff process for three-component flow. In Figure B-1, I_T and ϕ_T are the precipitation and total runoff, respectively. The subsystem for which I_1 and ϕ_1 are the input and output can be used to represent the surface flow portion of the precipitation. The

time distribution of surface flow is changed as it traverses the watershed and the parameter K_1 serves as a transformation coefficient. The subsystems involving I_2 and I_3 can represent the flow of water in the zones of aeration and saturation, respectively. The precipitation is separated at summing point S_1 and the outflow from each flow regime is summed at summing point S_2 . For this example, the arrows can be identified with the flow of matter through the system. For other models, such correspondence might not exist. The output ϕ_L from summing point S_1 represents water loss from the system which does not appear as streamflow.

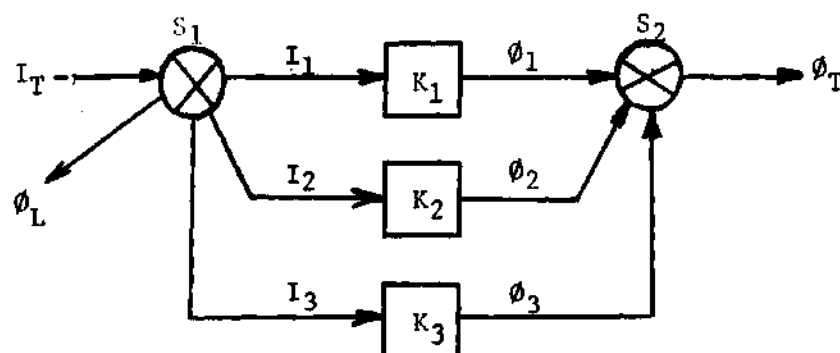


Figure B-1. Block Diagram Representation of the Rainfall-Runoff Process

APPENDIX C

SYSTEM CLASSIFICATION

Classifying systems according to properties provides a convenient basis for the comparison of models. The following paragraphs briefly describe properties which will be used to describe models which are analyzed and compared as part of this study.

Linear and Non-Linear Systems

A linear system is loosely defined as one which satisfies the principle of superpositioning. Specifically, if $\phi_1(t)$ and $\phi_2(t)$ are the responses of a system to inputs $I_1(t)$ and $I_2(t)$, respectively, and $c_1\phi_1(t) + c_2\phi_2(t)$ is the response of that system to the input $c_1I_1(t) + c_2I_2(t)$ for all values of c_1 , c_2 , $I_1(t)$ and $I_2(t)$, then the system is linear. For models which can be represented by a system of differential equations, the model is said to be linear only when all derivatives of the input and output are of the first power and there are no products of derivatives.

For a non-linear system the principle of superpositioning will not be valid. For such systems the response of the various components will vary with the input. Non-linear differential equations are often used to represent such systems.

Static and Dynamic Systems

The response of a static, or instantaneous, system only depends on

the input at the time of occurrence of the response. Since inputs at a given time will have no influence on any future responses, such systems are also classified as zero-memory systems. Static systems contain no means for information storage.

Systems which can store information such that responses from the system will depend on past inputs are said to be dynamic. Such systems can have either finite or infinite memory. Models of dynamic systems use time delay mechanisms to store information.

Time-Invariant and Time-Varying Systems

The output for a time-invariant linear system will not vary in time for a given input. If the system is represented by a linear differential equation the coefficients will be constant.

The output for a time-varying linear system will depend on both the input and the time at which the input is applied to the system. Such systems can be represented by differential equations having at least one coefficient which is a function of time.

Deterministic and Non-Deterministic Systems

Deterministic models are defined by explicit mathematical relationships. Such models produce data which can be predicted with certainty when the input and system response functions are given. The linear conceptual models investigated here are examples of deterministic models.

Non-deterministic models are, in general, defined by combinations of explicit mathematical relationships and elements which produce random fluctuations in the data. The random fluctuations are often characterized

by statistical properties but exact predictions of the output are impossible. The height and frequency of occurrence of ocean waves are examples of processes producing random data.

APPENDIX D

THE UNIT IMPULSE FUNCTION

Singularity functions, mathematical functions which are discontinuous or have discontinuous derivatives, are useful in the analysis of complex systems. Singularity functions usually have simple mathematical representations which can simplify the approximation of complex functional forms. Examples of such functions include the unit ramp function, the unit step function and the unit impulse function. The unit ramp and unit step functions have precise mathematical representations while the unit impulse function is usually defined by its properties. The ramp function is expressed mathematically as

$$f_2(t) = \begin{cases} 0, & t < 0 \\ t, & t \geq 0 \end{cases} \quad (D-1)$$

and the mathematical definition of the unit step function is

$$f_1(t) = \begin{cases} 0, & t < 0 \\ 1, & t \geq 0 \end{cases} \quad (D-2)$$

The time at which singularity functions begin can be changed by a translation of the time argument. Thus,

$$f_1(t - t_1) = \begin{cases} 0, & t < t_1 \\ 1, & t \geq t_1 \end{cases} \quad (D-3)$$

is a step function which begins at time $t = t_1$ and not $t = 0$. Time translation of mathematical functions are important when two functions must be convolved (see Appendix F).

Singularity functions can be combined to form many other functions of elementary and complex form. A rectangular pulse of magnitude $1/\Delta t$ and duration Δt can be derived by differencing two step functions of magnitude $1/\Delta t$ which are separated by a time interval of Δt .

A rectangular pulse is used as a finite approximation of the unit impulse function. The rectangular pulse of duration Δt and magnitude $1/\Delta t$ encloses an area of unity which is a property of the unit impulse function. The mathematical representation of the pulse used to approximate the unit impulse function is

$$u(t) = \begin{cases} 0 & t \geq |t_0/2| \\ 1/t_0 & -t_0/2 < t < t_0/2 \end{cases} \quad (D-4)$$

The limit of $u(t)$ is

$$u_0(t) = \lim_{t_0 \rightarrow 0} u(t) = \begin{cases} 0 & t \neq 0 \\ \infty & t = 0 \end{cases} \quad (D-5)$$

The unit impulse function is usually defined heuristically as

$$f_o(t) = \frac{df_1(t)}{dt} \quad (D-6)$$

This definition is not valid from a theoretical standpoint since the derivative of the step function $f_1(t)$ does not exist. Thus, the finite approximation, equation D-4, must be used. As the duration of the pulse is decreased the magnitude of $u(t)$ increases in order to maintain a constant area of unity.

For the analysis of complex linear systems the unit impulse function is extremely useful. The response of the system to the unit impulse function can be used as a mathematical model of the system and the output for any complex input function can be determined through the convolution of the input with the output of the system due to a unit impulse input. The convolution of such functions is particularly easy when the system response is time-invariant. For time-varying systems the analysis is generally more difficult since it is necessary to state the system response function for the various possible times and conditions.

APPENDIX E

THE SYSTEM RESPONSE FUNCTION

Figure E-1 shows an elementary linear system with input $x(t)$ and output $y(t)$, and $h(t)$ as a function which transforms the input $x(t)$. In the time domain $h(t)$ is called the system response function and equals the output from the "black box" when the input is a unit instantaneous impulse function, equation D-5.

In the frequency domain the system response function is called the system transfer function $H(j\omega)$ and equals the quotient of the output $Y(j\omega)$ to input $X(j\omega)$. From a sample of Laplace transformable input and output data the transfer function can be easily approximated. For complex input and output functions which cannot be transformed to the s domain, it is necessary to resolve the complex functions into sets of singularity functions. If the inverse Laplace transform of the estimated transfer function exists or can be approximated an estimate of the system response function can be determined. A system response function computed from sample data represents an approximation to the true, but usually unknown, system response function.

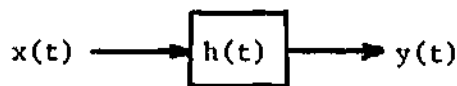


Figure E-1. "Black Box" Linear System

APPENDIX F

CONVOLUTION

Definition

The convolution integral defined as

$$y(t) = \int_0^t x(\tau)h(t - \tau)d\tau \quad (F-1)$$

can be used to determine the output from a linear, time-invariant system. The convolution of the complex input function $x(t)$ and the system response function $h(t)$ can be performed analytically, numerically or graphically. An analytical representation of the output function can be determined when the convolution of the input and system response functions can be performed analytically. If such integration is not possible, or considered too difficult, a solution must be determined by numerical or graphical convolution.

Numerical Convolution

When an analytical solution to the convolution integral is not possible, the input can be resolved into a series of impulses. The response to each impulse equals the product of the system response function and the strength of the impulse. The total response is determined by properly translating with time each of the products and summing the

individual pulse response. The total output is then

$$y(t) = \sum_{\tau=0}^t x(\tau)h(t-\tau) \quad (F-2)$$

For example, if

$$x(t) = \{0.5, 1.5\} \text{ and } h(\tau) = \{0.2, 0.5, 0.3\}$$

then the output will be found by

$$y(1) = x(1) h(1) = (0.5)(0.2) = 0.1$$

$$y(2) = x(1) h(2) + x(2) h(1) = (0.5)(0.5) + (1.5)(0.2) = 0.55$$

$$y(3) = x(1) h(3) + x(2) h(2) = (0.5)(0.3) + (1.5)(0.5) = 0.90$$

$$y(4) = x(2) h(3) = (1.5)(0.3) = 0.45$$

Digital programming of the numerical convolution procedure is relatively simple and quite useful in the analysis of hydrologic data.

APPENDIX G

FEEDBACK SYSTEMS

Feedback is a property of a system which enables a controlled variable of the system, such as the output, to be compared with the input to either the system or a component of the system. Such comparison of output with input results in control action. Feedback systems, a closed loop control system, are common in the analysis of electrical networks and mechanical devices. The water closet tank filling system is an example of one of the most frequently used control systems. The system contains a float which maintains a constant water level in the tank. When the water has been flushed from the tank, the outlet closes and the water level in the tank rises. As the water level approaches tank capacity, a valve which controls the input is slowly closed and the input of water is reduced. When the tank capacity has been reached, the valve is closed. Knowledge of the water level in the tank then controls the input and thus, acts as feedback. The electric light switch system is an example of an electrical feedback system.

For electrical network systems feedback has been used to increase the accuracy of signal regeneration in steady-state systems, reduce the effects of non-linearity of system components and to reduce the sensitivity of the output to variations in the system components (48).

Figure G-1 shows a block diagram of a feedback, or closed-loop,

control system. The feedback loop, the subsystem with the transfer function $h_2(t)$, controls the input $x(t)$ to the system. Thus, the input will depend on the state of the system output at summing point S_2 . For negative feedback, indicated by a negative sign at the feedback arrowhead, the input is reduced as the output is increased. Positive feedback will increase the input as the output increases. The system response function of the feedback loop determines the time translation of information from summing point S_2 to summing point S_1 .

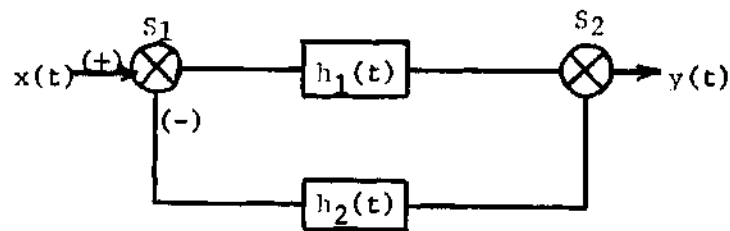


Figure G-1. Block Diagram of a Negative Feedback System

APPENDIX H

FACTOR ANALYSIS

Factor analysis, a multivariate statistical technique, determines a set of orthogonal axes which reduces the variance of a correlation matrix to a minimum. The characteristic equation

$$[R - \lambda_i I] = \emptyset \quad (H-1)$$

where R is the correlation matrix of a set of variables, I is the identity matrix, λ_i is the i^{th} eigenvalue, $i = 1, 2, 3, \dots, n$, n is the number of variables, and \emptyset is the null matrix, can be solved (47) to find the n eigenvalues and eigenvectors. The eigenvector \mathbf{V}_i , which corresponds to λ_i , can be determined by substituting the eigenvalues into the homogeneous set of linear equations

$$\begin{aligned} 0 &= (r_{11} - \lambda_1) \mathbf{V}_1 + r_{12} \mathbf{V}_2 + \dots + r_{1n} \mathbf{V}_n \\ 0 &= r_{21} \mathbf{V}_1 + (r_{22} - \lambda_2) \mathbf{V}_2 + \dots + r_{2n} \mathbf{V}_n \\ &\vdots \\ 0 &= r_{n1} \mathbf{V}_1 + r_{n2} \mathbf{V}_2 + \dots + (r_{nn} - \lambda_n) \mathbf{V}_n \end{aligned} \quad (H-2)$$

or

$$[R - \lambda I]Y = 0 \quad (H-3)$$

The system of homogeneous equations H-2 has a nontrivial solution if, and only if, the determinant of the coefficients vanishes, i.e., if $[R - \lambda I] = 0$. For normalized eigenvectors $\sum_{i=1}^m Y_i^2$ the vector corresponding to the largest eigenvalue produces the factor loadings (see below) of maximum variance. The variance of the i^{th} set of factor loadings is the i^{th} eigenvalue. The largest eigenvalue corresponds to the axis which results in the greatest reduction in unexplained variance. Each successive eigenvalue corresponds to the axis which reduces the variance the most.

The elements of each normalized eigenvector are multiplied by the square root of the corresponding eigenvalue to determine the factor pattern coefficients. The varimax procedure (40, 43) can be used to rotate the vectors $\lambda_i^{0.5} Y_i$. The resulting vectors, which no longer correspond to a particular eigenvalue, were modified such that the loadings are near ± 1 for a few related variables and the remaining elements of the vectors are near zero. Such factor loading patterns are much easier to interpret. Those variables which have factor loadings near ± 1 are highly correlated and tend to explain similar information.

APPENDIX I

PRINCIPAL COMPONENTS REGRESSION

Principal components regression (PCR) is a multivariate statistics technique which can be used, in a capacity similar to that of multiple regression, when the "independent" variables of a prediction equation are correlated. The structural coefficients of a PCR equation represent orthogonal contributions from the individual terms of the equation. As with factor analysis (Appendix H) the mathematical procedure of PCR involves an eigenvalue-eigenvector analysis of the characteristic equation of the correlation matrix. The resulting factor structure expresses the relationship between established orthogonal components and the original set of "independent" variables. For variables which are uncorrelated the PCR analysis will provide structural coefficients identical to those obtained using multiple regression analysis.

PCR determines n structural coefficients for the linear model

$$y_j = \sum_{i=1}^n a_i x'_{ij} \quad (I-1)$$

where y_j is the computed value of the j^{th} observation, a_i is the structural coefficient for the i^{th} orthogonal variates x'_{ij} . The computed value of the j^{th} observation equals the sum of the orthogonal elements y_j , $j = 1, 2, \dots, m$

$$y_j = {}_1y + {}_2y + \cdots {}_my \quad (I-2)$$

where m is the number of independent variables. Each orthogonal element is computed by

$${}_jy = \alpha_j \sum_{i=1}^m l_{ij} x_i \quad (I-3)$$

where α_j is the orthogonal weighting coefficient of the j^{th} orthogonal variate x_j and l_{ij} is the corresponding direction cosine.

APPENDIX J

COMPUTATION OF TOPOGRAPHIC PARAMETER VALUES

1. A : Horizontally Projected Area of Watershed
2. L : Length of Mainstream
Length of mainstream measured along the mainstream and extended to the basin divide.
3. S_{10-85} : Mean Channel Slope--Benson Method : $S_{10-85} = (H_{85} - H_{10})/D_{10}$
 H_{85} = Elevation at a point 85 percent of the distance from the gage to the end of the mainstream.
 H_{10} = Elevation at a point 10 percent of the distance from the gage to the end of the mainstream.
 D_{10} = Distance between the two (10 percent and 85 percent) points measured along the mainstream.
4. S_j : Basin Slope--Justin Method : $S_j = (H_g - H_l)/5280 A$
 H_g = Elevation of highest point in basin
 H_l = Elevation of lowest point in basin
 A = Area in square miles
5. S_L : Basin Slope--Landreth Method :

$$S_L = \frac{\sum_{i=1}^n (a_i \Delta h_i)}{(d_i A)}$$
 n = Number of subareas which the basin is divided into
 a_i = Area of i^{th} subarea
 A = Total area of basin
 Δh_i = Difference in elevation between highest and lowest points in the i^{th} subarea
 d_i = Distance between the highest and lowest points in the i^{th} subarea
6. S_m : Mean Basin Slope : $S_m = DL_c/A$
 D = Contour interval in feet
 L_c = Total length of all contours in feet
 A = Basin area in square feet
7. S_w : Mean Slope of Mainstream : $S_w = \Delta E/L$
 ΔE = Elevation difference between the gage and the point on the basin divide used to determine L
 L = Channel length in feet

8. S_T : Mean Slope of Mainstream : $S_T = (n/k_1)^2$
 n = Divide the mainstream (not extended to basin divide) into n segments.

$$k_1 = \sum_{i=1}^n 1/(\Delta e_i/l_i)^{0.5}$$

Δe_i = Elevation difference between endpoints of i^{th} segment

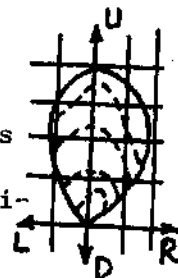
l_i = Length between endpoints of i^{th} segment

9. S_L : Land Slope:Intersection-Line Method : $S_L = N_R D/L_R$

D = Contour interval in feet

N_R = The number of times the contour lines cross the grid lines in the L-R direction

L_R = Length of grid lines (within the basin perimeter) in L-R direction



10. S_D : Land Slope:Intersection-Line Method : $S_D = N_D D/L_D$

N_D = The number of times the contour lines cross the grid lines in the U-D direction

L_D = Length of grid lines (within the basin perimeter) in the U-D direction

D = Contour interval in feet

11. S_{IL} : Land Slope : $S_{IL} = 1.57(N_D + N_R)D/(L_D + L_R)$

12. R_R : Basin Slope : $R_R = \Delta H/\Delta L$

ΔH = Difference in elevation between gage and point farthest from the gage

ΔL = Straight line distance between the two points

13. R_S : Slope Ratio : $R_S = S_m/S_T$

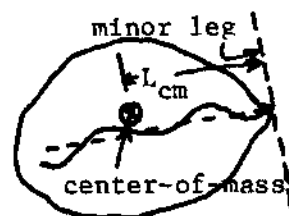
14. F_c : Circularity Ratio : $F_c = P/\sqrt{4A}$

P = Perimeter of basin in feet

A = Basin area in square feet

15. L_{cm} : Length to the center of area

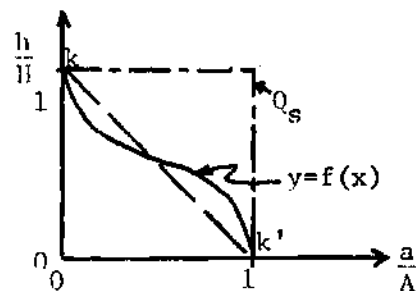
Draw a set of coordinate axes which has one leg parallel to the mainstream and passes through the gage; compute the center-of-mass around the minor leg. L_{cm} is measured in feet.



16. L_{cal} : Length to the center of area

The straight line distance from the center-of-mass to the gage point (measured in feet).

17. L_{ca} : Length to the center of area
The distance in feet measured along the mainstream from the gage to the point on the mainstream opposite the center of mass.
18. L_L : Shape Factor : $L_L = (L L_{ca})^{0.30}$
19. R_e : Elongation Ratio : $R_e = (4A/\pi)^{0.5}/L$
 A = Basin area in square feet
20. F_r : Circularity Ratio : $F_r = 4\pi A/P^2$
 P = Perimeter of basin in feet
 A = Basin area in square feet
21. F_f : Form Factor : $F_f = A/L_f^2$
 L_f = The straight line length from the gage to a point on the basin divide opposite the end of the mainstream (measured in feet)
 A = Basin area in square feet
22. F_s : Shape Factor : $F_s = A/L$
23. F_L : Shape Factor : $F_L = L^2/A$
24. H_A : Area Under Hypsometric Curve
 H_A = The ratio of the area under the curve y to the area of the square Q_s
25. H_s : Mean Slope-Hypsometric Curve Method
 H_s = The slope at the point of inflection on the hypsometric curve
26. H_f : Profile Factor : $H_f = D_H/L_H$
 D_H = The maximum deviation (perpendicular to line $k-k'$) of $y = f(x)$ to the line $k-k'$
 L_H = Length of line $k-k'$



Watershed	A sq ft x10 ⁵	L ft	S ₁₀₋₃₅	S _T	S _L	S _m
1	1.109	299	.1422	.1536	.1787	.1856
2	0.984	470	.02685	.0383	.02821	.0277
3	0.842	325.5	.0154	.0283	.02223	.0256
4	1.643	624	.0693	.08395	.05244	.0521
5	496	10710	.01379	.01173	.01589	.0464
6	3.49	854	.01422	.02085	.01555	.0188
7	32.2	3224	.0822	.1174	.13344	.1506
8	1.831	625	.0655	.0974	.07953	.0805
9	1.92	648	.0645	.0959	.06765	.0820
10	1.603	750	.0364	.0853	.0656	.0690
11	909	15880	.00543	.0189	.02041	.00773
12	28.48	2380	.0262	.101	.10716	.1613
13	5.45	1235	.100	.2313	.16507	.1730
14	0.1082	171	.0281	.02386	.03634	.02865
15	0.1076	171	.0299	.02455	.02568	.02885
16	0.1069	174	.02892	.02425	.02839	.02905

Watershed	S _w	S _T	S _L	S _D	S _{IL}	R _R	R _S
1	.164	.1867	.1609	.0571	.1681	.1368	0.993
2	.0213	.02263	.01694	.01972	.0288	.0215	1.427
3	.02582	.0259	.0186	.00833	.0211	.01975	0.989
4	.047	.0530	.0295	.0190	.0394	.0524	0.985
5	.01027	.01045	.02543	.03026	.0436	.0128	4.435
6	.01193	.01472	.00964	.01362	.01812	.01252	1.278
7	.03878	.1246	.0645	.1253	.1524	.0665	1.209
8	.0664	.0670	.05105	.05470	.08295	.0664	1.200
9	.0649	.0735	.0490	.0495	.0781	.0652	1.117
10	.0387	.0452	.0602	.0419	.0799	.0471	1.527
11	.00945	.00595	.0449	.0398	.0665	.01209	1.300
12	.0484	.02615	.0505	.1345	.1451	.065	6.18
13	.1320	.1212	.1290	.0715	.1578	.1458	1.426
14	.0275	.0280	.0292	.00201	.0248	.0278	1.022
15	.0287	.0295	.0283	.00201	.0240	.029	0.978
16	.0287	.0279	.02895	.0010	.02395	.0278	1.041

Watershed	F _c	L _{cm}	L _{cal}	L _{ca}	L _L	R _e	F _r	F _f
1	1.281	123	133	142	0.1237	1.253	.734	1.498
2	1.121	244	248	259	0.158	0.748	.791	0.456
3	1.106	190	194	190	0.1304	1.004	.816	0.843
4	1.149	339	342	352	0.1987	0.730	.756	0.442
5	1.371	3355	3475	3590	1.111	0.741	.529	0.624
6	1.126	420	422	401	0.2305	0.789	.790	0.523
7	1.182	1482	1504	1518	0.560	0.627	.717	0.325
8	1.121	295	298	300	0.1884	0.771	.796	0.477
9	1.120	293	295	308	0.1923	0.760	.796	0.4615
10	1.392	374	341	335	0.2802	0.600	.520	0.318
11	1.600	5890	5930	6355	1.539	0.676	.605	0.610
12	1.190	1142	1151	1162	0.463	0.799	.667	0.528
13	1.122	489	495	662	0.308	0.674	.799	0.482
14	1.300	87	87	87	0.08108	0.683	.593	0.370
15	1.284	89	89	89	0.0785	0.680	.609	0.3675
16	1.300	91	91	91	0.08265	0.670	.595	0.352

Watershed	F _s	F _L	H _A	H _s	H _f
1	370	0.816	.585	0.653	.0669
2	209.5	2.250	.590	0.622	0.1009
3	258.5	1.257	.618	0.750	0.1151
4	263.8	2.365	.588	0.600	0.1027
5	4640	2.318	.605	0.476	0.0978
6	409.5	2.085	.647	0.475	0.1469
7	999	3.232	.614	0.589	0.0923
8	793.5	2.135	.541	0.581	0.1111
9	296	2.18	.560	0.571	0.0888
10	214	3.15	.540	0.625	0.0835
11	5730	2.775	.585	0.700	0.0865
12	1199	1.99	.414	0.500	0.09745
13	441	2.80	.468	0.690	0.057
14	63.4	2.70	.485	1.000	0.01328
15	62.9	2.72	.502	0.999	0.0181
16	61.4	2.84	.493	1.000	0.0348

APPENDIX K

WATERSHED AND STORM EVENT INFORMATION

Watershed Number	Watershed Location	Storm Event Number	Runoff Gage	Rain Gage	Date of Storm Event
1	Lacrosse, Wis.	1	CW	CPR*	8/16/40
		2	CW	CPR*	6/29/41
2	Cherokee, Okla.	3	1	4	6/24/58
3	Cherokee, Okla.	4	7	9	6/24/58
4	Hastings, Nebr.	5	5-H	B-36-R	6/12-13/58
5	Oxford, Miss.	6	28	5	9/9/59
6	Cherokee, Okla.	7	9	8	6/9/42
		8	9	8	3/18/48
7	Coshocton, Ohio	9	183	RG 119	6/16/46
		10	183	RG 108	6/16/46
8	Bethany, Missouri	11	D3	R-2	6/17/35
		13	D3	R-2	5/1/35
9	Bethany, Missouri	12	D3	R-2	5/21/33
10	College Park, Md.	14	6	R-4	8/27/43
11	Oxford, Miss.	15	4	R-7	5/22/57
12	Pullman, Wash.	16	GS2	F-3	4/20/43
13	Newberg, Oregon	17	1	R-1	5/21/39
14	Riesel, Texas	18	P1	W-9	6/25/61
15	Riesel, Texas	19	P2	W-9	6/25/61
		20	P2	W-9	7/16-17/61
16	Riesel, Texas	21	P3	W-9	6/25/61
		22	P3	W-9	7/16-17/61
17	Lafayette, Ind.	E1	5	R-2	6/24/57
18	Lafayette, Ind.	E2	6	R-2	6/24/50
19	College Park, Md.	E3	7	R4	8/27/43
20	Hastings, Nebr.	E4	18-H	B-33-R	6/15/57

*Control Plot Raingage

APPENDIX L

SENSITIVITY AND CORRELATION VALUES

SE*	R*	SLR ₂ S ₁ *	R	ELWF S ₁	R	DR S ₁	S ₂ *	R	DRWF S ₁	S ₂
1	.74	.0065	.62	.0038	.94	.0214	.0167	.90	.0122	.0080
2	.98	.0362	.95	.0436	.93	.1428	.1169	.94	.1050	.0804
3	.92	.0038	.83	.0024	.97	.0110	.0087	.94	.0070	.0058
4	.55	.0019	.42	.0011	.84	.0056	.0045	.72	.0033	.0026
5	.73	.0136	.66	.0084	.96	.0707	.0576	.94	.0452	.0375
6	.75	.0014	.69	.0005	.93	.0025	.0020	.91	.0010	.0008
7	.67	.0071	.59	.0028	.93	.0123	.0096	.92	.0049	.0043
8	.97	.0039	.89	.0029	.98	.0114	.0093	.97	.0085	.0067
9	.65	.0019	.60	.0006	.90	.0038	.0030	.87	.0016	.0012
10	.72	.2738	.69	.3787	.94	.0157	.0134	.95	.0060	.0048
11	.80	.0227	.88	.0295	.98	.0721	.0581	.97	.0437	.0368
12	.82	.0175	.74	.0112	.92	.0598	.0482	.89	.0332	.0251
13	.55	.0133	.49	.0036	.79	.0238	.0186	.77	.0089	.0073
14	.83	.0049	.76	.0027	.98	.0160	.0130	.93	.0091	.0074
15	.76	.0092	.74	.0303	.94	.0009	.0007	.93	.0004	.0003
16	.55	.4014	.55	.1437	.93	.0025	.0018	.93	.0009	.0006
17	.97	.0226	.92	.0170	.99	.0747	.0592	.98	.0472	.0384
18	.93	.0055	.86	.0032	.99	.0152	.0121	.96	.0091	.0074
19	.99	.0176	.95	.0167	.98	.0359	.0293	.98	.0253	.0198
20	.84	.0029	.77	.0017	.98	.0106	.0086	.95	.0062	.0052
21	.93	.0039	.86	.0024	.99	.0114	.0093	.97	.0072	.0059
22	.75	.0197	.70	.0508	.92	.0266	.0208	.89	.0114	.0088

*SE = Storm Event

R = Correlation Coefficient

S₁ = The absolute value of the maximum ordinate of the sensitivity function

S₂ = The absolute value of the sensitivity function ordinate at the peak of the response function

SE*	Nash			LCLR-R			LCLR-LT		
	R	S_K	S_n	R	S_K	S_{T_C}	R	S_K	S_{T_C}
1	.90	.0079	.0495	.80	.0115	.0804	.78	.0115	.0493
2	.95	.1029	.2624	.95	.0825	.3169	.95	.0852	.1703
3	.97	.0048	.0493	.92	.0068	.0797	.92	.0068	.0310
4	.82	.0022	.0205	.54	.0037	.0480	.53	.0037	.0283
5	.94	.0310	.1019	.87	.0404	.2003	.87	.0409	.1143
6	.95	.0005	.0278	.95	.0004	.0077	.95	.0004	.0050
7	.98	.0029	.0366	.95	.0035	.0326	.95	.0038	.0135
8	.99	.0054	.0557	.97	.0077	.0749	.97	.0075	.0303
9	.96	.0009	.0270	.86	.0012	.0097	.86	.0012	.0092
10	.94	.0032	.0376	.96	.0041	.0393	.96	.0042	.0189
11	.98	.0316	.1396	.98	.0364	.1824	.98	.0352	.0950
12	.89	.0240	.1135	.87	.0284	.1506	.86	.0287	.0854
13	.78	.0062	.0578	.90	.0030	.0048	.92	.0032	.0022
14	.94	.0064	.0486	.85	.0093	.0923	.85	.0093	.0355
15	.97	.0002	.0108	.95	.0002	.0001	.95	.0002	.0001
16	.90	.0007	.0108	.93	.0010	.0006	.93	.0010	.0004
17	.99	.0344	.1633	.98	.0372	.1580	.98	.0357	.0999
18	.97	.0062	.0652	.94	.0083	.0877	.94	.0083	.0462
19	.99	.0184	.1438	.99	.0194	.0800	.99	.0188	.0735
20	.94	.0036	.0445	.87	.0051	.0670	.87	.0051	.0366
21	.98	.0048	.0538	.94	.0068	.0650	.94	.0067	.0422
22	.90	.0065	.1078	.94	.0052	.0186	.93	.0051	.0101

*SE = Storm event